Dipl. Ing. Claudia Payerl

Sorption-induced creep of pulp fibers

PhD Thesis
Dissertation

Zur Erlangung des akademischen Grades
Doktorin der Technischen Wissenschaften
eingereicht an der
Technischen Universität Graz

Betreuer:

Ao.Univ.-Prof. Mag. Dr.rer.nat. Robert Schennach

Institut für Chemische Technologie von Materialien (ICTM)

Graz, Oktober 2019

EIDESSTATTLICHE ERKLÄRUNG

Ich erkläre an Eides statt, dass ich die vorliegende Arbeit selbstständig verfasst, andere als die angegebenen Quellen/Hilfsmittel nicht benutzt, und die den benutzten Quellen wörtlich und inhaltlich entnommenen Stellen als solche kenntlich gemacht habe. Das in TUGRAZonline hochgeladene Textdokument ist mit der vorliegenden Dissertation identisch.

_____   _____

Datum   **Unterschrift**

Acknowledgements

Index of Abbreviations

Abbreviations	Unit	Description
SP	-	Spruce
DP	-	Degree of polymerization
MFA	-	Microfibril angle
FSP	-	Fiber saturation point
RH	-	Relative humidity
EMC	-	Equilibrium moisture content
VdW-forces	-	Van der Waals interactions
PEK		Parallel exponential kinetic
MC	-	Moisture content
MSC	-	Mechano-sorptive creep
UTS	-	Ultimate tensile strength
Tg	°C	Glass transition temperature
ε	%	Strain
l	µm	Gauche length
ε_c	[-]	Creep strain
ε_r	[-]	Recovery strain
$\dot{\varepsilon}$	%ε/LOG$_{min}$	Strain rate
σ	MPa	Stress
F	mN	Force
A	µm^2	Cross sectional area
J	MPa^{-1}	Creep compliance
G	MPa	Relaxation modulus

Content

Abstract

The present study was designed to independently study the sorption-induced creep and the creep induced by an externally applied load. As the key incentive was the separation of these frequently overlapping effects, special focus was put on the experimental design. Therefore, the moisture content was evaluated from dynamic vapor sorption experiments at the applied three moisture levels of 25%, 50% and 80% relative humidity. In order to verify, whether the applied pre-load affects the sorption induced strain-rate, the cross-sectional area of the previously tested fibers was obtained from microtome slices and the resulting stress was calculated. The results indicate that the applied pre-load does not significantly affect the sorption induced strain-rate, which, indeed, enables for studying the long-term deformation behavior of pulp fibers exclusively induced by sorption. The strain during wetting can be clearly categorized in three parts, including (1) initial surface adsorption, (2) swelling during RH increase, and (3) creep at constant RH. The swelling strain-rate at the applied moisture levels follows a second order polynomial growth, whereas the creep strain-rate linearly increases with elevating moisture levels. In the present study, when the fibers were exclusively stressed by the sorption process between 50% and 80% RH and the applied pre-load, MSC was not observed. The absence of MSC is related to matrix polymers entering their rubbery state enabling facilitated stress migration. In addition to this, creep experiments were performed with dry pulp fibers in order to study the impact of the mechanically applied load. The results further suggest that during drying the MFA decreases as the cell wall significantly deformed even when the fibers had reached their maximum dry state. After load application this process is reversed, and the MFA continuously increases while the fibers plastically deform to a high extent.

Kurzfassung

Das Quellverhalten von Zellstofffasern wirkt sich negativ auf die dimensionale Stabilität von Papier aus, das daraus resultierende beschleunigte Kriechverhalten und dessen zugrundeliegende Prozesse sind jedoch bis heute nur unzureichend verstanden. Ein Grund dafür ist die gleichzeitige Einwirkung einer von außen aufgebrachten Last und der Umgebungsfeuchte auf die Faser, die in weiterer Folge zu kriechen beginnt. Das Hauptaugenmerk der vorliegenden Arbeit liegt auf der Beobachtung dieser beiden Effekte unabhängig voneinander mittels eigens entworfenen Experiment-Designs. Der Feuchtegehalt von Zellstofffasern und dessen Auswirkungen auf deren Kriechverhalten wurden bei drei verschiedenen Umgebungsfeuchten von 25, 50 und 80% bestimmt. Um zu überprüfen, ob die angelegte Vorspannung die sorptionsinduzierte Dehnungsrate beeinflusst, wurden die Querschnittsflächen der zuvor getesteten Fasern an Mikrotomschnitten bestimmt und der resultierende Stress berechnet. Die Ergebnisse zeigen, dass die angelegte Vorspannung die sorptionsinduzierte Dehnungsrate nicht signifikant beeinflusst, wodurch die Untersuchung des langfristigen Verformungsverhaltens auf Grund des Quellvorgangs von Zellstofffasern ermöglicht wird. Die Faserbeanspruchung während des Quellvorgangs kann in drei Bereiche eingeteilt werden, die (1) anfängliche Oberflächenadsorption, (2) Quellung während des Anstiegs der relativen Luftfeuchtigkeit und (3) Kriechen bei konstanter relativer Luftfeuchtigkeit. Die Dehnungsraten während des Quellens bei den vorab definierten Umgebungsfeuchten folgen einem Polynomwachstum zweiter Ordnung, die Dehnungsraten während des Kriechens bei konstanter Feuchte nehmen mit steigender Umgebungsfeuchte linear zu. Weiters wurde bei den Experimenten kein beschleunigtes Kriechen (*mechano-sorptive creep, MSC*) beobachtet, wenn die Fasern ausschließlich durch den Quellvorgang zwischen 50% und 80% relativer Luftfeuchtigkeit und der applizierten Vorspannung beansprucht wurden. Das Nichtauftreten von MSC kann durch den überschrittenen Glasübergangszustand der Matrixpolymere und die damit einhergehende erleichterte Stressmigration erklärt werden. Darüber hinaus wurden Kriechversuche mit trockenen Zellstofffasern durchgeführt, um den Einfluss der mechanisch aufgebrachten Last zu untersuchen. Die Ergebnisse legen ferner nahe, dass der Microfibrillen-Winkel *(micro-fibrillar angle, MFA)* während des Trocknens abnimmt, da sich die Zellwand kontinuierlich weiter verformt, selbst wenn die Fasern bereits einen Großteil ihre Feuchte an die Umgebung

2

abgegeben haben. Nach dem Aufbringen der Last kehrt sich dieser Vorgang um und der MFA steigt kontinuierlich an, während sich die Fasern in starkem Ausmaß plastisch verformen.

Motivation

Modern society is filled with products made of plastics and many of them are treated as single-use plastics. These plastics, however, do not biodegrade but slowly break down into smaller pieces of plastic, known as micro- and nano-plastic [1]. Over the past decades these plastics have been polluting our planet and are still continuously accumulating on earth [2]. Fortunately, people all around the world now start to realize that we need an alternative to single-use plastics and even force politics to take action [1]. Products made of and derived from wood, therefore gain more and more attraction as a renewable- and biodegradable-solution in order to reduce and replace single-use plastics. Besides, wood already has a broad range of application, as it is used in paper and packaging materials, in furniture and in building constructions. In addition, the last few years have seen a growing interest in nature-based organic products, and there is good reason to believe that wood will remain an important and sustainable material for future generations.

Wood is by far the most abundant source for the production of paper. But pulp fibers can be extracted from almost any vascular plant found in nature. In addition to that, they exhibit a number of advantages that fulfill the requirements of the papermaking industry. As a hydrophilic material, the interaction between wood and water plays a key role. When wet fibers are brought together during the sheet forming process, the bonding between individual fibers is promoted by the attraction forces between water and the constitutive polymers, such as cellulose and hemicellulose. During sheet drying, water molecules evaporate, enabling individual fibers to interact and further bond with each other by means of hydroxyl groups [3]. The affinity of pulp fibers to water, however, has a serious effect on the dimensional stability of paper. Since the constitutive polymers in pulp fibers belong to a class of polymers based on cellulose and hemicellulose, they are sensitive to moisture. When pulp fibers are in contact with water they swell, thereby changing their dimensions and altering the material structure [4]. This phenomenon can crucially affect the performance of paper and with that its usage in many applications.

For wood engineering purposes, another interesting behavior affecting the product performance of wood-based materials is viscoelasticity. The viscoelastic nature of pulp fibers is described by their time-dependent mechanical response to stress. When a fiber is exposed to a constant load, it first rapidly changes its dimension in direction of the applied load and

further only slowly deforms. Upon load removal this process is reversed, hence the fibers quickly contract at first and then, slowly change their dimensions again. A total recovery of the initial dimension is favored as it determines the long-time applicability of paper-based products. In pulp fibers, however, a residual deformation, called permanent set, remains, even after a prolonged recovery time [3].

Besides, the viscoelastic nature of wood-based materials is strongly influenced by moisture. Moisture-induced structural changes inside the fiber cell-wall have a dramatic effect on the mechanical properties of pulp fibers and consequently affect the performance of nearly every paper-based product such as corrugated containers, printing and writing papers, and laminates [5]. The time-dependent deformation upon change in relative humidity can cause significant deterioration in the load-bearing capacity of paper-based materials during storage. A box under load, for instance, fails within 72 days at constant ambient environment. When the same box is exposed to a cycling ambient humidity between 30% and 80% relative humidity every 12 hours it fails already within four days [6]. This so called mechano-sorptive creep or accelerated creep, is still not fully understood. Understanding the effect behind mechano-sorptive creep, however, is crucial in order to predict macroscopic paper performance and to ensure product quality. As paper is a composite, it consists of many individual but interconnected pulp fibers, all responsible for the resulting creep. Consequently, there is a need of study creep on the single fiber-level as well, in order to separate the paper-creep from the individual fiber-creep. These investigations of the tensile creep are usually performed under the additional influence of moisture [7,8]. The main drawback of these methods is that the obtained creep of the tested fibers is always induced by both, an external load and the sorption process itself. Accordingly, there is a need to independently study the sorption-induced and the mechanically induced creep in order to understand the fiber response to either one of these two performance-influencing factors. The aim of this thesis therefore is to provide an experimental design which enables to independently study the creep of individual pulp fibers induced by either the sorption process or by the externally applied load. The study offers some relevant insights into the time-dependence of sorption-induced strain and provides information which can further extend our knowledge about the viscoelastic nature of dry pulp fibers. This, in turn, can help to minimize dimensional instability and may even encourage the use of paper in other relevant industrial fields.

Chapter 1: Wood polymers and their purposes

Cellulose for industrial use is mainly obtained from wood pulp and cotton. Both are hierarchically structured materials with several levels of organization. The characterization and interpretation of the behavior of wood pulp-fibers therefore requires profound knowledge of the composition and structural organization from the molecular level up to the macroscopic structure [9]. The main constitutive polymers of wood are the biopolymers cellulose, hemicellulose and lignin. Cellulose, an organic compound with the formula $(C_6H_{10}O_5)_n$, is a polysaccharide consisting of several hundred to many thousands of $\beta(1\rightarrow4)$ linked D-glucose units. Cellulose is one of the most important structural components in nature, and as such it is an essential ingredient in green plants, many forms of algae and of oomycetes. The cellulose content in cotton fibers is about 90%, that of wood about 40–50%, and that of hemp is about 57% [10]. The smallest unit of cellulose are anhydroglucose units, which when linked together by a $\beta(1\rightarrow4)$ covalent-bond, polymerize as a straight chain, figure 1. Cellobiose units condense with their reducing end, and no coiling or branching occurs in contrast to other polymers present in plant fibers.
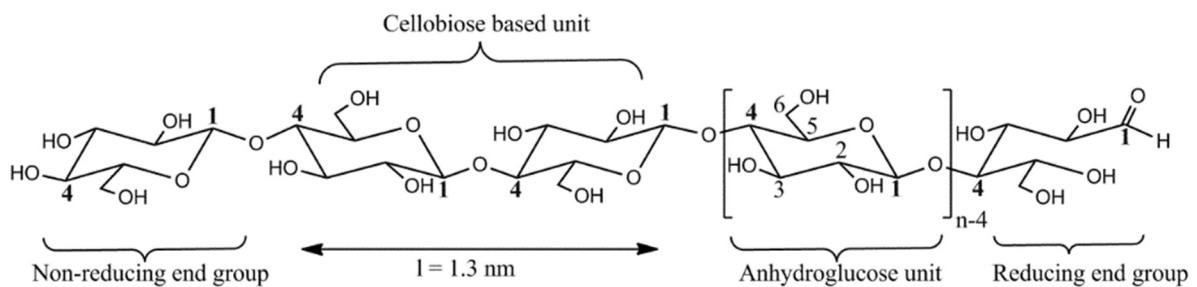
Fig.1 Cellulose polymer chain consisting of cellobiose units, which are two single anhydroglycose units $\beta(1\rightarrow4)$ covalently-bound. Each cellulose polymer has a reducing and non-reducing end group [11].

The degree of polymerization (DP) of cellulose varies to a high extent, depending on its source and the processing steps during cellulose isolation. The DP of cellulose in wood can be up to 10000 [12]. Once processed, the DP of cellulose in pulp decreases, varying between 300 to 1700. Regenerated cellulose has a DP of only 250 to 500. Still regenerated cellulose is characterized by a high tenacity and strength [10]. This is based on its superior ability to interact with itself using the hydroxyl-groups at the positions C2, C3 (both secondary, equatorially bonded) and C6 (primarily bonded). Those hydroxyl-groups build up hydrogen-bonds to neighboring cellulose polymers, thereby they agglomerate to form fibrils. Up to 36 cellulose chains

intermolecularly bond to form hexagonally aligned microfibrils in softwood [13], figure 2(a). Cellulose in nature-based fibers usually obtain a cellulose I$_\beta$ crystal lattice structure, figure 2(b).
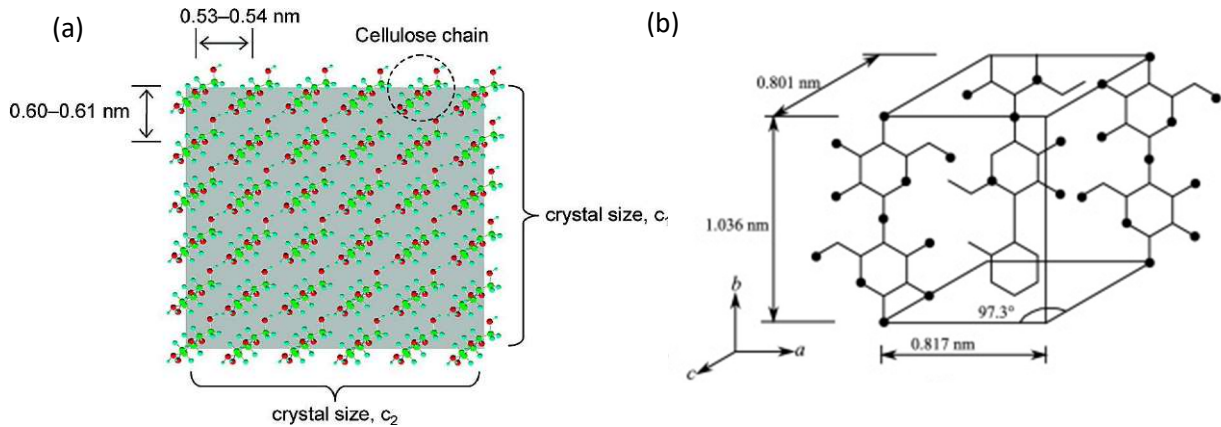
Fig. 2 (a) Cellulose unit cell[3] and (b) Cross-section of a microfibril with 36 hexagonally aligned cellulose chains [13].

The unit cell has dimensions of a = 0,817 nm, b = 1,036 nm, c = 0,801 nm, and α = 97,3°. The *a-b* plane bears the planes of the anhydroglucose units, whereas the axes of the cellobiose units are parallelly aligned to the *b*-axis. In sum, three types of forces hold together the unit cell. The β1,4-glucosidic primary valence bond holds the glucose units together along the *b*-axis [3]. Along the *a*-axis, cellulose chains are held together by hydroxyl groups with an estimated distance of about 0,53 nm. Along the *c*-axis the nearest distance of the cellulose chains are reported to be in the range of 0,60 nm, indicating that van der Walls forces are holding the lattice together [13]. Aggregated celluloses, traditionally called crystalline fibrils, occur in nature in two polymorph-states, cellulose I$_\alpha$ and cellulose I$_\beta$. The relationship of celluloses I$_\alpha$ to I$_\beta$ varies with the source of the cellulose, with the I$_\beta$ form being dominant in higher plants, such as in trees [14,15]. The next higher level of organization is termed microfibril [16]. Cellulose within a wood cell wall can exist either as a part within the fibrils, in its crystalline form, or in its amorphous form. Crystallization is, however, favored by the linearity of the molecule and its tendency to form hydrogen bonds with adjacent cellulose chains, which allows a tight packaging of the polymers [3].

In wood, another important constituent within a single cell wall is hemicellulose. Whereas cellulose is based on anhydrous glucose units as its constitutive monomer, hemicellulose consists of several different sugar units. The most abundant monomers used to build up the polysaccharide are xylose and arabinose. Besides these sugars, built up from five carbons,

mannose, galactose and rhamnose are building blocks for hemicellulose [4]. Thus, a large family of several wood polymers exists in a single cell wall, with arabinoglucuronoxylan and galactoglucomannans being present in the largest amount in softwood [17], figure 3. As their building blocks are far more versatile than those of cellulose, hemicelluloses are branched polysaccharides with a rather low degree of polymerization.
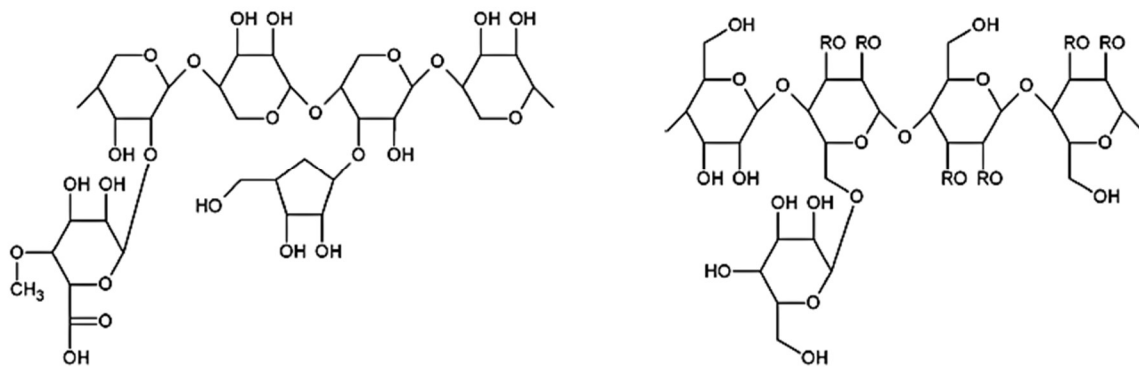
Fig. 3 Chemical structure of two most common hemicelluloses present in wood: arabinoglucuronoxylan (left) and galactoglucomannans (right). R=CH₃CO- or H- [4]

Like hemicellulose, lignin is a branched polymer and the third essential polymer necessary to build up the cell wall. In contrast to hemicellulose and cellulose, lignin contains aromatic monomers. Three types of building blocks are used for its polymerization, called mono-lignols. Liginins present in softwood are mainly built up by the mono-lignol coniferyl alcohol [17]. According to the route of polymerization, two different types of lignin are found in softwood; condensed and non-condensed ones [4,18], figure 4.
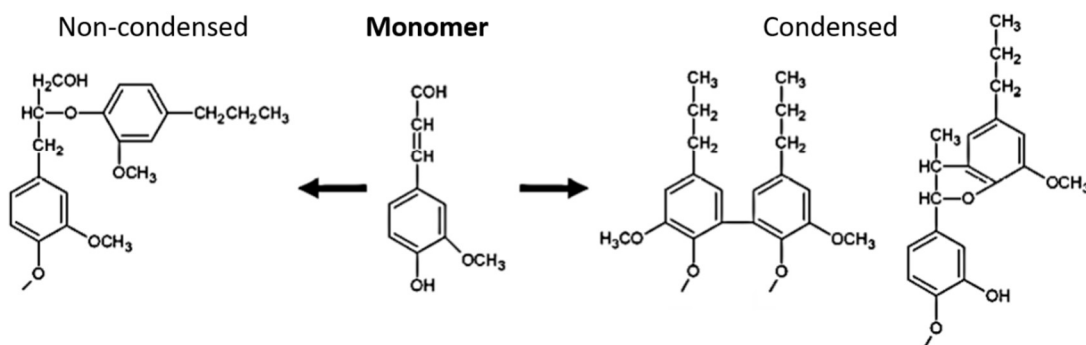
Fig.4 Typical structures and bonding patterns of lignins as found in wood [4].

Hemicellulose is sometimes also referred to as matrix-polysaccharide, as it is found accompanied by condensed lingnin between the cellulose microfibrils. Glucomannan

hemicellulose was observed to be the component closest to the microfibrils [19,20], followed by xylan and condensed lignin, which are covalently bonded to each other [21]. Non-condensed lignin is found farthest from the microfibrils and forms the outermost layer of the cell wall. There is evidence that glucomannan, xylan, and lignins are all parallelly oriented to the microfibrils [9,22]. The constitutive biopolymers are organized into composites and form the cell walls of the tracheid, figure 5. Several tracheid cells are further parallelly arranged into wood tissues. A tracheid cell is a hollow tube typically, about 2-4 mm long and 0,02-0,04 mm wide, figure 5(a). The inner void volume is called cell lumen which is surrounded by the 0,002-0,008 mm thick cell wall [23]. The cell wall can be further divided into the primary (P) and the secondary (S) cell wall, where the secondary cell wall is the dominating layer, building up about 80% of the total cell wall [24]. The secondary cell wall consists of three more layers, namely S_1, S_2, and S_3.
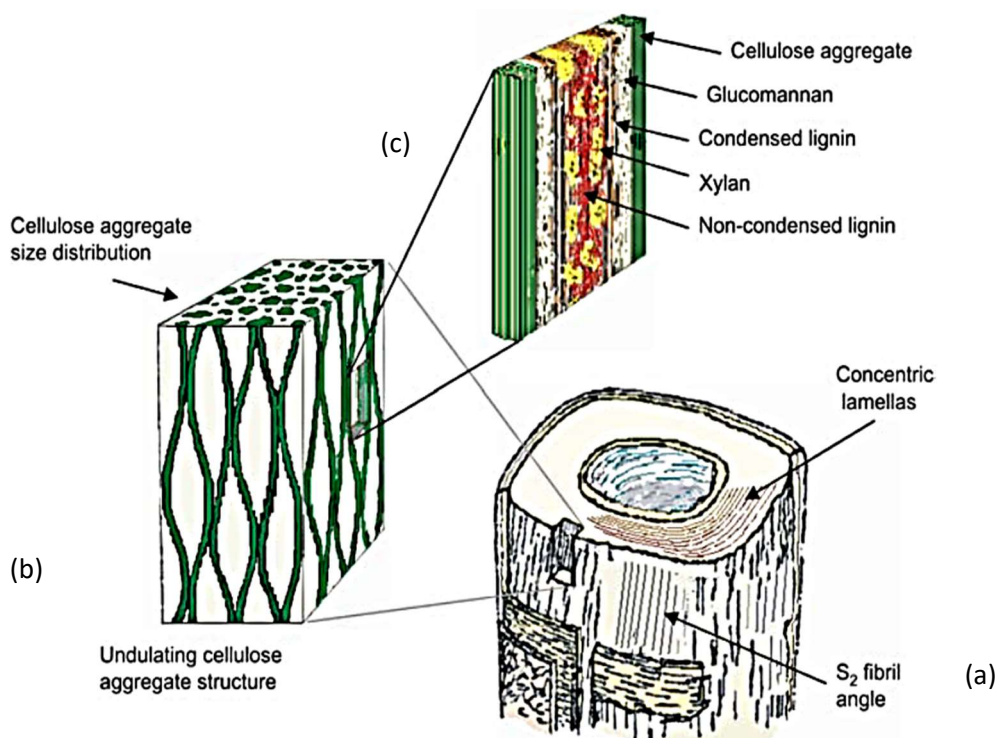
Fig. 5 (a) Schematic drawing of the wood cell-wall in softwood (tracheid). (b) Section of the S2 layer, where aggregated cellulose (fibrils) is embedded in the amorphous matrix, showing undulating cellulose aggregate structure and variability of cellulose aggregate sizes (c) Constitutive polymers of the cell-wall matrix, all parallelly arranged between fibrils [19,22].

The S2 layer is characterized by the highly ordered pattern of cellulose fibrils and hemicellulose and as such is key to an in-depth understanding of the mechanical performance of the whole cell wall, figure 5 (b+c). These fibrils align in a helical structure which varies

between the different layers. Regarding the secondary cell wall, the helix has a rather low inclination towards the fiber axis within the S1 and S3 layer, whereas the inclination of the helix is rather large within the S2 layer [22]. A more random alignment of the fibrils was observed in the primary cell wall. The inclination of the fibrils towards the fiber axis is known as microfibril angle (MFA).

All wood polymers are more or less hydrophilic. Accordingly, wood can accommodate a substantial amount of water inside the wood cell wall. This affinity to water derives from the presence of hydroxyl groups in all wood polymers. Therefore, the so-called sorption sites are the most important chemical groups in terms of attracting water. Other chemical groups, such as carboxyl groups are also capable of adsorbing water, but their amount in the cell wall, compared to the amount of hydroxyl groups, is negligible [25]. The maximum amount of water able to accumulate inside a wood cell wall is referred to as fiber saturation point (FSP), although definitions vary throughout the literature. The FSP in softwood was obtained by several authors and was shown to be in the range of 35- 42wt% moisture content [26–28]. For an in-depth understanding of the definition and measurement techniques available to define the FSP, the reader is referred to the review "a critical discussion of the physics of wood-water interactions" [29].

Chapter 2: Interaction between wood and water

One question has the attraction of researchers since the early 1980s, when a profound knowledge of wood-water interaction became increasingly important in order to predict the performance of wood-based materials: Does water freeze in wood? Back then, Nakamura et al. observed two different phase shifts in a temperature range of 10 to -70°C by applying Differential Scanning Calorimetry (DSC) on wood samples, which they related to the freezing point of water [30]. The initial phase shift occurred between 10 to -20°C and was therefore referred to as freezing bound water, whereas the phase shift at lower temperatures down to -70°C was referred to as non-freezing bound water [25]. Accordingly, it would seem natural to separate water present in wood into three categories, namely; free water, freezing bound water and non-freezing bound water. This nomenclature is still frequently used, although there is reasonable doubt whether water freezes in wood at all. Low field nuclear magnetic resonance relaxometry (LFNMR), for instance, did not reveal the presence of any freezing bound water down to -20°C in wood [31]. Zelinka et al. in 2012 further found considerable doubts on the interpretation of the DSC signals previously made by Nakamura and Berthold. They suggested that the DSC-signal, previously referred to as freezing bound-water, is identical with the homogeneous nucleation of free water and as such, water inside a wood cell wall would not reach the frozen state. Zelinka et al. argued that water being bound close to the constitutive hydrophilic polymers of wood, might be ordered in a defined pattern which could induce nucleation [32]. Nucleation describes the primary step in order to establish a new thermodynamic phase and is defined as the process that determines the speed of transition into a new stable phase. If an amount of water, for instance, gets cooled down below 0°C it will freeze. If the same amount of water, although cooled down only a few degrees below 0°C, it often stays completely free of ice for a long period of time. That is because nucleation under these conditions is very slow. Depending on its environment, water can be kept in the state of nucleation without reaching a new thermodynamic frozen phase. Within a wood polymer it is therefore probable that water does not reach the frozen state. Thus, the newer interpretation of Zelinka et al. clearly points out the difficulty of the observation of wood-water interactions. These observations require a continuum, hence a thermodynamic equilibrium, which is difficult to reach with nearly all applied measurement techniques [29]. Moreover, the more general question that arises from the results of Zelinka et al. is, how to correctly interpret the freezing point depression of water in wood. In wood the strong effect of bonding and the

formation of a possible bonding pattern of adsorbed water molecules largely influence the freezing point of water. Naturally, water bound directly to the constitutive polymers experiences attraction forces larger than water located only in the proximity of such polymers [33]. Accordingly, freezing bound water has been assumed to be less confined and only loosely bound to the cell wall, whereas non-freezing bound water was argued to largely experience the attraction forces of the constitutive polymers [34,35]. Analytical techniques in order to quantify and visualize bound and free water are: Differential Scanning Calorimetry (DSC), Nuclear Magnetic Resonance (NMR), Raman spectroscopy and infrared spectroscopy [30,36,37].

Chapter 2.1: Water accessibility inside wood structures

From a chemical point of view rather than from a physical one, one can determine the amount of possible sorption sites. Sorption sites are known as possible sites for water to adsorb. Hydroxyl-groups are the most important chemical components in terms of attracting water molecules [38] and as such characteristic for most of the available sorption sites in wood. It is well known that hemicellulose has the highest number of sorption sites, followed by cellulose and lignin [29]. As previously mentioned, cellulose interacts with itself in order to form aggregates, and two-third of its hydroxyl-groups are bound already to neighboring cellulose chains constituting the microfibril [39]. As a consequence those hydroxyl groups are not accessible to water and only hydroxyl groups present on the fibril's surface are potential sorption sites [40,41]. Some sorption sites located in the amorphous matrix are additionally inaccessible for water. Constitutive matrix-polymers interact with themselves and sterically hinder water to adsorb at few more sorption sites. Nonetheless, the hemicellulose-rich matrix is the region where most of the water molecules primarily adsorb. However, this evaluation could be used as an estimation only and it expresses a theoretical upper limit. The estimated number of water molecules per sorption site indicates that only 1 to 2 water molecules bond to each sorption site [25,42]. By measuring the sorption enthalpy of adsorbed water in amorphous cellulose, Joly et al. found a threshold after which the previously constant sorption enthalpy suddenly decreases [43]. The sorption enthalpy was reported to be constant up to 40% - 50% RH and related to the binding of one water molecule per glucose unit. A similar observation was made by Fringant et al. on various other polysaccharides, and in both studies the sorption enthalpy decreased in the range of 50 to 85% RH. The decreased sorption

enthalpy was further related to the increased water uptake of a second water molecule per glucose unit. Interestingly, the adsorption of a single water molecule on the cellulose crystal-surface obviously is energetically favored, as the obtained sorption enthalpy was increased at lower humidity levels. The authors therefore concluded, that water favorably adsorbs to two neighboring sorption sites of the constitutive polymers [43].

Chapter 2.2: The sorption isotherm of wood

The amount of moisture present in the wood cell wall depends on the surrounding environment. By performing dynamic vapor sorption measurements, the amount of water held by a wood cell wall at specific ambient conditions can be obtained. Thereby a defined mass of wood is exposed to a defined relative humidity at constant temperature and vapor pressure while the increasing mass during water adsorption is detected. If the moisture content is further plotted against the surrounding relative humidity the so-called sorption isotherm could be obtained. Thus, a sorption isotherm illustrates different equilibrium moisture states between wood and its environment, attained at constant temperature and water vapor pressure. Sorption isotherms of wood typically show a sigmoidal relation between water content and relative humidity and illustrates either water uptake (adsorption) or release (desorption) from the cell wall, both processes with long duration, figure 6.
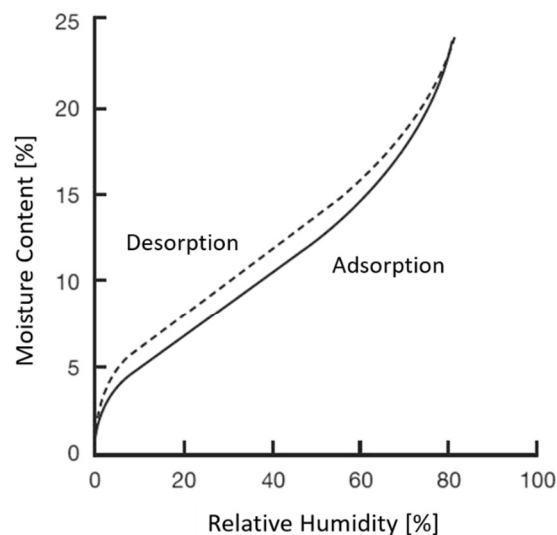

Fig. 6 Wood sorption isotherm during adsorption and desorption illustrated by hysteresis.

Sorption is a thermodynamically complex process involving both a change in temperature and volume, thereby heat and work are involved in the process of attaining the new thermodynamic equilibrium. In dynamic vapor sorption (DVS) measurements an equilibrium

moisture state of wood is attained when there is no measurable exchange of moisture between a defined amount of wood and its surrounding. Again, this method expresses a theoretical upper limit as the sorption process constantly progresses. Besides the necessity of long-time measurements in order to attain a new thermodynamic equilibrium, applied measurement conditions are unsuitable for detecting and compensating small fluctuations in temperature, vapor pressure and mass. In addition to the dependency of the sorption isotherm on relative humidity and temperature, the sorption isotherm of wood is influenced by its moisture history. This becomes obvious as drying (desorption) from a saturated state in defined climatic conditions yields a higher equilibrium moisture content (EMC) than moistening (adsorption) from a dry state to the same conditions. Therefore, sorption isotherms from adsorption to desorption follow a characteristic shape called hysteresis.

However, sorption isotherms of hydrophilic porous media are usually obtained as a type II sorption isotherm which represents the sorption of deformable solids accompanied with significant heat of sorption [44]. Various phenomena were suggested to be responsible for the physical background leading to this shape of the isotherm. The more general interpretation, based on the Park's model, divides the absorption process into three parts [45,46]: The initial water uptake up to around 10% RH, proceeds according to Langmuir's mode and is related to the adsorption of single water molecules gradually covering the internal surface of the cell wall [47]. As previously discussed, those sorption sites are hydroxyl-groups of amorphous cellulose and hemicellulose, or carboxylic functions of pectins [48]. As the ambient humidity increases, the inner surface becomes fully covered by water, which leads to a linearly increasing water concentration with the ambient relative humidity. This part of the isotherm can be mathematically described by Henry's law up to an ambient relative humidity of about 65%. This behavior is related to the porous structure of wood, where water is free to diffuse. The third part is mathematically well described by a power law which is related to the agglomeration of water and capillary condensation [49]. The precise mechanisms governing the transport and the distribution of water through the cell wall in nature-based fibers, however, are still unknown. Capillary condensation for instance has been speculated to be possible only above 90% RH, whereas the upward bend of the sorption isotherm starts already at around 60-70% RH. In addition, Thygesen et al. showed that capillary condensation apparently does not play any significant role in water vapor sorption of wood below 99,5% RH [31].

Interestingly, the sorption isotherm of many polymeric materials has been shown to follow a sigmoid shape. For amorphous polymers, such as hemicellulose, it has therefore been suggested by various authors that the upward bend in sorption isotherms is related to the softening of these polymers [50–52]. The softening of amorphous polymers is usually related to increased temperature levels. The glass transition temperature (Tg) of amorphous polymers describes the transition from a glassy state to a rubbery state. Thereby both, viscosity and rigidity, decrease, accompanied by an increased free volume, which thus could increase the sorption capacity of wood at higher humidity-levels. The same process is further suggested to be responsible for the appearance of sorption hysteresis. It is well known that the glass transition of such polymers could be shifted to lower temperatures by the presence of moisture, which is known as plasticization, figure 7.
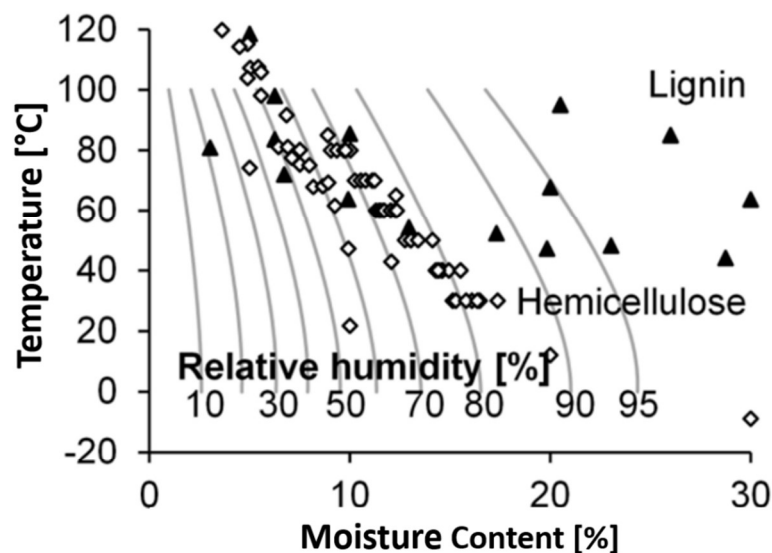
Fig. 7 Softening of hemicellulose (diamonds) and lignin (triangles) in wood as function of the moisture content. Isohumes between 10% and 95% RH are illustrated in grey [29].

Under dry conditions hemicellulose has an estimated glass transition temperature between 150°C and 220°C [53]. Salmén et al. have shown that around 60% RH hemicellulose in wood softens already at room temperature, whereas pure hemicellulose extracted from wood softens at around 80% RH and room temperature [20,54]. In contrast to that, lignin's glass transition temperature never drops below room temperature in the entire sorption range up to the FSP [55,56]. Thus, at room temperature and at a relative humidity between 60 to 80% RH, corresponding to 11-15wt% moisture, hemicellulose enters the rubbery state. This range

15

further is characterized by a percolation threshold, after which moisture-induced structural damage becomes increasingly important [57].

Chapter 2.3: Modeling of wood sorption isotherms

The complexity of the sorption process itself made it hardly possible to invoke every single thermodynamic step into a mathematical model and fully describe the sorption isotherm in its hygroscopic range. Thus, a large number of models has already been proposed for sorption isotherms with sigmoid shape, many of them being empirical approaches. Excluding the empirical models in order to predict sorption isotherms, two theoretical models describing the typically s-shaped sorption isotherm can be found in literature. One model, the BET-model, considers sorption to be a surface phenomenon [44], whereas the other model considers sorption to be a solution phenomenon [58]. A drawback of the BET-model and its newer modification into the Dent model is the inconsistency with the thermodynamic aspects of sorption [29]. The second approach, attributable to the Hailwood and Horrobin model, considers different grades of hydrated wood, dry wood and dissolved water as an ideal solution [58]. This model thus fits best to experimentally obtained data, as evaluated by Simpson [38]. Nonetheless, this model does not accurately describe the thermodynamics behind sorption as it does not consider heat of sorption and other accompanying quantities typically occurring during a thermodynamic state change. Even though some empirical models adequately fit experimentally obtained data, all sorption models proposed for wood in literature obviously show several flaws related to the actual thermodynamics behind the sorption process. Until now, there are too many assumptions necessary in order to model and predict the sorption behavior of wood. In most cases these assumptions are questionable, since significant parts of the complex process of attaining equilibrium moisture state are not considered [29]. As Engelund has argued in his critical review concerning the physics behind wood-water interactions: the sensitivity of a seemingly simple test, which concerns the measurement techniques to quantify the mass difference of wood specimen at two different equilibrium moisture states has been and still is apparently underestimated.

Chapter 2.4: Water transport in wood

The previously discussed studies of wood-water interaction unfortunately do not reveal anything about the actual water distribution inside a cell wall. Water transport through the cell wall is a complex mass transfer including coupled processes of water in different phases,

and in many aspects it is still not understood. Thus, the focus will be put on the presence of vapor inside the cell wall only, as this is the most common case when moisture transport through wood is observed. This assumption is valid as long as the wood specimen being observed are not in direct contact with water, and therefore true for the whole sorption range up to at least 90% RH. For this most common case, water transport theoretically is governed by the initial diffusion of vapor in the porous system, adsorption of water on the inner available surface, and diffusion of adsorbed/bound water through the wood cell wall [59]. Each diffusion step can be mathematically described by a Fickian equation, thus having a different diffusion coefficient when vapor diffuses through the porous structure or when bound water diffuses inside the cell wall [60]. The diffusion of vapor through the cell wall is further controlled by the chemical properties and by structural resistance of the material [61]. The adsorption step between vapor and bound water diffusion influences the water transport trough the cell wall in several aspects: Energy set free during adsorption increases the interface temperature based on the positive sorption enthalpy of the system. This leads to an increased activity of bound water and thus decreases the driving force of adsorption. The driving force could be explained as the gradient in water activity between water vapor and interface bound water [29]. The increased water activity at the interface further increases the transport of bound water into the cell wall, which is driven by the bound-water concentration-gradient between different regions of the cell wall. Hence, even small temperature fluctuations as occurring during sorption drastically influence the moisture transport. In addition, the observation of bound water diffusion is experimentally difficult, as diffusion of molecularly adsorbed water is several times slower than the diffusion of vapor through the porous cell wall. For that reason, the transport of bound water is of little significance at least in larger wood specimen [62].

However, diffusion characteristics are obtained by measuring the water vapor permeability through thin films. Thereby obtained diffusion coefficients were reported to be in the range of 10^{-12} m^2/s for thin hemicellulose films and uncoated cellophane films [63]. It is expected that the diffusion coefficient for bound water in the wood cell wall is in a similar range. Furthermore, permeability measurements have revealed that the diffusion coefficient increases exponentially with increasing moisture content [64]. Accordingly, an equilibrated moisture state should be achieved faster the higher the initial moisture content is, although contradictive results have been reported [65]. The experimental observations of Christensen

have shown that the time to reach equilibrium increases with increasing initial moisture content. In agreement, the sorption rate was shown to decrease with the initial moisture content for hemicellulose thin films. These observations consequently indicate that water transport is not controlled by diffusion and that another mechanism is responsible for the obviously increasing sorption capacity of wood polymers at higher moisture levels.

Chapter 2.5: Relaxation as driving force of sorption

Since the early 1950s authors have been suggesting that polymer relaxation might largely influence the speed of sorption. In material science relaxation can be obtained from the stress response of polymers to strain, which is decreasing as the polymers relax. Thereby polymer chains deform as a function of time which leads to structural changes at the molecular level. Stress relaxation in wood was described by shearing of constitutive polymers in material direction [66–68]. As stress relaxation progresses, the sorption capacity of the cell wall increases, as predicted by several authors [29]. This might be explained by the total free volume increase induced by relaxation. As a consequence thereof, the cell wall's sorption capacity increases, which is even more pronounced, once the amorphous polymers soften, figure 8. During the incorporation of water, constitutive polymers are forced apart, a process which could further induce a slippage of polymers between the microfibrils [68]. This includes the breaking and re-bonding of hydrogen bonds, a process strongly dependent on time and the applied stress.

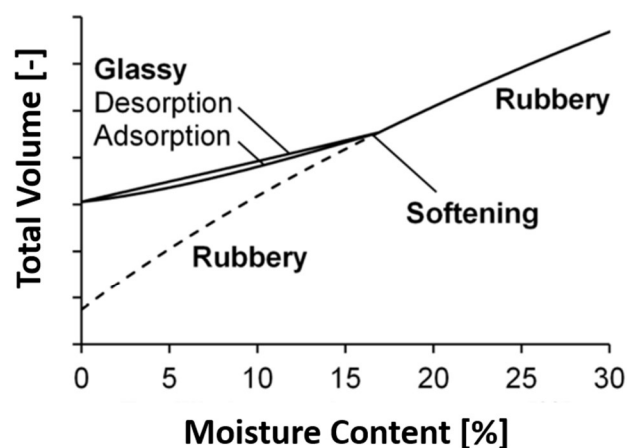**Fig. 8** Relationship between free volume change and the moisture content in amorphous polymers. As the moisture content increases the free volume increases which is highly pronounced above the glass transition [4,52].

The hierarchically structured wood cell-wall might further produce stress concentrations and induce stress gradients based on the restraining effect of the cellulose fibrils on the swelling

amorphous polymers. Thus, this effect would additionally insert a significant amount of stress relaxation, which influences moisture transport and sorption capacity to a large extent. Consequently, the sorption rate should be related to the speed of relaxation, which was first addressed by Crank et al. Crank suggested non-Fickian sorption behavior in polymers due to relaxation of adsorption (moisture)-induced shear stresses [69]. In order to model creep in wood Engelund et al. have already used an expression for time dependent swelling as a function of the swelling pressure [70], thereby considering stress relaxation. The glass transition significantly influences stress relaxation and consequently the equilibrium moisture state. Softening further increases the polymers' flexibility in order to adjust structural changes on the molecular level and to accommodate the volume change induced by sorption [4,51]. Above 75°C, after hemicellulose has entered the rubbery state, sorption hysteresis therefore disappear, as suggested by some researchers [52,71]. Vrentas further related the theory of free volume to the sorption hysteresis in order to explain the increased sorption behavior of wood specimen after drying and remoisturizing. When amorphous polymers enter their glassy state during desorption, an amount of free volume could be temporarily locked in a new thermodynamic state, which is re-accessible once the polymers are remoisturized. Therefore, the equilibrium moisture content during adsorption of amorphous polymers increases with each sorption step and is further significantly influenced by their moisture history [51]. However, in order to model the diffusion kinetics of water through the cell wall, most of the authors historically used a classical Fick diffusion model [72]. Although, the results often differ from the experimental observations. From a mathematical standpoint Hill et al. have shown that the sorption kinetics can be modeled as the sum of two exponential decays; a fast and a slow sorption process [73]. This model is known as the parallel exponential kinetic (PEK) model, and thus correlates well with the obtained data from sorption experiments.

To sum up, water transport in nature-based materials are complex phenomena, and comprehensive understanding is still missing. The urgent need of simulating and modeling the long-term deformation behavior of wood-based materials under the influence of moisture have led to several approaches to mathematically describe the phenomena. A single mathematical law to describe and predict sorption still does not exist. Theoretically, all water is directly or indirectly bound to the constitutive polymers. Possible sorption sites are mainly hydroxyl groups covalently bound to the constitutive polymers. The largest number of hydroxyl groups are found in hemicellulose. Cellulose agglomerates to form fibrils and only

the surface hydroxyl-groups are accessible to water. In consistence with the measured sorption enthalpy, one to two water molecules can bind to a single hydroxyl-group. Wood changes its sorption capacity with each drying step. Thereby the fiber-saturation point increases, leading to the typically derived sorption hysteresis of wood. The phenomenon still is not fully understood, but undeniable, the behavior of wood largely depends on its sorption history. In order to explain the hysteresis effect, the theory of the free volume of amorphous polymers was developed. The theory is based on the softening and hardening of amorphous polymers, processes strongly influenced by moisture. Several researchers have described the adsorption of water inside the cell wall by a two-stage process. The first stage of water adsorption obviously could be mathematically described by means of the Fickian law, whereas the second stage proceeds quicker and becomes increasingly pronounced as the concentration of bound water increases [74,75]. The second stage of adsorption is highly pronounced above 40-50% RH, where stress relaxation proceeds faster as hemicellulose enters the rubbery state. Water distribution through constitutive polymers was therefore suggested to be influenced by stress relaxation due to the swelling pressure and by phase changes with respect to the present moisture content. Meanwhile, researchers have realized that the sorption process is rather governed by the swelling process and induced stress relaxation than by Fickian diffusion kinetics. Stress relaxation becomes increasingly important when wood materials are stressed in the moisturized state, as the mobility on the molecular level is enhanced. Understanding and predicting the mechanical behavior of wood-based materials under the influence of moisture is one of the main goals of wood-researchers all over the world.

Chapter 3: The mechanical behavior of wood

On the macroscopic level, the fibers' ability to withstand mechanical stress is generally governed by the orientation of the constitutive polymers and their interaction with each other. As stress is applied, the fiber deforms (on the macro-level) and polymers relax (deformation on the molecular level) in dependence of their initial orientation. Upon external loading stress migration proceeds from the pliant matrix polymers to the stiff cellulose and vice versa [22]. Matrix polymers are highly flexible polymers and crucial in order to transmit and distribute the stress along the fibrils. The specific bonding pattern at the interface between fibrils and matrix, which is mainly governed by strong hydrogen bonds, therefore plays an essential role. The non-covalent bonding pattern yields a flexible and strong composite structure being able to withstand stress [22]. The stress response on the molecular level differs, between the aggregated cellulose and the amorphous matrix polymers. The load is carried by both, covalent and hydrogen bonds in the case of cellulose, which has been observed by applying infrared and Raman spectroscopy [19]. Micromechanical in situ tests combined with nano-structural observation are commonly used to observe and study the deformation behavior on the molecular scale and to identify the load bearing unit. In these experiments the fibers are strained by applying an external load and the applied stress is detected. The initial stress response, defined by the linearly increasing stress with the applied low strain-rate, is referred to as elastic modulus. The elastic modulus describes the fibers ability to elastically and reversibly deform under an applied strain. The elastic deformation is mainly governed by the long cellulose chains agglomerated to fibrils, which deform through changes in cellulose fibril orientation and stretching of the C-O-C bridge between two glucose molecules in a cellulose fibril [19,22]. In contrast to cellulose, the covalent bonds of hemicellulose and lignin do not seem to respond upon loading [76]. Modeling studies have confirmed these observations, showing that the covalent bonds of amorphous cellulose under small loads are not affected. However, lengthening of hydrogen bonds has also been reported [77]. Similar results were achieved by other modeling studies, which have shown that secondary chemical bonds, such as hydrogen bonds and van der Waals interactions are the physical bonds primarily affected by the externally applied load [78,79]. Accordingly, it is assumed that the mechanical properties of the matrix polymers, hemicellulose and lignin are entirely dominated by hydrogen bonding. The stiffness of the fiber therefore is governed by the covalent bonds

of the cellulose fibrils, which are known to be the load bearing unit of the whole cell wall. The inclination of the fibrils further plays a key-role to either store or release the applied stress [4].

Studies on individual single fibers [80–82] and on tissues [83] have revealed that a relation between the MFA and the fibers' elastic modulus exists. Fibers which initially had a high MFA usually show a decreased elastic modulus in comparison to those fibers which initially had a low MFA, figure 9.
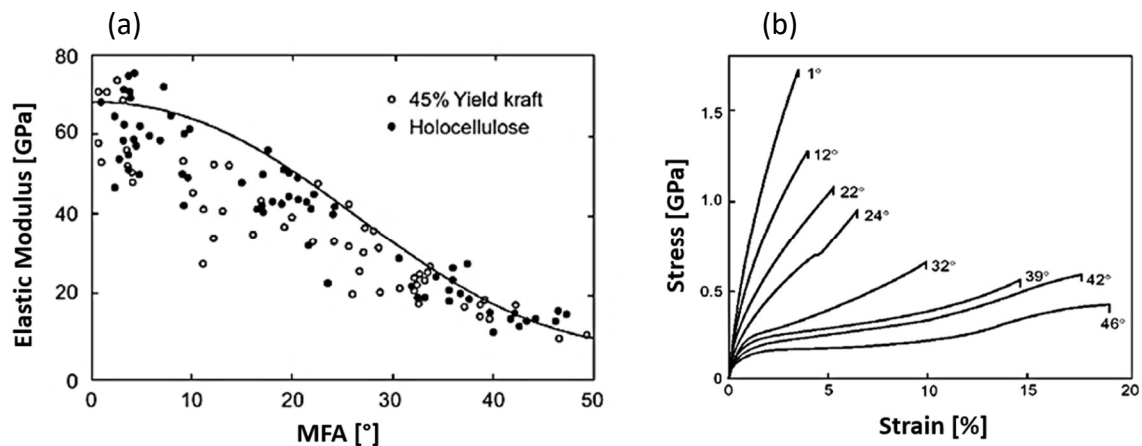
Fig. 9 (a) Relationship between elastic modulus and fibril inclination within the S2 layer [179]. (b) Stress-strain curve of individual softwood fibers in dependence of their MFA [180].

A much higher resolution can be achieved by applying X-ray diffraction techniques, in order to detect and observe the reorientation of the fibrils under an applied load. Thereby the distance between the crystal lattice of the cellulose-fibrils is monitored by X-ray diffraction techniques [68,84,85]. By following the lattice spacing, d_{200} and d_{004} of the crystalline cellulose within the cell wall under an applied stress one can follow the mechanical stress response of the fibrils in-situ. Studying the deformation of the crystal-lattice enables the calculation of the Poisson's ratio, which describes the ratio of relative contraction to relative expansion of the fibrils [84]. Pronounced changes of the initial fibril orientation were observed for wet wood tissues with high initial MFA by Keckes et al. The results suggest a relationship between the applied strain-rate and the observed decrease of the MFA, indicating that the cellulose fibrils are continuously shifted towards the cell axis. Keckes et al. also reported a slight increase of the MFA, which spontaneously occurred after rupture. This observation was referred to the partly elastic characteristic of the fibrils [68]. Thus, when the applied stress exceeds a certain stress-level, the MFA decreases with the applied strain. It is believed that trees utilize this functional relationship to re-orientate the fibrils in order to achieve optimum mechanical

resistance against stress. Thereby they can naturally adjust their MFA to the site of stress application and are better prepared to react towards growth-stresses such as bending- and stretching- stresses. Young trees are known to have more cells with a high MFA, which are less stiff but highly flexible in order to resist different wind-loads [83]. During wood ageing the MFA changes and matured wood fibers exhibit a significantly lower MFA. Another typical characteristic of a wood fiber with high MFA upon loading is their tendency to plastically deform to a large extent. In contrast, fibers with low MFA show only small deformation before rupture [22,80,86], figure 10.
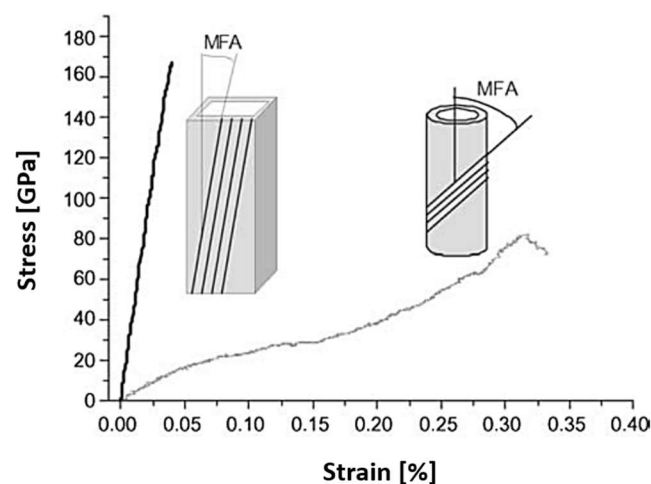
Fig. 10 Stress-strain curves of two individual wood fibers with high and low MFA, respectively. In contrast to fibers with low MFA (black line), fibers with high MFA (grey line) show a broad region of plastic deformation [22].

The underlying mechanism has been discussed several times in literature, and it is generally accepted that a decrease of the MFA occurs [22]. This theory is only applicable for fibers with initially high MFA. For fibers with low MFA, the decrease of such upon external loading has not yet been observed. However, the mechanical properties of wood are substantially influenced by moisture. Several experiments have shown that the initial fiber stiffness decreases with the moisture content. This influence of moisture is attributable to the formation of hydrogen bonds. In the absence of water, constitutive polymers use their hydroxyl groups to form hydrogen bonds with each other. When water enters the cell wall, single water molecules force the constitutive polymers apart, leading to the breakage of the existing hydrogen bonds [29]. Upon adsorption, hydrogen bonds between constitutive polymers are replaced by water. Thereby single water molecules occupy space between constitutive polymers and the fiber cell wall starts to swell, figure 11.
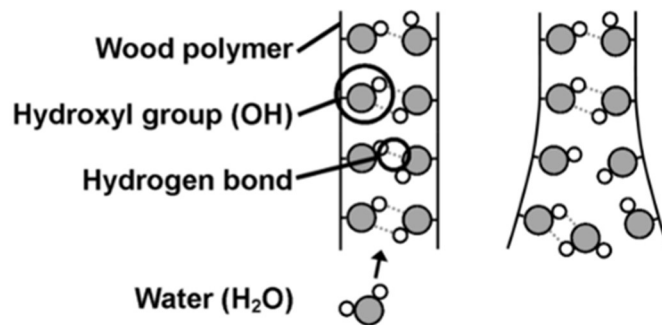
Fig. 11 Schematic illustration of swelling in wood and the effect of a water molecule on the spacing between constitutive polymers (hydroxyl-group interactions are illustrated by dotted lines) [4].

Consequently, the breaking of the hydrogen bonds by water molecules weakens the cell structure. Several studies addressing the mechanical properties of wood under the influence of moisture have shown that elastic modulus and stiffness decrease with the moisture content [22]. This effect is originally described by the theory of hydrogen bond dominated solid materials [87]. However, the wood cell wall does not only elastically respond to external loadings. A significant portion of the fibers' deformation is non-elastic. Depending on the duration of the mechanical excitation, wood fibers plastically deform. The time-dependent non-elastic response has been described by the sliding of polymers between microfibrils [54,66]. This process is governed by the breaking and reforming of hydrogen bonds between constitutive polymers, as they continuously slide past each other. When water enters the cell wall, this slippage is further facilitated as the constitutive polymers are forced apart. Water therefore is commonly known as a plasticizing agent. The sliding of constitutive polymers past each other is documented by molecular modeling and mainly responsible for the time-dependent mechanical properties [88]. Notably, this time-dependent sliding of amorphous polymers was observed for different polymeric fibers [89]. Eyring and co-workers have developed a model describing the deformation kinetics beyond the sliding of polymers [90,91]. In their theory, the sliding of polymers is described as an activated process, where polymers must pass a certain energy barrier in order to attain a new configuration. When no external load is applied, the potential energy of the molecules equals the thermally induced molecular motion. The highest energy level is known as the activation energy, figure 12. A certain percentage of the polymers' potential energy will have a potential energy equal to the activation energy, and hence, can move freely [92].
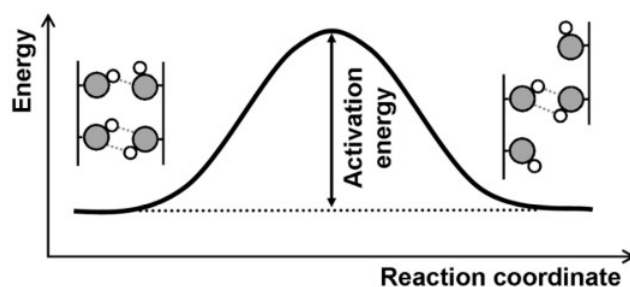
Fig. 12 Energy barrier (activation energy) of moving polymer segments between the energy ground level and the energy level after successful interlocking in a new position [4].

For any chemical and physical reaction, the lowest energy level is generally favored. Consequently, the favored movement is limited to the lowest energy level which yields an intermediate state with lowest free energy. Although the process is defined by the breaking and re-forming of hydrogen bonds, the actual process might be a more continuous one [4]. Jeffery and Saenger therefore suggested that an intermediate state with a three -center bond dominates the deformation kinetics. In their work a three-center bond is described by a single hydroxyl group simultaneously interfering with two further hydroxyl groups of the constitutive polymers [93]. The energy of such an intermediate state is lower than that of an intermediate state with completely broken hydroxyl groups (unbonded state), figure 13. The same is possibly true for the sliding of wood polymers past each other.
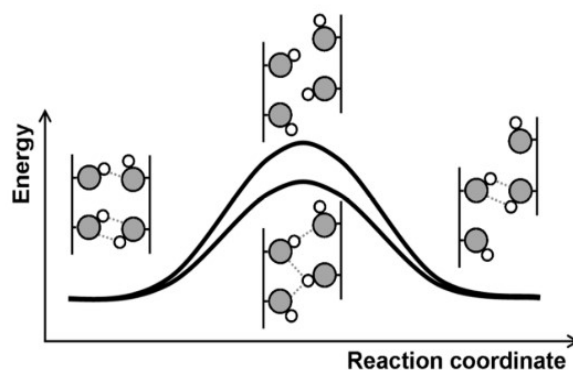
Fig. 13 Activation energy of two different intermediate states: a non-bond intermediate state (upper activation energy level) and a three-center hydrogen-bond intermediate state (lower activation energy level) [4].

If no external load is applied the probability of mobile units moving both forward and backwards is equal. Consequently, the overall movement of the polymers appears to be zero, and the polymers are in "rest". If an external load is applied, the energy needed to pass the energy barrier of the activated state is enhanced, figure 14.
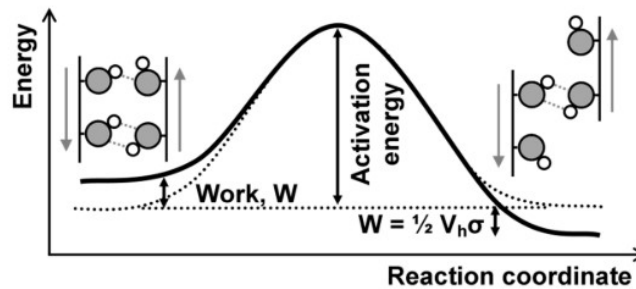
Fig. 14 Change of the energy barrier during stress application [4].

Thereby, the sliding along the direction of the applied force is favored over that in the opposite direction. The deformation rate can be further described by the mechanical work and the contribution of the movement of a polymer-segment. The induced mechanical work increases the initial energy ground-level and further lowers the energy level on the opposite side of the energy barrier [94,95]. For cellulosic materials the moving segment has been estimated to be 0,68 nm^3 [94]. The volume is similar to that of the cellulose unit cell, which was experimentally determined to be around 0,65 nm^3 at room temperature [96].

However, besides the understanding of the decrease of the MFA of fibers and tissues with initial high MFA, the influence of moisture on the long-term deformation behavior is less understood. This is based on the unpredictable contribution of polymer relaxation when the moisture content increases. In addition, all mechanical tests performed under the influence of moisture show a coupling effect between the stress relaxation due to externally applied loads and the stress relaxation induced by moisture. Until now, it has not been possible to separate these two effects in order to study either the stress response from the externally applied load or the stress response due to moisture adsorption. Besides the essential role of the MFA, the influence of moisture to the stress response becomes highly dominating when the available moisture content (MC) increases [31]. Thereby stress-relaxation increases and might even affect the decrease of the MFA. As stress-relaxation on the molecular-level increases, shear-forces towards the fibrils increase which, after exceeding a critical shear-stress, might even result in gliding or slipping of the cellulose fibrils. Exceeding the critical shear-stress implies that the matrix adapts a highly viscous state in order to transfer sufficient shear-stress onto the fibrils [68]. This state might even imply reaching the Tg and is highly correlated with the present MC in the cell wall. Adding to the complexity of the fibrils' ability

to move within the matrix, the possible transition of the matrix from rather glassy to rubbery does not facilitate the prediction of the long-term deformation behavior of wood-fibers. However, it is not sufficient to translate the global deformation-pattern to a single observed mechanism. The MFA clearly plays a fundamental role predicting the mechanical performance of single wood fibers. Additionally, the impact of the matrix, more precisely the interface between the matrix and the fibrils, becomes increasingly important in order to understand the deformation pattern of wood.

Chapter 4: Creep in wood fibers and tissues

Cellulose-based fibers exhibit viscoelastic material properties when exposed to an externally applied load. Viscoelasticity is a term describing a material characteristic that combines both, elastic and flow-like behavior, related to either solid or viscous material properties. The time-dependent deformation could be described by the tendency of the solid material to creep or flow under the influence of a persistent mechanical stress, previously discussed as the sliding of amorphous polymers. Thereby, creep could increase during long-term exposure to high levels of stress that are still below the yield strength of the material. Theoretically, creep experiments allow to distinguish between the initially occurring elastic material response and the time-dependent viscous response after a mechanical load has been applied. The creep compliance usually is separated into three components; primary, secondary and tertiary creep, figure 15. The primary creep describes the initially rather elastic material property, whereas the secondary creep describes the time-dependent creep component. The secondary creep is responsible for the occurrence of permanent material deformation, also referred to as permanent set. The rate of deformation is a function of a material's initial properties, exposure time and the applied stress. Depending on the magnitude of the applied stress and duration, material deformation largely increases and may lead to accelerated creep, normally indicating material failure. Accelerated creep is described by the tertiary creep component.
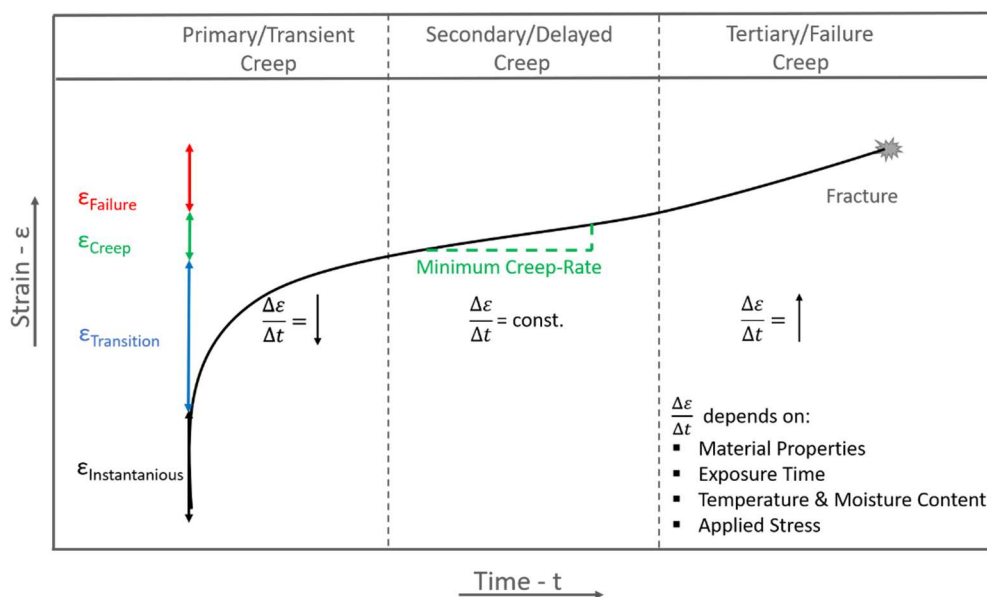

Fig. 15 Schematic illustration of a creep experiment and its evaluation.

Primary creep represents the time-dependent, recoverable creep component which is thought to be due to configurational changes of the molecular structure induced by the mechanically applied load. The molecular structure of amorphous polymers is rather randomly aligned and void spaces, known as the free volume, are present in the solid configuration. Accordingly, the packaging of the polymers is less than optimum, enabling the polymers to move in a new position when they are subjected to an external stress. Molecular movement, also known as relaxation, therefore can occur when void spaces are available for polymers to be occupied [97]. In addition, sufficient energy has to be inserted to the system in order to overcome the attraction forces between constitutive polymers, defining the initial molecular configuration. In pulp fibers such a movement requires the breaking of secondary bonds which are able to re-bond in a new position, e.g. in void spaces. However, after the externally applied stress has been removed, the release of the inserted stress, also known as elastically stored energy, forces the polymers to return to their normal, rather randomly aligned molecular configuration. Thus, primary creep describes a reversible phenomenon. Unlike primary creep, the secondary creep describes the time-dependent non-recoverable component of the creep.

The amorphous matrix of pulp fibers is reinforced by crystalline regions, and both differently respond to the applied stress. As fibrils have far stiffer mechanical properties than the amorphous matrix, their response to an applied tensile stress is expected to be fully elastic. The co-existing crystalline- and amorphous-regions exhibit a large number of interfaces, which are only governed by weak secondary bonds. These secondary bonds are predetermined to break during stress exposure and may or may not re-bond in a new position. Depending on the amount and stability of the newly formed bonds between constitutive polymers, a material may change irreversibly its mechanical behavior, making the theoretical treatment of creep in hierarchically structured materials difficult. As creep is a time-dependent phenomenon, a material could return to its initial mechanical properties during a long period of time, after the stress has been released. A distinctive boundary between primary and secondary creep, in order to distinguish between reversible and non-reversible mechanisms, therefore is difficult. Thus, a portion of primary creep may not be recoverable at the experimental conditions but might be restored at evaluated temperatures or in the swollen state. Accordingly, the experimental conditions largely influence the reversibility of the material mechanical properties.

However, if a viscoelastic material is stressed configurational changes occur, leading the material to deform and under some circumstances, the material irreversibly changes its mechanical properties. The formation of new secondary bonds can therefore lead to an irreversible creep after removal of the applied stress, if the stored energy of the system is insufficient to break the newly formed bonds [3]. The breaking and formation of secondary bonds and accompanied molecular configuration changes are thermodynamic processes. The time required to attain a thermodynamic equilibrated state is one of the factors largely influencing the resulted mechanical properties and the creep. If a metastable equilibrium state is reached, permanent deformation will occur. Permanent deformations thereby are caused by (1) viscous flow, (2) irreversible crystallization and (3) molecular chain rupture. The term viscous flow is used to explain the stress response and as a consequence thereof, permanent deformation in amorphous polymers when these polymers enter the glassy state. In crystalline materials the flow or relative movement of entire molecules is prohibited by the firmly formed network. Fibrils establish much stronger secondary bonds than amorphous polymers and far more energy is necessary to induce a phase change enabling them to melt. True viscous flow, therefore, is limited to amorphous polymers. In contrast to that, irreversible crystallization is limited to cellulose. Induced crystallization requires a huge amount of energy, as the growth of crystals demands a very high secondary bond density at the fibril surface. Some researchers argue that shear forces at the interface between fibrils and amorphous matrix might become sufficiently high in order to induce crystallization of the para-crystalline cellulose located at the fibrils surface. But the evidence for this phenomenon is indirect and inconclusive.

A typical phenomenon observed during creep experiments often wrongly referred to as "increased crystallinity" is strain hardening. Although strain hardening is a phenomenon simply described by a final configuration exhibiting a higher ordered configuration than the initial one. Only amorphous regions are considered to contribute to strain hardening. This could be explained as the amorphous, previously entangled polymers, tend to realign towards the applied stress. After the stress has been released a highly oriented structure could be achieved, yielding a different mechanical performance. Thus, strain hardening should not be mistaken for real crystallization, which could only occur at the surface of the fibrils. A final important response mechanism during creep is the rupture of primary valence bonds. Thereby

premature material failure is induced, which is described by an accelerated strain towards the end of the experiment.

Chapter 4.1: Accelerated or mechano-sorptive creep in wood

For hydrophilic polymers, such as present in pulp fibers, water adsorption additionally stresses the material, often causing increased creep behavior. This accelerated creep should not be mistaken for induced material failure and the breakage of primary valence bonds, as described by the proper meaning of accelerated, tertiary creep. Another, more meaningful expression therefore is mechano-sorptive creep (MSC), which describes the coupling between an externally applied stress and stresses induced due to the sorption process. Surprisingly, materials such as paper deform much more during moisture cycling than in their most compliant state when exposed to a mechanically applied load, even in the humid state [98]. The proclivity of materials to perform MSC has unfortunate practical ramifications, as they fail much sooner when stored in an inconstant environment. Obviously, it is necessary to understand the causes of accelerated creep to profit from this phenomenon rather than to suffer from its consequences.

Accelerated creep was first reported to occur in wood-based products in the early 1960s by the pioneers Armstrong and Kingston [99]. They have shown that cellulose-based materials under load exhibit an extra compliance when alternatingly exposed to adsorption and desorption processes. Contemporaneously, a similar observation was made on concrete, first triggering the discussion of the mechanism behind such a phenomenon. It took ten more years to initially demonstrate the occurrence of accelerated creep in paper-based products [98]. Afterwards, many researchers have contributed to the verification and the extent of accelerated creep in paper-based products [100–103]. However, after nearly fifty years of trying to understand and predict MSC, still no generally accepted mechanism explaining MSC exists.

In the early 1960s, accelerated creep was described to be an unknown consequence of stress coupling between the moisture transport and the mechanically applied load. Accelerated creep established a status of a totally new phenomenon requiring its own unique explanation [104]. In various ways, moisture diffusion was directly related to the decrease of the mechanical compliance. This was explained by the moisture transport, causing additionally existing bonds between constitutive polymers to brake, leading to an extra portion of creep. In 1972, Amstrong was the first who studied creep on individual pulp fibers, namely hollow

wood cylinders [99,105]. In his work he was unable to demonstrate accelerated creep on single fibers. He argued that accelerated creep is a consequence of an uneven stress distribution, and as such does not occur on the single fiber-level when it is exposed to a constant moisture gradient, e.g. a constant moisture gradient from the inside to the outside of a hollow cylinder. Based on his results he claims that a link between moisture transport and compliance exists.

Led by Ranta Maunus in 1975, the next generation of researchers directly related accelerated creep to the changing moisture content [106]. They claimed that accelerated creep is a function of the time-rate of the changing moisture content [107,108]. Hence, the creep is related to the moisture increase, whether the material is instantaneously exposed to a changed environmental humidity or whether the humidity was increased by a defined rate. In 1980, Salmèn et al. have revealed the moisture induced glass transition of amorphous cellulose at room temperature and 11 to 13wt% present moisture [109]. 10 years later, these results were further used to define a completely new interpretation of accelerated creep by Padanyi in the early 1990s.

Padanyi et al. have done some provocative and pioneering thinking regarding the influence of the moisture history on the mechanical compliance of paper. He made a connection between accelerated creep and physical aging, a phenomenon observed in the field of polymer rheology. Back then, physical aging was observed when an amorphous polymer was cooled from above to below its glass transition temperature. The consequence was a reduction of the specific volume or enthalpy, and an apparent shift of the creep response to longer times. In its proper meaning, physical aging of polymers was referred to the progression of polymers in order to attain a thermodynamic equilibrium after it had been exposed to a temperature below its glass transition. Above its glass transition temperature, an amorphous polymer in its glassy state shows a high entropy, accompanied by considerable free volume and by appreciable polymer backbone mobility. Such a condition is characterized by a high material compliance. The transition from one physical state to another cannot be achieved immediately and needs time to progress. When the temperature falls below the glass transition temperature a part of the previously available free volume could be preserved, leading to an increased free volume once the polymer again passes its glass transition temperature. Thus, a thermodynamic phase change requires polymer backbone motion, which requires available free volume. The increased polymer mobility at evaluated

temperatures allows the rapid progression of the phase change. In contrast to this, decreasing the temperature leads to the solidification of the polymers with considerably less backbone mobility. Thereby the polymer continually loses some of its compliance. The rate of attaining a new equilibrated state greatly depends on the availability of free volume, which is steadily decreasing. Hence transition processes are self-retarding processes, as the free volume is gradually occupied by the polymers passing their glass transition. The phase change from a rubbery to a glassy state with the accompanied loss of compliance is called physical aging. It differs from chemical aging, as its original compliance could be restored by exposing the material again to temperatures above its glass transition. Padanyi's provocative thinking was based on the argument that moisture adsorption additionally impacts the available free volume. He concludes that aging could be triggered by moisture changes as well as by temperature changes, as previously seen in paper. The results reported by Salmèn et al. were further argued to be a consequence of the increased free volume, achieved as the material was quickly passing from a high to a low moisture content. Thereby, the material very slowly approaches a new thermodynamic equilibrium with increased free volume. Thus, the material after desorption would be more compliant than it was initially and ages during the process of slowly approaching a new thermodynamic equilibrium. To prove evidence, Padanyi performed standard aging creep tests after dropping the moisture content instead of the temperature and the experimental results were remarkably similar to standard aging curves. Therewith, accelerated creep was proposed to be a manifestation of sorption-induced physical aging [110].

Since then, several materials have shown to exhibit larger creep compliances under moisture cycling conditions than under humid but stable conditions. Accelerated creep has been reported in wood [99], concrete [111], paper [98], polyurethane foams [112] and Kevlar-composites [56]. Still, some approaches have been made, trying to link the phenomenon to a paper specific, fiber-level mechanism. Sorenmark and Feller, for instance, presented a "physico-mechanical" model that employs moisture induced stress re-distribution inducing extra dislocations, whereas Haslach proposed a long explanation including anisotropic swelling and the motion at the interface between individual fibers [6,101]. In addition, specific cell wall mechanisms were sometimes proposed to be responsible for the putative sorption rate dependence of creep. To verify whether accelerated creep in paper is based on individual fiber properties or whether it originates from the fiber-network, it was necessary to test single pulp fibers rather than paper. However, individual fibers were small, fragile and therefore unable to be observed in

common testing devices. Individual fiber experiments, therefore, started in the late 1990s accompanied with the development of self-made tensile testers. Since then, creep experiments further prove the occurrence of accelerated creep in several polymeric fibers. Besides Kevlar, accelerated creep was reported to occur in regenerated cellulose fibers, and to a small extent, in nylon fibers [110]. Nature-based fibers such as pulp, however, have a far more complex structure than single component polymeric fibers. Pulp fibers are composites and characterized by a sophisticated hierarchical structure designed by nature. Sedlacheck first performed creep experiments on individual pulp fibers and unfortunately was unable to show accelerated creep [3]. Whether accelerated creep occurs in pulp fibers obviously is dependent on the experimental conditions. Haberger and Coffin argued that the moisture-rate increase and the sorption time of the material are crucial parameters in order to observe accelerated creep [110]. In Sedlacheck's experiments, the moisture-rate increase was at least as large as the sorption time (pulp fibers adsorb moisture rapidly and the rate of moisture increase to sorption time was estimated to be 15:1 seconds), and the cycle time was much larger than the sorption time. According to Haberger et al., accelerated creep also demands long sorption times and rapid changes in the ambient humidity in order to occur, as based on the theory of moisture induced stress-gradients. Sedlacheck's creep experiments with pulp fibers therefore were argued to be on the verge of showing accelerated creep. Recently in 2014, Salmén et al. were able to prove the occurrence of accelerated creep in pulp fibers, which led to the acceptance that accelerated creep in paper is rather a phenomenon based on individual fiber properties than on the fiber network formation [7,8]. For nature-based fibers accelerated creep was reported to occur in ramie and in wood fibers [110]. Still physical aging and moisture induced stress gradients are largely discussed to be responsible for accelerated creep. But all above mentioned hypotheses are plausible and each mechanism may contribute to the mechano-sorptive creep to some extent. Making this topic even more complex, recently accelerated creep was observed in nanocellulose thin films and aerogels. Nanocellulose thin films consist of mainly crystalline regions and the film thickness of a few μm does not allow the development of large moisture induced stress-gradients. The results provided by Lindström et al., however, revealed that accelerated creep occurs to a similar extent in both, thin films and aerogels [113,114]. This is surprising as aerogels have a far higher porosity than nano-cellulose thin films. These results further suggest that none of the aforementioned mechanisms alone is responsible for the observation of accelerated creep. The effect of

physical aging and accompanied induced glass transitions should be much more pronounced in aerogels than in highly crystalline cellulose thin films. In addition, the through-thickness stress gradient plausibly established during humidity changes is diminishingly small in thin films. Therefore, none of the aforementioned theories has become generally accepted as the primary mechanism for mechano-sorptive creep and once again accelerated creep or mechano-sorptive creep has the attention of the researchers all over the world.

Chapter 5: Method and experimental design

The mechanical performance of paper in terms of tensile strength and elastic modulus is known to be highly affected by the moisture content of the fiber network [109,115]. Paper is a viscoelastic material which exhibits a distinctive creep behavior [116–121]. The pulp fibers forming the network in paper-based materials are also known to show viscoelastic response. Quantification of the creep-rate of pulp fibers therefore is of high importance to be able to predict long-term creep behavior of paper. Recently, the creep behavior of individual pulp fibers has been studied by Salmén et al.[7,8] Also for other plant fibers the creep behavior has been evaluated [122–129]. As pulp fibers are derived from wood, their creep deformation is related to the one of wood, which has been researched extensively [5,8,66,130–138]. The creep in pulp fibers results from a combination of differently induced stresses such as mechanical stress combined with temperature and moisture gradients. Accordingly, the mechanical properties differ with respect to the ambient environment and the amount of moisture adsorbed by the cell wall. Increase in temperature or moisture content of the fibers increases the creep of the material [139]. Indeed, the creep intensity of paper is enhanced when it is exposed to varying relative humidity, e.g. adsorption and desorption cycles. This coupling between varying moisture content and load-induced creep-deformation is referred to as mechano-sorptive creep or accelerated creep [140]. A widely accepted explanation for accelerated creep has been given by Habeger and Coffin who concluded that accelerated creep was driven by the non-uniform moisture uptake of the individual fiber. Thereby, locally induced stress-gradients during the process of swelling increase the creep intensity [110]. As stress migration on the molecular level, in particular the mechanism of cell-wall creep, has been a topic of research for decades, several proposed mechanisms exist trying to manifest the underlying phenomenon behind creep. But besides significant progress, the creep of wood fibers under moisture influence still is not yet fully understood [133,141,142]. The extraction of reliable data and their comparison aggravates in many cases, due to differences in sample treatment prior to testing, the testing device itself and the coupling effects between varied ambient humidity and the mechanically applied load [122,137]. Mechano-sorptive creep in wood [107,132,133,135,137,141] and in cellulose related fibers [7,8,110,143] has been studied extensively, as it correlates with the long-term creep behavior. To the author's knowledge, no literature is available emphasizing the creep of single fibers exclusively under steady-state moisture influence. The first section of this thesis will therefore examine the influence of relative

humidity (RH) on the sorption-induced creep of pulp fibers at three different moisture levels: 25%, 50% and 80% RH. After knowing the sorption induced creep at constant ambient conditions, pulp-fibers were exposed to a cycling ambient humidity between 50% and 80% RH in order to investigate mechano-sorptive creep. The second part of this thesis treats the creep of dry pulp fibers. The experimental design specifically addresses the following influencing factors, relevant for the creep-behavior of pulp-fibers under moisture influence:

1. Dynamic vapor sorption (DVS) measurements were performed in order to estimate the present moisture content at given relative humidity.

2. The fiber specimen in the present study, monitored under the influence of moisture were exclusively stressed by the applied pre-load of 1mN and the increasing ambient humidity. All experiments were started from a dry fiber-state. Accordingly, the strain-rate in tensile direction of individual pulp-fibers during swelling was obtained. This is in contrast to traditional creep experiments, which require the application of a mechanically applied load before determining the creep-rate. It is well known that polymers under strain can increase their orientation in direction of the applied stress which alters the mechanical properties. In order to separate the effect of the mechanically applied load from the applied stress due to moisture sorption on the deformation behavior of pulp fibers, no further external load was applied before determining the strain-rate at each moisture-level.

3. The creep experiments were performed on the single fiber-level. The stress applied by the pre-load used to keep the fiber in tensile direction was obtained by evaluating the cross-sectional area of each previously tested fiber. The influence of the applied pre-load on the obtained creep rate was further examined. Commonly, the material stress is calculated by direct or indirect measurement of the mean fiber cross-sectional area. It is, however, well known that the true cross-sectional area of pulp fibers differs to a huge extent, according to the site of harvest and the natural variation of the fibers within the trees. In order to know the stress applied on the individual fibers it is therefore necessary to evaluate the actual cross-sectional area of the previously tested fibers.

Chapter 5.1: Fiber preparation

Fiber sample preparation followed the procedure according to Jajcinovic et al [144,145]. A water-suspension containing 0.01wt% of soft-wood pulp was prepared. One droplet of the suspension was placed between two Teflon-foils and subsequently dried in a Rapid-Köthen sheet former for 1 h at 94 ± 2°C. The dried fibers were carefully chosen (fibers with kinks and bends were sorted out) and glued to a custom designed acrylate-based sample holder with solvent free 2-component epoxy resin [144] [145]. After gluing the individual fiber onto the sample holder, the bridges were afterwards molten through, figure 16. After separating the upper from the lower part of the sample holder, the sample holder is only connected by the fiber, figure 16 (a) and (b). As the sample holder is several orders of magnitude stiffer than the mounted fibers the forces and displacements recorded in the dynamic mechanical analyzer (DMA) originated from the fiber in the free span. The tested fibers were named after the source of the wood and chronologically ordered. SP is the abbreviation for spruce, and the following number shows the consecutive sample number. At that point, it is worthwhile to mention, that during the experiment not a single fiber broke before it was demounted from the DMA afterwards. Fiber fraction during demounting from the testing device occurs primarily in the middle of the fiber-length. Nevertheless, some fibers broke at the site of fixation and were further excluded from the evaluation. Tensile experiments involving the use of resins to glue the fiber on sample-holders should be carefully evaluated in order to identify any contribution of the resin to the tensile strain measured from the fiber. Therefore, left fiber samples, which were not further subjected to the microtome addressing those fibers which break on the side of fixation, were additionally examined, employing scanning electron microscopy (SEM). SEM images indicated the influence of the resin. Hereby it was observed that approximately 10% of the fiber-surface might have been covered with resin. Still, epoxy resins are frequently used to apply single fibers to sample holders though it could affect the tensile strain.

Chapter 5.2: Evaluation of true fiber cross-sectional area and true stress

Following the creep measurement, each fiber tested in the DMA was embedded in resin, cut in a microtome and the fiber's cross-sectional area was imaged using light microscopy. The effective fiber cross-section was then analyzed from three different images obtained from the same fiber. The outlines of the fiber cross section, shown in figure 16 (d), were drawn manually and the cross-sectional area was calculated using a MATLAB routine. The effective cross-sectional area was used to calculate the true stress applied for each fiber during measurement. A detailed description of the embedding, cutting and imaging procedure is given in [146].
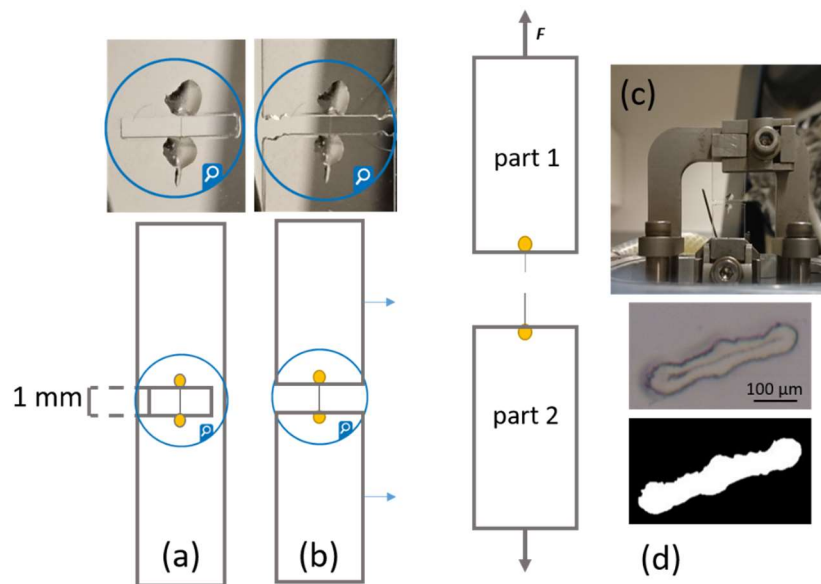

Fig. 16 (a) Sample holder (b) Sample holder with molten bridges (c) sample installation in the DMA testing device (d) Fiber cross-section as obtained from the microtome.

Chapter 5.3: Dynamic vapor sorption (DVS)

DVS measurements were performed using a dynamic vapor sorption instrument (DVS Intrinsic, Surface Measurement Systems, Alperton-London, UK). The sorption kinetics were evaluated at three different moisture levels to obtain an estimated moisture content present in the cell wall at specific ambient humidity under isothermal conditions.
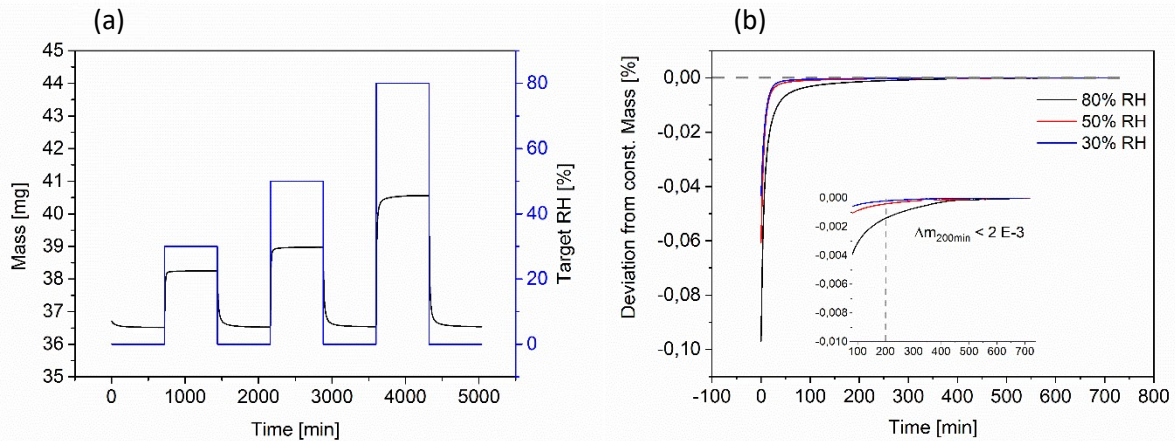
Fig. 17 Evaluation of the equilibration time (a) measurement method (b) equilibration time with respect to the % of moisture content obtained after 210 min.

For the estimation of the MC at each humidity-level, the relative humidity (RH) was cycled between 0% and 30%, 50% or 80 %, and back to 0% RH, figure 17 (a). The resulting changes in sample mass were recorded with the DVS at constant 25°C for 12 hours. The deviation from constant mass after 200 minutes is below 0,002% for pulp at 80% RH (black line in figure 17 (b)) and below 0,0002% for pulp at 30% and 50% RH (red and blue lines in figure 3(b)). The amount of absorbed water is 9,7wt% at 80% RH, 6,9wt% and 4,7wt% at 50% and 30% RH, respectively. It is important to note, that an accurate sorption-kinetic could not be calculated from the DVS-measurement, as depicted. The sorption-kinetics are influenced by the rate of humidity increase, whereas the DVS uses a defined volume of either dry gas (nitrogen) or gas loaded with a defined amount of water. This mixture is further instantaneously supplied to the measurement chamber, as soon as the experiment starts. As pulp fibers are known to adsorb water from the environment very quickly, the sorption rate during the first five minutes of continuous exposure to moisture was obtained. After the first five minutes, the sorption-rate drops below E-3.

Chapter: 5.4 DMA measurements

All experiments were performed using a Dynamic Mechanical Analyzer (DMA, Q800 purchased from TA Instruments), in controlled force mode. The instrument provides control of force, temperature and the ambient humidity. Typical operating ranges of 0–90% RH are possible, whereas at very high or very low adjusted humidity the maximum deviation is defined with ± 1%pt. The driving shaft is decoupled from friction and the displacement is detected by an optical encoder showing a resolution of 1 mN. All other results were calculated from the recorded displacement and the applied force, using the following equations:

Strain $[\varepsilon]$ $\qquad\qquad\qquad\qquad\qquad\qquad\qquad\qquad\qquad\qquad \varepsilon = \frac{\Delta l}{l}$

where l is the applied gauche length and Δl is the changing length after load application.

Recovery Strain $[\varepsilon]$ $\qquad\qquad\qquad\qquad\qquad\qquad\qquad\qquad \varepsilon = \varepsilon_c - \varepsilon_r(t)$

where ε_c is the strain during load application (creep strain) and ε_r is the strain after load release (recovery strain).

Stress $[\sigma]$ $\qquad\qquad\qquad\qquad\qquad\qquad\qquad\qquad\qquad\qquad\qquad \sigma = \frac{F}{A}$

where F is the applied force and A is the true cross-sectional area.

Strain Rate $[\dot{\varepsilon}]$ $\qquad\qquad\qquad\qquad\qquad\qquad\qquad\qquad\qquad\qquad \dot{\varepsilon} = \frac{\Delta \varepsilon}{\Delta t}$

where $\Delta \varepsilon$ is the changing strain during the time interval Δt.

Creep Compliance $[J]$ $\qquad\qquad\qquad\qquad\qquad\qquad\qquad\qquad J = \frac{\varepsilon(t)}{\sigma}$

where $\varepsilon(t)$ is the changing strain and σ is the applied stress.

Relaxation Modulus $[G]$ $\qquad\qquad\qquad\qquad\qquad\qquad\qquad G = \frac{1}{J(t)}$

where $J(t)$ is the creep compliance.

The instantaneous and delayed modulus were obtained from the highest and the lowest value of the relaxation modulus during stress exposure.

Chapter 6: Sorption induced creep

The mechanical performance of paper in terms of tensile strength and elastic modulus is known to be highly affected by the moisture content of the fiber network [109,115]. As a viscoelastic material, paper exhibits a distinctive creep behavior and single pulp fibers, which paper consists of, essentially contribute to this long-term creep behavior [116–121]. Mechanical analysis under defined ambient conditions of wood-based materials are very often performed on the sheet level of either paper- or wood-slices. The small length and only a few µm in diameter make fiber handling and application to testing devices difficult. As the time- and moisture-dependent creep of individual pulp fibers is characterized by complex physical and chemical processes, several parameters significantly influence the results of mechanical analysis, such as the true cross-sectional area, applied ambient conditions and the fiber history, e.g. degree of processing and storage conditions. In addition, water accessibility in pulp fibers is highly dependent on their hierarchical structure, composition and porosity. A major problem when it comes to the simulation of the time- and load-dependent deformations of wood-based materials is the moisture content of the individual fibers. An increased moisture content induces a shift of the composites glass-transition (Tg) towards lower temperatures, known to highly influence the mechanical fiber properties. Several authors, therefore, have examined the influence of hemicellulose on the creep behavior of plant-based materials.

Whereas the mechanical properties under continuously increasing loads are fairly well known, little has been reviewed on the topic of moisture-induced creep. The reason behind the lack of knowledge of moisture-induced creep is a phenomenon called mechano-sorptive creep (MSC). During the observation of MSC, specimens are alternatingly exposed to adsorption and desorption processes, while they are stressed by a mechanically applied load. Necessarily, stress-coupling related to both, the moisture uptake and the applied tensile stress, occurs within the material. The phenomenon of MSC was observed in several wood- and paper-based materials, on the individual fiber level, however, results are highly contradictive. In addition, the generalizability of much published research on this issue is problematic because experimental conditions, sample preparations and pretreatment (often not even mentioned) differ to a huge extent from experiment to experiment. Hence, there exists a large variety of approaches to simulate and to describe the mechanism governing viscoelastic properties of

wood-based materials, but no mechanism is known by the author, which entirely captures the mentioned phenomena. It is further doubtful that a single mechanism exists describing MSC of pulp fibers. The present chapter treats the moisture-induced creep.

The lack of knowledge is further aggravated by the rather unknown dry fiber properties, when moisture is absent from the cell wall. Only a few studies, for instance have investigated the creep of a dry pulp fiber. Although, in order to understand the moisture induced creep, the knowledge behind dry fiber creep is inevitably necessary for a deeper understanding. Little has also been reviewed on the topic of defects influencing the mechanical performance of pulp fibers. During wood processing a variety of defects are induced and processing conditions can even dissolve constitutive polymers from the fiber cell wall. In addition, water accessibility to the fiber cell wall is known to significantly increase after processing. Thus, these defects may influence the mechanical performance of pulp fibers to a huge extent. Chapter 7 treats dry fiber creep.

However, most simulations are based on the results generated from wood-fibers separated by hand and the experimental data are rather controversial, as there is no general agreement about the mechanism beyond sorption-induced creep [22]. This clearly indicates the need to generate reliable results for pulp fibers and to further investigate the physical and chemical mechanism beyond the long-term creep behavior of these fibers. Therefore, the major objectives of this study were to investigate an experimental design which enables the use of the results in simulations and the deeper understanding of the interaction between water and pulp fibers.

To date various methods have been developed and introduced to measure the mechanical behavior of pulp fibers. Traditionally, the stress response of pulp fibers has been assessed by continuously increasing the fiber strain. In the simplest way, the fiber behavior during drying can be visualized by measuring the strain of a fixed fiber as the ambient RH decreases. In order to shrink, the fiber has to compensate the constantly applied stress, until a negative strain can be detected. One advantage of such a measurement method is that the fiber drying can be studied in-situ. Therefore, the fibers were previously fixed onto a sample-holder according to the procedure of Hirn et al. and stored at 25°C and 25% RH. The measurement method, as explained, was used here to study 12 individual pulp fibers during 8 hours of drying at 25°C, figure 18. Thereby, the fibers were kept in position by the applied tensile load (=preload) of 1 mN throughout the experiment and the displacement was recorded, figure 18 (a). From each fiber previously tested the cross-sectional area was obtained from microtome slices. A preload of 1 mN corresponds to a stress of about 5±2 MPa, according to a cross-sectional area of about 235±73 μm^2. The evaluation of the resulting strain trajectory during drying was performed by using a logarithmic time-scale. The longitudinal shrinkage of pulp fibers non-linearly proceeds with time and is further separated into three parts, figure 18 (b). Part I and III are characterized by a linear decrease of the strain with the logarithmically scaled time, illustrated in red and blue, respectively. Part II, illustrated in black, is characterized by a non-linear strain decrease, indicating a change in the porous structure.
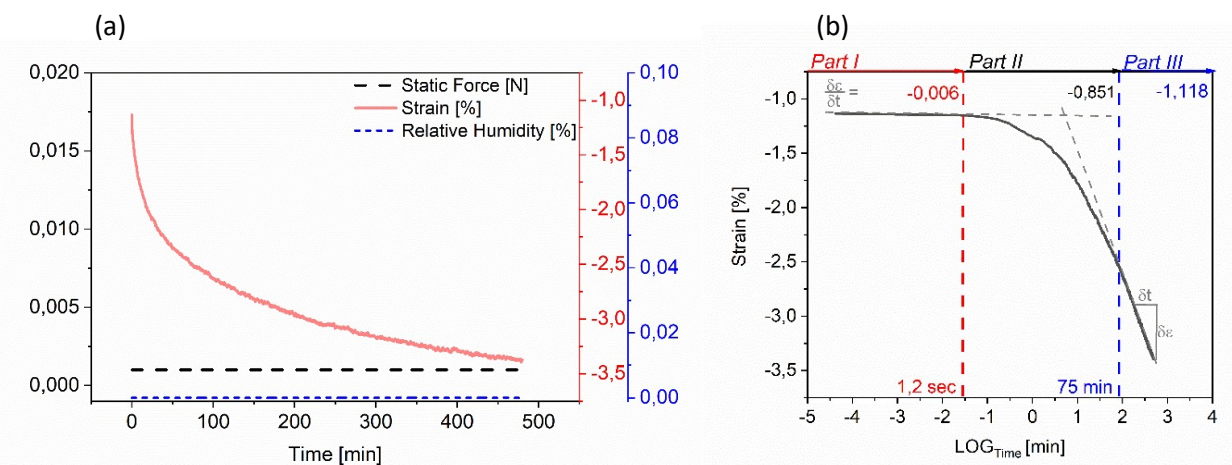

Fig. 18 (a) Measurement schedule for load (black) relative humidity (blue) and strain evaluation (red) (b) average resulting strain obtained from 12 individual pulp fibers during drying.

As the surface is the first area in contact with the dry environment the first linear segment (red) illustrates water removal from the surface, which is quickly achieved after 1,2 seconds

(-1,5 LOG$_{min}$). The second segment (black) after the first yield-point is characterized by the induced pore collapsing and successive water desorption, which dominates the strain for further 75 minutes (1,9 LOG$_{min}$). Afterwards the inclination [dε/dt] significantly changes, initiating the third strain segment, characterized by a linear decrease of the strain over 400 minutes (2,8 LOG$_{min}$). The strain-rate [dε/dt] for pulp fibers is further obtained from Part III of the strain-curve by linear regression after 200 minutes (2,3 LOG$_{min}$) of exposure to dry nitrogen, figure 19 (range of linear regression is indicated by a grey dotted line).
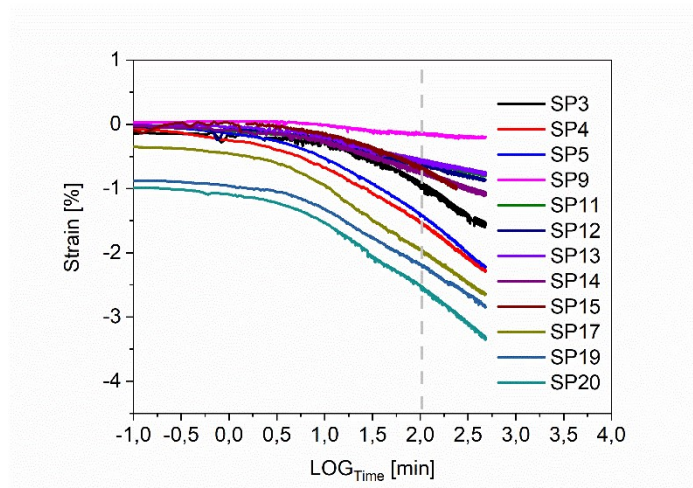
Fig. 19 In-situ drying strain of 12 individual fibers during 8 hours of exposure to dry nitrogen at 25°C.

The fiber cell wall starts to collapse immediately after the surface has been dried. The transition from surface drying to pore collapsing is characterized by a change of the drying strain from a rather restricted shrinkage behavior (*Part II* -1,0 LOG$_{min}$) to a progressive, accelerated one (*Part II* 1,0 LOG$_{min}$). Clearly, this region of transition is described by the decreased amount and size of the present pores and voids. In addition, the tensile shrinking of the fiber increases as the moisture content decreases, which is in agreement with previous studies [147]. As drying proceeds, the strain continuously develops, seemingly initiating further accelerated pore collapsing.
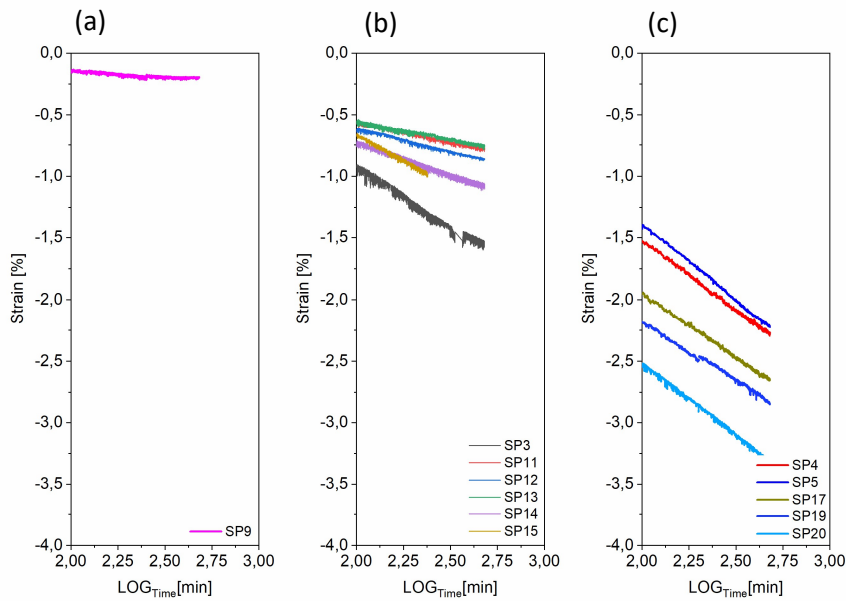
Fig. 20 In-situ drying strain of 12 individual fibers classified according to the obtained strain-rate (a) equilibrium strain (b) dry pulp-fibers that have obtained a low strain rate and (c) dry pulp-fibers that have obtained a high strain rate.

The average strain-rate of 12 individual pulp fibers after 8 hours of exposure to dry nitrogen at 25°C is $-0,8 \pm 0,4$ %ε/LOG$_{min}$, but it differs to a high extent from sample to sample, figure 20. An equilibrium state is observed for a single fiber sample, namely SP9, whereas all other samples still show a persistent and progressive shrinking at very low moisture content, table 1.

Tab. 1 Strain-rates of 12 individual pulp fibers in the dry state with an applied pre-load of 1 mN.

dε/dt	%/LOG$_{min}$	%/LOG$_{min}$	%/LOG$_{min}$	%/LOG$_{min}$	%/LOG$_{min}$	%/LOG$_{min}$
Equilibrium	-0,03_SP9	--	--	--	--	--
Low	-0,8_SP3	-0,3_SP11	-0,3_SP12	-0,3_SP13	-0,5_SP14	-0,8_SP15
High	-1,1_SP4	-1,2_SP5	-1,0_SP17	-1,0_SP19	-1,2_SP20	--

As estimated from the DVS-measurements the moisture content insignificantly changes by 0,002% after 60 minutes of exposure to dry nitrogen (1,75 LOG$_{min}$), while the cell wall collapses with decreasing moisture content. The results therefore suggest, that the fiber has reached its maximum dry state according to the applied drying treatment. The pulp fibers' drying strain after 75 minutes of exposure to a dry environment linearly proceeds with the logarithmically

scaled time, indicating exponentially decreasing sorption kinetics. Obviously, the last drying segment has the highest impact on the overall deformation pattern and continuously develops, which might be an important information for ongoing research simulating the pulp fiber long-term creep behavior. The results further prove evidence that the fiber after drying for 8 hours in dry nitrogen at 25°C still has not reached a thermodynamically equilibrated state. Consequently, DVS-measurements are not appropriate to predict the time necessary to achieve a thermodynamic equilibrium. This is explained by a structural reorganization on the molecular level, which can still proceed even after long-time stress exposure, and may additionally release some strongly bound water. Besides the willingness of the fiber to achieve a thermodynamic equilibrium, the viscoelastic nature of pulp fibers is based on intense Van-der-Walls interactions (VdW-forces) between constitutive polymers. VdW-forces further strongly depend on the distance between the constitutive polymers. As the fiber contracts, the distance between the constitutive polymers decreases and attraction and/or repulsion increases. The increased attraction between constitutive polymers might enable the supramolecular structure to highly densify as the distance between constitutive polymers decreases. Modelling studies have shown that hydrogen bonds and van der Waals interactions dominate the strain energy. Thereby, they are controlling most of the deformation upon loading and unloading of amorphous polymers [70,78,79]. Contrary to the amorphous matrix, which rather randomly collapses, the crystalline parts do not alter due to drying, as the interior of a fibril is not accessible to water. There is further evidence that the microfibrils as a whole experience a change in dimensions [147–150]. As mentioned in the literature review, by applying FTIR spectroscopy it was shown that cellulose elastically deforms at the side of the C-O-C bridge, which connects the adjacent glucose-rings [19]. Within the past ten years, XRD-measurements have favorably been used to describe the crystalline lattice of the cellulose microfibrils [68,71,84,147,148,151–155]. From the obtained diffraction pattern one can determine the length and the width of a single cellulose crystal-unit described by the d_{200} and d_{004} lattice distance, respectively [152]. The findings confirmed a dimensional change of the microfibrils when they were stressed. After drying of wood-based samples, an expansion of the microfibrils in direction of the MFA was reported, although on the macroscopic scale, the fiber length decreased [147]. When dry wood samples are further strained, the fibril width was reported to additionally decrease, which was shown to correlate with the applied strain. Peura et al. showed for dried wood fibers of small MFA, that the d_{004} lattice space continuously

decreased with increasing strain [84], although a change of the MFA was not observed. This indicates that the cellulose microfibril elongates in the direction parallel to the cellulose chains, whereas the distance between the hydrogen bonded sheets of cellulose chains decreases. Similar results were obtained by Hill et al., who studied the MFA of wood tissues during drying [71]. Both authors reported that the observed dimensional changes of the fibrils were partly reversible, when either the strain was released, or the fibers were rewetted. In addition to that, Hill et al. found a decrease of the monoclinic angle of a single cellulose unit-cell when the MFA was obtained from an un-strained specimen during drying. The expansion of the cellulose fibrils was attributed to the collapsing matrix during drying, inducing a transversal stress onto the fibrils, forcing them to elongate and further reduce the distance between single cellulose chains. More recently, Lube et al. found that the initial MFA of wood specimen significantly decreases after drying at evaluated temperatures to a target moisture content of 15wt% and 8wt% [155]. The observed increase of the MFA was even more pronounced the more the moisture content was decreasing. Abe and Yamamoto observed the MFA of wood specimen after drying to a certain moisture content below 25%, where the specimens were previously dried at different relative humidity and at 20°C. The weight and length of each specimen was further found to correlate with the changing MFA, with the moisture content and with the shrinking behavior. Similar to the observed shape of the drying strain in the current study, Abe and Yamamoto observed a nonlinear relation between the longitudinal shrinkage of the wood specimen and the moisture content. The degree of nonlinearity was further reported to increase as the initial sample MFA decreases. More captivatingly, the deviation from linearity increased as the moisture content dropped below 10% [147,148]. These findings further support the idea that differences in the obtained drying strains in the current study can be attributed to the pulp fibers' initial MFA. In agreement, the current study confirms accelerated longitudinal shrinkage at a moisture content below 10%. The accelerated shrinkage might be explained by the VdW-attraction forces between the constitutive polymers, which considerably increase as the moisture content decreases and the fiber shrinks. However, the phenomenon described by following the lattice space of the fibrils during drying, clearly captures the fibers' willingness to rotate or twist. This would cause an increased elongation of the cellulose chains accompanied by a decreased distance between the hydrogen-bonded microfibrils. Mentionable, the fiber samples in the current study were previously glued onto a sample-holder, and the single cell wall is only minorly allowed to twist.

In wood tissues the cell walls are parallelly aligned and glued together by lignin, so that rotation of the single cell wall should be allowed up to a comparable, small extent. For that reason, the mechanical behavior of a single cell wall and the behavior of thin wood tissues are often reported as being essentially the same, or at least similar to each other [68]. Besides the initial MFA, torsion of the pulp fibers additionally might play a huge role during drying and swelling and might even enable the fiber to reversibly decrease its MFA as the pore volume collapses. In summary, it is suggested that the observed shrinking behavior of pulp and wood is characterized by an initial expansion of the fibrils in direction of the MFA, as the matrix starts to collapse. Once a certain low moisture content is reached, the elongated microfibrils start to linearly shrink in tensile direction, decreasing the fibril width when they are strained. Accordingly, the drying stress might be explained by an elastically elongated and densified microfibril which, in order to release the stress, tends to elastically deform back to its initial dimensions once the fiber is rewetted.

However, once a dry fiber is remoisturized swelling stresses occur, which are described by the debonding and separation of the solid polymers due to the adsorbed water. The water forces constitutive polymers apart, thereby generating free volume. Thus, in the wet state cellulose fibers, be they native or processed, have a porous structure [156]. According to the applied humidity change, sorption does not necessarily occur uniformly. As a consequence, induced moisture- and stress-gradients were previously suggested to produce unpredictable creep behavior [143]. In addition, the mobility of polymers and, more precisely, the relaxation behavior is triggered by the moisture uptake and defined by their physical state, whether they are solid or in a more viscous state. In contrast to the dry state, relaxation of wetted polymers is enhanced, leading to the well-known plasticizing effect of water on hydrophilic materials [116]. When moisture desorbs, amorphous polymers enter the glassy state. Thereby an amount of free volume apparently is "frozen" and further re-accessible once the fiber is remoisturized [51]. Therefore, the total volume of swollen glassy polymers is less than the total volume of glassy polymers and swelling agents [52,157]. Hence, the free volume is locked in a local thermodynamic equilibrium and is not necessarily equal to the global thermodynamic equilibrium. Thus, excess free volume might occur once the fiber is remoisturized and accordingly, one memorized thermodynamically stable state is approached again by relaxation. The mechanical behavior under the influence of moisture therefore is much more complex than that of dry polymers. The creep of wood-based materials exhibits a phenomenon called mechano-

sorption, which is a collective term describing accelerated deformation under an applied load once the specimen is exposed to cyclically changing humidity of the ambient atmosphere. In comparison to the achieved deformation under a constant high ambient humidity, the average creep rate under cyclic conditions is significantly higher [140]. Mechano-sorptive creep (MSC) was first observed in the late 1950s and further found to occur in many wood- and paper-based materials [3,118,121]. Besides, mechano-sorption was also observed in other hydrophilic polymers, whether they were nature-based or synthetically spun, suggesting that mechnano-sorption is induced by physical aging. Indeed, MSC was also reported to occur in single pulp fibers [8]. But the topic is highly contentious and results exist in contradiction to the observed MSC in pulp fibers [3,110]. Accordingly, no widely accepted explanation for accelerated creep in wood exists. In general, MSC in cellulose-based materials has been related to either moisture-induced physical aging of glassy materials or macroscopic moisture gradients accompanied by enhanced stresses [143]. The induced stress is further discussed to affect the supramolecular structure, such as changes in the fibril structure [113]. However, the phenomenon of moisture induced creep critically affects the use of wood in composite materials, and thus deserves to be studied in more detail. Following the proper meaning of the word creep the observed specimen has to be instantaneously stressed by a mechanically applied load. Up to now, moisture induced creep has only been studied under mechanically applied stresses. In addition, the macroscopic swelling of individual wood fibers due to sorption has only been approached by comparing fiber dimensions before and after moisture uptake [158]. So far, no study exists describing the in-situ deformation of pulp fibers during continuously increasing (swelling) and under constant ambient humidity (creep) without additionally stressing the specimen with a mechanically applied load. A change of the initial MFA was usually related to the mechanical application of a certain tensile stress, although it is yet unknown to which extent water influences the fibril structure. In order to prevent stress-coupling between mechanically applied loads and sorption-induced stresses, pulp fibers were only subjected to an applied pre-load of 1 mN and further exposed to dry environmental conditions. After drying the specimen for eight hours, the fibers were subsequently remoisturized at three different moisture levels and the deformation rate was obtained at constant ambient humidity. The resulting strain curves were separated into three parts, namely (1) surface adsorption, (2) swelling and (3) creep, figure 21. Surface adsorption and swelling were induced by the continuously increasing humidity, whereas creep was obtained under constant ambient

humidity. The deformation rate was calculated during swelling (referred to as swelling-rate), immediately after the RH had been kept constant (referred to as minimum strain-rate) and during creep (referred to as maximum strain-rate). After the experiment the true cross-sectional area was obtained from microtome slices of each previously tested fiber and the applied stress induced by the required pre-load was calculated. By increasing the ambient humidity with a defined rate of 2% per minute, non-uniform moisture uptake resulting in concentration- and stress- gradients was minimized [143].
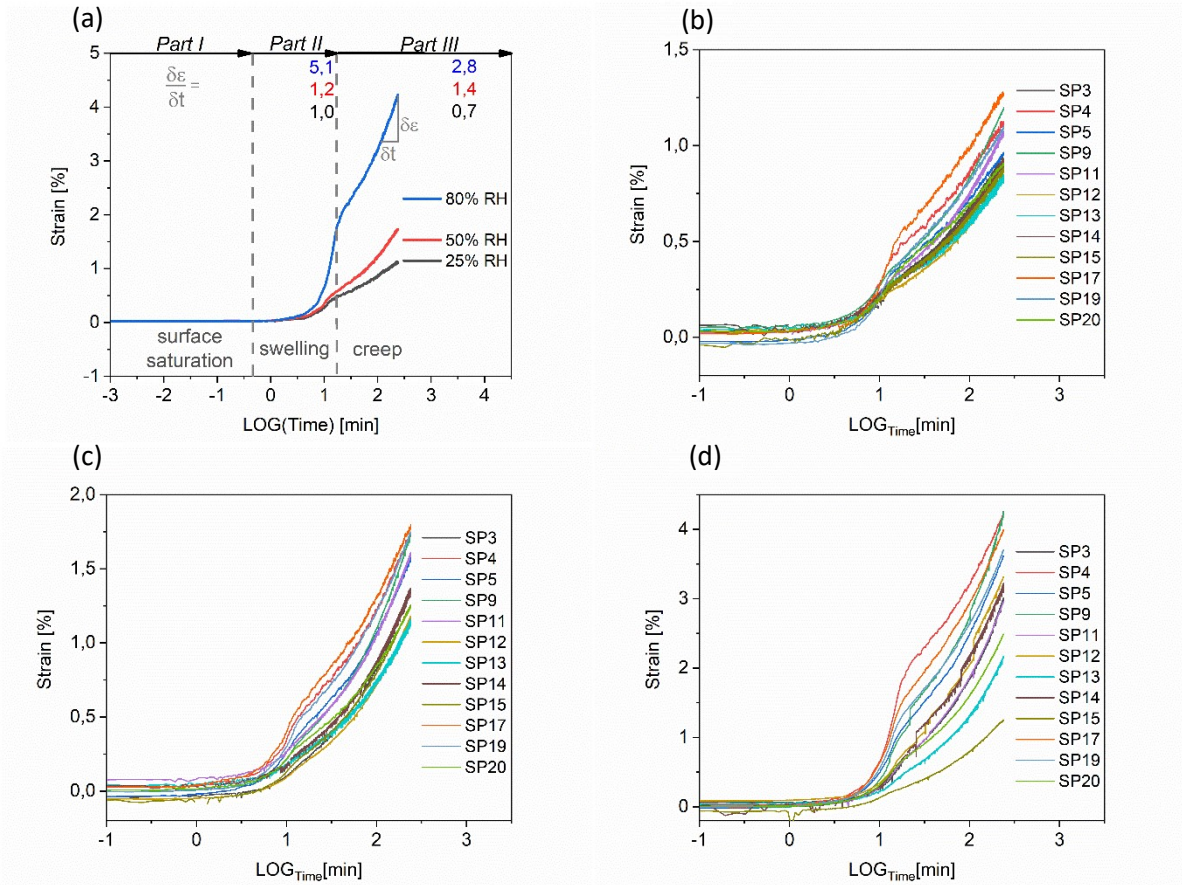
Fig. 21 Evaluation of the average in-situ strain of 12 individual fibers at three different moisture levels (a) Interpretation (b) in-situ strain at 25% RH (c) in-situ strain at 50% RH (d) in-situ strain at 80% RH.

The results show that during RH change the strain increases faster than during constant RH, which is related to the spontaneous moisture uptake during swelling. Thus, the water uptake proceeds slower at lower moisture content and further accelerates with increasing moisture content. This is in agreement with the observed sorption behavior of fibrous, hydrophilic polymers, which were reported to follow at least two stages of sorption [159]. Thereby, the sorption kinetics of cellulose-based fibers, be they natural [74,75] or regenerated, [160,161] have been satisfactorily described by the parallel exponential kinetic model (PEK). The PEK-model

describes two stages of adsorption of different speed both following an exponential growth. The slow process is further associated with the initial moisture uptake, referred to as mono-layer adsorption, whereas the fast process is related to poly-layer adsorption, describing the mobile water phase. A differentiation between these two processes is necessary as water molecules bound to constitutive polymers experience much stronger cohesive forces than single water molecules within the poly-water layers [162]. Mono-layer adsorption therefore is directly associated with the binding capacity of the constitutive polymers. Notably, these processes could also occur simultaneously once the RH changes instantaneously. Accordingly, the rather slow increase of the strain during the initial RH increase might be attributed to the reopening of the internal porous structure due to mono-layer adsorption. After the yield point, the previously closed pores seem to be sufficiently reopened to allow poly-layer adsorption, leading to a linearly increasing strain with the logarithmically scaled time, figure 22 (a) (range of linearly increasing strain is separated by the black dotted line). Thus, poly-layer adsorption is induced after approximately 10 minutes of RH-increase with 2%/min. The linearly increasing strain until constant ambient conditions thereby indicates an exponential growth of the tensile deformation during RH change. To achieve a constant humidity of 25% and 50% RH, 12,5 minutes corresponding to 1,1 LOG_{min} are necessary, whereas 15 minutes corresponding to 1,2 LOG_{min} are necessary to increase humidity from 50% RH to 80% RH. The linearly increasing strain with the logarithmically scaled time clearly indicates exponential growth.
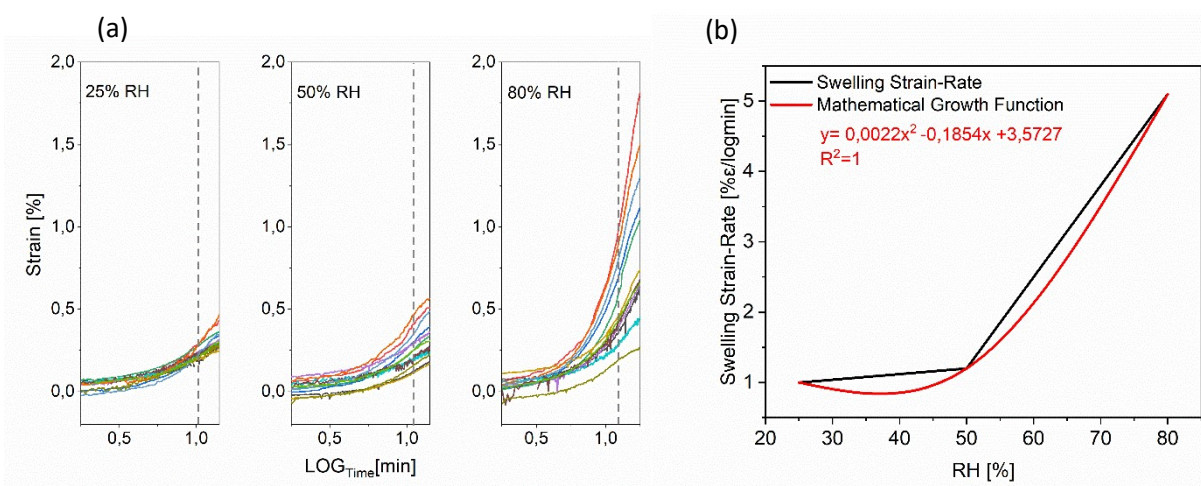

Fig. 22 (a) Swelling during RH increase to three different moisture levels (accelerated creep indicated by a grey dotted line) (b) Evaluation of the swelling strain-rate at three different moisture levels, obtained in the region of linear strain-increase.

The average swelling strain-rate, obtained within the linear regime increases from 1 %ε/LOGmin to 1,2 %ε/LOGmin and even up to 5,1 %ε/LOGmin, when the humidity is increased from 0% to 25%, to 50% and from 50% to 80%. The fitting of the data with various mathematical growth functions further reveals that the swelling strain-rate follows a second order polynomial growth with the increased moisture-level, figure 22 (b). This result suggests that it is possible to separate the observed two sorption-processes by increasing the ambient humidity by a defined and slow rate. With a moisture-rate of 2% per minute, the system obviously has sufficient time to adequately respond to the changed environment, resulting in a polynomial increase of the swelling strain when the ambient humidity is doubled. But in order to evaluate which growth function could be applied for the sorption behavior of pulp fibers at different moisture levels, additional experiments should be carried out. However, when a previously dried pulp fiber is re-wetted, water molecules first adsorb at available sorption sites on the inner and outer surface of the cell wall. Thereby they occupy space between constitutive polymers in the matrix and at the surface of the fibrils, which leads to an opening of the transient microcapillary network [133]. Since there are about three sorption sites per glucose unit in wood polymers, one water molecule per glucose unit corresponds to around 0,33 H_2O per sorption site (= 1 water molecule per glucose unit), not counting the unavailable hydroxyl groups within the microfibril [29]. It was shown that 0,33 H_2O per sorption site roughly correspond to 5-6wt% moisture, which represents the amount of moisture absorbed by the cell wall at 25% RH, as estimated from DVS measurements [25,42]. Accordingly, up to 25% RH only strongly bound water, experiencing the attraction forces of the constitutive polymers, is adsorbed by the cell wall.

Moisture induced fiber creep is often referred to as the interaction of single water molecules with the surrounding matrix when hydrogen-bonds break, move and re-form. As the sorption enthalpy decreases at higher moisture content, water is expected to be highly mobile, thereby facilitating stress migration [5]. Thus, water can more easily migrate to those sorption sites exhibiting a smaller energy barrier to overcome, thereby enabling the systems' entropy to decrease. During transition from an increasing ambient humidity to a constant one, both mechanisms, elastic- and creep- compliance, simultaneously contribute to the stress relaxation. Whereas during swelling the elastic fiber-compliance is expected to be dominated by the volume expansion, the creep-compliance is mostly dominated by the water-migration [5]. The transition from the instantaneous fiber response, referred to as swelling, to

the delayed fiber response, referred to as creep, seemingly expands at higher humidity, figure 23. Accordingly, the contribution of the delayed creep- compliance increases at higher moisture levels.
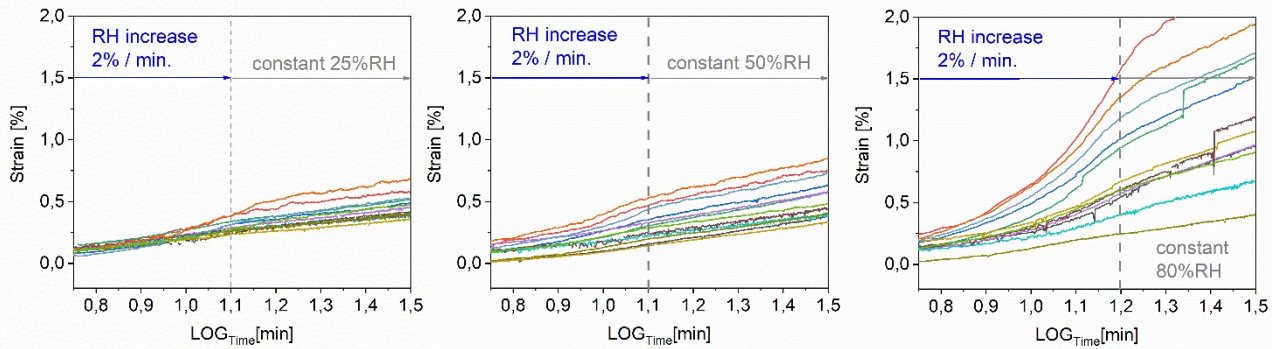

Fig. 23 Transition zone between RH increase and constant RH at three different moisture levels (constant conditions are indicated by a grey dotted line).

It is generally accepted that a mechanically applied load stresses the load-bearing fibrils more than the amorphous matrix, and stress relaxation is performed by the controlled lengthening and/or rotation of covalent (backbone-relaxation) and hydrogen bonds (side-chain relaxation) inside the fibrils, which could be described by polymer-vibration [22]. Thereby the polymers have to be able to transmit the stress towards and through the amorphous matrix. However, a significant portion of stress is also put on the fibrils by the matrix during swelling, as the cell volume increases. Thereby, the fibrils are not able to fully release the stress by backbone-relaxation and VdW-interaction seemingly have a growing effect on stress-migration when the moisture content increases. This is further shown as the creep-strain at each moisture level accelerates after one hour (=1,75 LOG_{min}) of exposure to constant RH and non-linearly proceeds with the logarithmically scaled time. The divergence from a linear relationship of the creep is rather small at 25% RH, but it increases with the moisture level and becomes highly pronounced at 80% RH. Thus, the first stage adsorption related to the adsorption of strongly bound water appears to be almost independent of the overall sorption history, as the creep-strain rather linearly increases at constant 25% RH. At higher humidity levels the creep-strain largely deviates from linear growth, figure 24 (a).
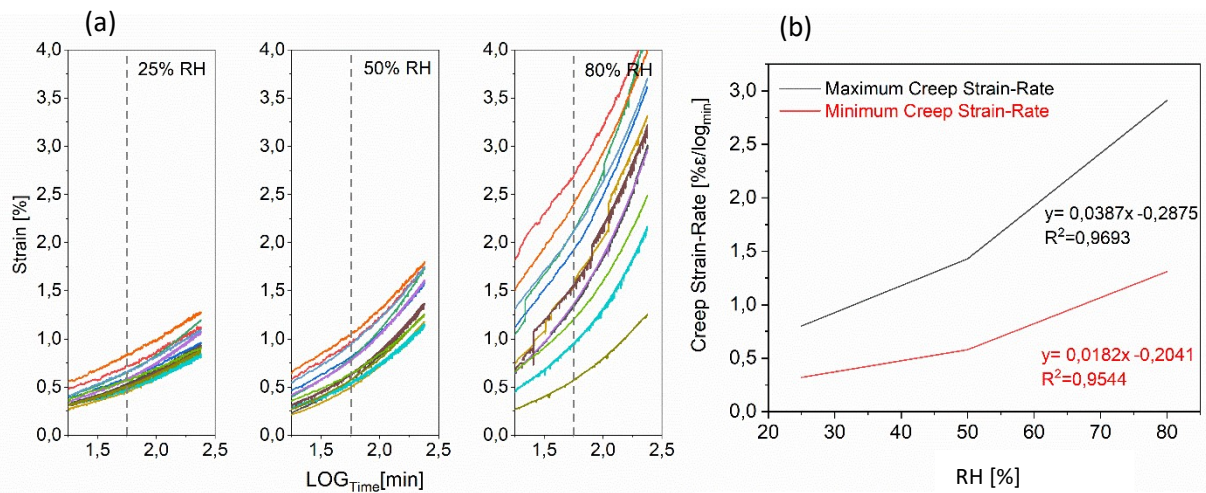
Fig. 24 (a) Creep during constant RH at three different moisture levels (accelerated creep indicated by a grey dotted line) (b) Evaluation of the minimum and maximum strain-rate, obtained instantaneously after the RH was kept constant and during the last 20 minutes of exposure to constant RH.

Consequently, up to 25% constant ambient humidity water molecules directly bond to the constitutive polymers and might lead to additional cross-linking of the fibrils with the surrounding matrix, thereby forming a hydrogen-bond network. Besides, the swelling strain-rate during sorption up to 25% RH is similar to that of the long-term creep strain-rate under constant conditions (1,0 vs. 0,8 %/LOG_{min}).

A continuously developing, load-induced creep-strain above 25% RH has also been observed by other researchers, and discussed as the influence from the sorption history [3,5]. Creep experiments of wood-based materials at an ambient humidity below 30% RH have not been reported in literature. In the present experiment the fibers were previously dried under tension before rewetting. Thereby the fibrils were found to partly increase their length and to decrease their width. Accordingly, upon rewetting, the fibrils are expected to elastically deform back into a more extended cross-section, but shortened length. A decrease in fibril length and an increase of the fibril width upon rewetting was also shown to occur in cellulose thin-films[163]. In the present experiment, this process might be responsible for the initially observed slower creep strain, as soon as the RH was kept constant. Thus, the pulp fibers did obviously not reach a thermodynamic equilibrium, as polymer relaxation still proceeds after the main water uptake was accomplished. Consequently, when a dry wood-based fiber is exposed to changing ambient humidity, its attainment of constant moisture content, as for instance obtained with DVS-measurements, does not necessarily mean that complete equilibrium has been reached. Obviously, significant relaxation processes (and perhaps barely

detectable moisture- and pressure-gradients) continue for a long period of time, thus having profound effects on the fibers' subsequent behavior. Hence, it is necessary to additionally introduce substrate deformation, e.g. relaxation induced by swelling, as being a rate-limiting process during sorption [61,65,164]. Substrate deformation could originate from a decrease of the initial MFA, additionally generating free volume between the fibrils and the amorphous matrix, allowing more moisture to be adsorbed. The enhanced moisture content further induces an increased shear stress at the fibril surface. In order to withstand these shear stresses, the fibrils might adapt their fibril structure towards the fiber axis, thereby increasing the overall fiber stiffness. It is generally accepted that water preferably adsorbs within the amorphous matrix, thereby significantly increasing polymer relaxation. Besides preferred water adsorption at the amorphous matrix, Kulasinski et al. recently revealed that water additionally prefers to adsorb at the interface between fibrils and matrix. This sorption site was significantly preferred at high (above 10wt%) and at low (below 5wt%) moisture content. This is plausible, as the interface is characterized only by hydrogen bonds and weak interactions, whereas the polar interactions between hemicellulose are much stronger, also including covalent bonds. It is further known that water has no accessibility to the fibril inside, as the highly crystalline properties do not allow water adsorption. The incorporation of water between constitutive polymers of the matrix demands a larger energy barrier to be overcome, as hemicellulose needs to be stretched and reorganized, which efforts more energy than simply breaking up existing hydrogen-bonds and weak polar-interactions at the interface. Hence, there is evidence that water accumulates at the interface between the matrix and the fibrils, besides the generally accepted water accumulation in the amorphous matrix. Accordingly, the creep-strain does not linearly increase with time and accelerates during long time exposure to constant RH as excessive water adsorption at the interface might occur. This might be directly related to a change of the MFA, thereby generating additional free volume. Such behavior enables facilitated stress transmission through the amorphous matrix, as water placed between matrix and fibrils can function as stress transmitter. In combination, these two processes would increase the fiber strength by the reduction of the MFA and facilitate stress transmission through VdW-interactions.

However, the delayed creep response, both the minimum and maximum strain-rate, follow the same increase with the moisture content, indicating that the initial fibril contraction upon re-wetting influences the long-term creep behavior to a huge extent. The maximum and minimum strain-rate increase by a factor of 4 when the humidity changes from 25% to 80% RH and seemingly linearly increase with the moisture content, figure 24(b). This is in agreement with previously reported dimensional changes during moisture uptake of wood, which were observed to proportionally increase between a moisture content of 5 to 20wt% [35,158]. The pulp fibers tested in the present study have approximately achieved a moisture content in the range of 5 to 10wt% when exposed to an ambient humidity between 25 and 80%. In consistence with the linear growth of the creep-rate the moisture content linearly increases with the ambient humidity, whereas the swelling strain rate largely deviates from linear growth, figure 25 (a+b).
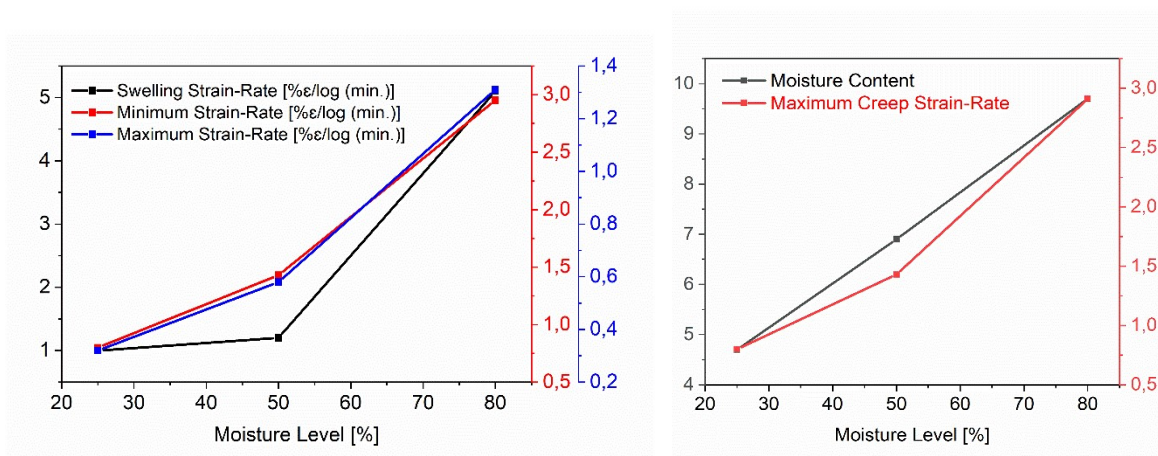
Fig. 25 (a) Evaluation of the strain-rate at different sorption stages (b) Increase of moisture content and creep strain-rate with RH.

From the results, it is further apparent that around 50% RH, corresponding to a moisture content of about 7wt%, some additional mechanisms significantly add to the delayed creep. An increased moisture content of 2wt% from 5 to 7wt% already leads to an increased strain-rate by a factor of two. After pores have been completely filled, the cell wall necessarily has to increase its free volume, which could be achieved by hemicellulose entering the rubbery state. The T_g of hemicellulose was reported to be at 25°C and about 60% RH [67,109]. More precisely, it seems plausible that the T_g of hemicellulose at 25°C already occurs at 50% ambient RH. From the experiment it is obvious that at 50% RH the swelling strain-rate increases, and the delayed creep-response significantly deviates from linearity, further

influencing the creep at 80% RH. In addition to this, evidence has been found as the swelling strain-rate is significantly enhanced at 80% RH. After passing the Tg the free volume tremendously increases, leading to excessive water adsorption and increased viscosity of the amorphous matrix. By that, shear forces at the fibril surface become increasingly high, which might even induce slippage of single cellulose-chains through the amorphous matrix. The softening of the matrix implies an enhanced strain-rate at 80% RH, additionally, the stiffness of the composite strongly decreases. Some fibers tested at 80% RH showed a typical strain pattern of fiber failure, figure 26 (a). Keckes et al. observed a similar strain pattern during tensile testing of wetted wood fibers when a certain mechanical stress was applied. Further loading resulted in a complete recovery of the initial fiber stiffness. Keckes et al. argued that the softened matrix carried along cellulose chains from the fibril structure. The delocalized cellulose-strains further re-bond at another position, thereby restoring some of the initial fiber stiffness. As the load-bearing unit, fibrils are highly stressed in direction of the applied tensile-load when their MFA is low. With increasing MFA, the fibrils are stressed more in their cross-direction than towards the applied tensile-stress, which leads to decreased stress transfer accompanied by deteriorated mechanical properties. Consequently, a significant loss of the elastic fiber-properties could be detected when the initial MFA was high [22]. Interestingly, the same fiber specimen which show a typical strain pattern of fiber failure at 80% RH were suggested to have reached a large MFA during drying, namely SP 9,12 and 14. As those fiber samples are suggested to experience higher stresses during the swelling process, it seems reasonable that these specimens first show characteristics of fiber failure.
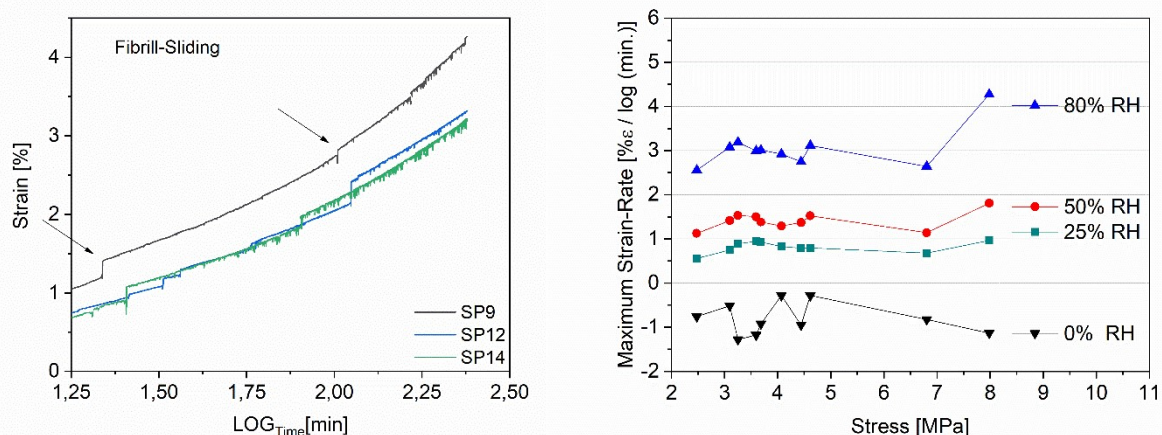

Fig. 26 (a) Characteristics of fiber failure at 80% RH (b) Individual fiber-relationship between the applied stress and the obtained creep strain-rate at each moisture.

The linear relationship between strain-rate and moisture level would imply that the effect of the pre-load is diminished or at least similarly influences the strain-rate at each moisture level. Indeed, the strain-rate according to the applied stress rather scatters in the same range at each moisture level, and suddenly increases, when the mechanically applied load exceeds 7 MPa, figure 26 (b). It is assumed that after 7 MPa the stress significantly impacts the moisture induced strain-rate, as it was shown in previous work [22]. At small stresses in the range of 2 to 7 MPa, however, fibril relaxation seems to be sufficiently compensated by the surrounding matrix. The results therefore suggest that the apparent strain-rate is rather controlled by the swelling than by the applied pre-load. Table 2 summarizes the obtained strain-rates according to their moisture content with an applied pre-load of 4 MPa in average.

Tab. 2 Average strain-rates of 12 individual pulp fibers according to their moisture content.

Moisture Level	Moisture content wt%	Swelling Strain Rate %ε/log$_{min}$	Maximum Strain Rate %ε/log$_{min}$	Minimum Strain Rate %ε/log$_{min}$	Max. Elongation %
25% RH	4,7	1,0±0,15	0,80±0,09	0,32±0,07	0.99±0,15
50% RH	6,9	1,2±0,21	1,43±0,13	0,58±0,09	1,47±0.24
80% RH	9,7	5,1±0,50	2,91±0,41	1,31±0,32	3.17±0,88

From the results it is further apparent that the deviation from the mean strain-rate is rather small compared to the deviation of the strain-rates obtained from dry pulp fibers (max. strain-rate: 0,8±0,40 %ε/log$_{min}$). In consistence with the increasing stress with the moisture content, the deviation from the mean value increases. Thus, the highest deviation from the mean strain-rate is achieved at dry conditions. This might imply that, in accordance with the moisture content, a maximum deflection of the MFA exists. According to the volume change, the highest stress at the fibrils occurs at 0% RH and at 80% RH, when the cell wall is either dry or in its fully swollen state. Under these conditions the fibrils are tremendously stressed, and the mechanical properties might be strongly controlled by the MFA. Thus, the strain-rate will more strongly deviate from the mean strain-rate. The maximum fiber elongation at each

humidity level further is increased by 1,0% at 25% RH, by 1,5% at 50% RH, and by 3,2% at 80% RH, which is in accordance with the linearly increasing creep strain-rates and the macroscopically observed tensile deformation between 5 and 20wt% moisture [165]. Notably, during demounting the individual fibers from the testing device, each fiber broke in the middle of the applied gauche length. Fibers previously tested, which broke at the site of fixation, were excluded from further evaluation. Nonetheless, all tested fibers obviously were at the edge of failing.

In order to evaluate the accelerated creep behavior in more detail, three pulp fibers were subjected to the same pre-drying step as applied in the previous experiment and subsequently exposed to changing ambient humidity-cycles. In a first step the ambient humidity was increased with a defined rate of 2% per minute to constant 80% RH and the fiber was allowed to relax for 20 minutes to ensure matrix softening. Afterwards, the humidity was cycled between 50% and 80% RH in an interval of 30 minutes, figure 27 (a). Once the respective RH had been attained, the RH was immediately changed again to the previouse moisture level. Thereby the fibers were not allowed to slowly equilibrate under the new environmental condition, and desorption and adsorption were limited to 15 minutes during the RH change.
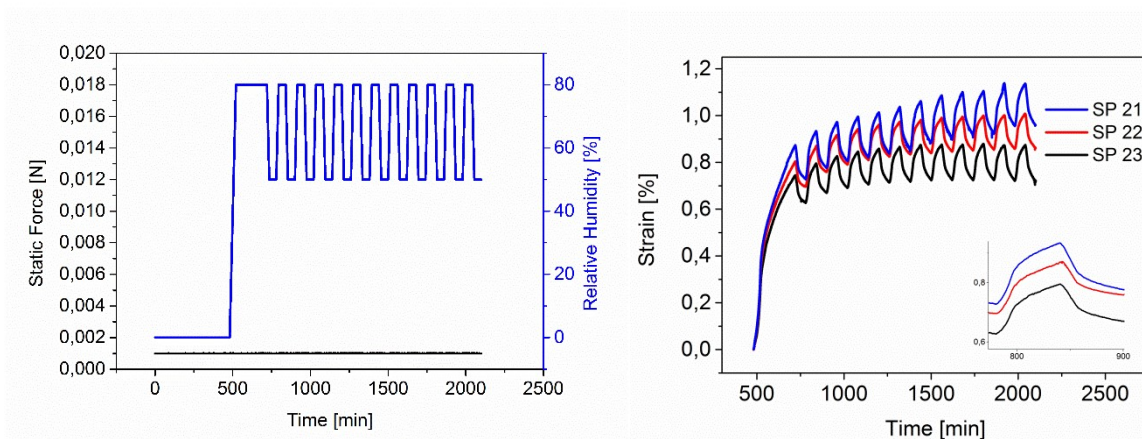
Fig. 27 (a) Measurement schedule for load (black) and relative humidity (blue) (b) resulting strain of three single pulp-fibers.

The tested pulp-fibers show flow-like behavior rather than a solid one. This is described by a steep strain increase when the humidity is increased from 50% to 80% RH and the quick fiber response when humidity is decreased again from 80% to 50% RH. Thereby, the cell wall is alternatingly exposed to drying- and swelling- processes. It is assumed that the matrix is present in its softened state, and therefore stress migration should be facilitated, resulting in

less accelerated creep. Indeed, accelerated or mechano-sorptive creep does not occur under the conditions applied in the present experiment. Thus, no external load was applied to the fibers prior to the humidity cycling, and the obtained strain illustrates the strain of pulp fibers obtained exclusively under the influence of adsorption and desorption cycles. The resulting creep-rate during cycling humidity thereby is five times lower than the observed creep-rate at constant relative humidity, figure 28.

Fig. 28 Average strain of three individual pulp fibers during humidity cycling between 80% and 50% RH at constant 25°C.

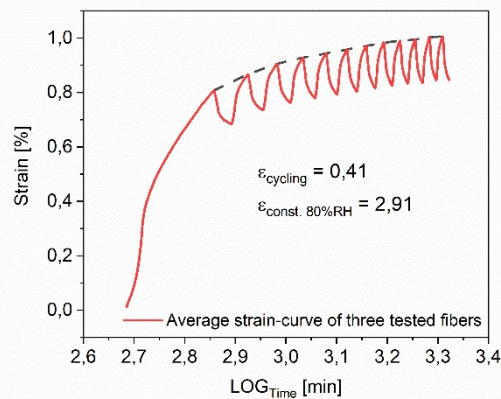The results are in agreement with previously evaluated creep-experiments performed by Sedlachek and Habeger et al., who studied sorption induced creep in pulp and cellulosic fibers [3,110]. Notably, the applied conditions in the present experiment are not conducive for the observation of strong moisture-gradient driven creep, as pointed out by Habeger et al. The sorption time, which is defined by the time of constant RH exposure, is kept as low as possible, which only allows surface swelling and drying. By keeping the sorption time lower than the applied moisture-rate increase, moisture-induced stress-gradients should also be minimized and the obtained strain should not accelerate as a result of the applied cycling parameters [110,143]. In addition, the matrix stays in its softened state, which seemingly plays a key role to mitigate and relieve stress. Mechano-sorptive creep in pulp fibers was observed in experiments in which the environmental humidity was cycled between 30% and 80% RH [7,8]. In addition to this an external load of 70 mN was applied to the tested fibers before determining the creep-rate. At 30% RH the matrix, however, is insufficiently moisturized in order to adequately relieve the stress from the sorption process by polymer relaxation due to the glassy state of the hemicellulose. In addition, drying the fiber from 80% to 30% RH generates a larger amount of free volume than drying from 80% to 50% RH. Besides, the influencing

factor of the softened matrix interfaces between fibrils and matrix seemingly play an essential role.

As stated by Habeger, the observation of accelerated creep on the single fiber level is difficult, as stress gradients, usually occurring through the thickness of the material, are minimized by the already thin individual fibers. The thicker a material becomes the larger the induced stress gradients are due to sorption from the materials' surface to the inner core of the material. In the case of hydrophilic pulp fibers, which are about 3 to 8 µm thick, sorption happens immediately through the whole fiber structure, and the presence of sorption-induced stress gradients is diminished [110,166]. Interestingly, accelerated creep or mechano-sorptive creep occurred in nanocellulose thin films of various film thickness as well. As reported by Lindström et al. mechano-sorptive creep in those films were independent of the film thickness. Moreover, for nanocellulose thin films, they found, that as long as there is sufficient time for moisture equilibration during each step of the RH cycle, the mechano-sorptive creep-rate does not significantly depend on the rate of moisture increase of the environment [113]. These results are in contradiction to the hypothesis of moisture-induced stress-gradients proposed by Habeger. When, however, moisture-induced stress gradients were induced on the single fiber-level, they were largely compensated by the softened matrix, as seen in the present results. The results of the present study in comparison with those of Lindström consequently lead to the suggestion, that stress migration changes, whether the amorphous polymers are in their softened or in their glassy state. Amorphous cellulose is not expected to soften through the whole applied sorption range, which implies that amorphous cellulose within the nanocellulose thin films was present in its glassy state [167]. Reported accelerated creep in nanocellulose thin films and in single pulp-fibers therefore might be a consequence of the amorphous polymers in their glassy state. In their non-softened state, interfaces between crystalline parts and amorphous parts of the material might become crucial for stress migration. When the matrix is not sufficiently moisturized and flexible, stress concentrations might occur especially at those interfaces. If the material further is dried insufficiently, those interfaces will stay intact and grow during each applied moisture cycle. As suggested by Lindström, mechano-sorptive creep might be a local phenomenon, occurring when crystalline polymers are embedded in a matrix of amorphous polymers. It is now further suggested that mechano-sorptive creep further depends on the physical state of the amorphous polymers,

namely their softened or their glassy state. Another influencing factor of mechano-sorptive creep is the sorption history of the material.

The sorption history of a material dictates the movement of the crystalline parts, once the material is remoisturized. It is generally accepted that amorphous polymers swell more than crystalline polymers of the same material. Once wetted, crystalline regions memorize their latest path and configuration, which might be induced by the swollen state of the amorphous polymers. During drying, the additionally generated free volume from moisture uptake, e.g. at the interface between crystalline and amorphous regions of the material, is apparently locked and remains accessible when the material is again rewetted. Repeated water adsorption at the interface promotes the reorientation of the crystal parts in direction of the applied stress, whereby the crystalline parts can adapt their configuration according to the swollen state of the amorphous polymers. From molecular dynamic simulations, it is known that water preferably adsorbs at interfaces, where VdW-forces are decreased. This would imply that free volume is generated at these very interfaces during sorption. Exposing the material to drying and rewetting cycles increases the volume of the interfaces. Hence, those interfaces might grow during each drying step, and with this the sorption capacity of the material. In addition, stress transfer is interrupted by the increased distance of the constitutive polymers at the interface. Consequently, interfaces are prone to stress concentrations, especially when the matrix is present in its glassy state and stress transfer is already diminished by the rigid matrix.

The present results illustrate how remarkably pulp fibers respond to rather quick changes of the ambient humidity when a sufficiently high moisture content facilitates polymer-relaxation. In addition, accelerated or mechano-sorptive creep was not observed. This can be referred to the matrix, which is supposed to be in its softened state. Creep observations made during pulp fiber testing are rarely found in literature, and authors include creep at constant RH addressing mechano-sorptive creep (MSC) and physical aging rather than constant creep [3,110,143]. In order to gain a deeper understanding of the underlying mechanism the moisture-induced creep of pulp fibers was obtained under diminishingly small loads. Strain-rates at constant humidity reported in literature were either evaluated from experiments carried out after successive loading- and unloading- cycles, or at varying temperatures [5,134,136,138]. Consequently, the methods used to determine creep strain-rates, differ to a high extent from the present

experiments in terms of fiber pre-conditioning and fiber stress-history. The main distinction from the presently discussed experimental design, however, is that no additional external load was applied to the pulp fibers before determining the creep-rate. The fibers, although kept in tensile direction by a pre-load of 1 mN, were therfore in a rather unstrained state. Conventional creep-experiments require the application of an external load before evaluating the creep-rate. Thereby the fibers are additonally stressed by a force corresponding to around 50% of the fibers' maximum tensile strength. Seemingly, the stress applied by an external load drastically prolongs the ability of pulp fibers to creep due to sorption. This becomes obvious when comparing the creep-rates obtained inhere with the creep-rates reported in literature. Presented sorption-induced creep-rates are increased by a factor of 10 as compared to those creep-rates obtained from fibers additonally stressed by an externally applied load. One reason could be that the applied external load directs the polymer relaxation, wheras during sorption the polymers are free to adjust their configuration to the randomly distributed stress. Thereby they can fully expand in any direction and are not restricted to the direction of the externally applied load.

The presented experimental set-up provides an important opportunity to advance the understanding of moisture-induced fiber creep. The pulp fibers tested were initially stressed by a preload of approximately 4 MPa, dried and subsequently remoisturized. After the experiment, the cross-sectional areas of the previously tested pulp fibers were obtained from microtome slices. The results in comparison with the available literature discussing wood-water interactions suggest that the MFA increases during drying, whereas upon rewetting the MFA decreases. From previous observations of moisturized wood-based specimen, it is known that the MFA influences the mechanical properties to a huge extent [9,22,168,169]. A strong relationship, for instance, was shown to exist between the elastic modulus and the initial MFA of wood-based materials [168]. Accordingly, stress-strain curves of wetted wood specimens as well as nature-based individual fibers, exhibited non-linearity [22,125]. The non-linearity occurred only for samples with initially high MFA, whereas fibers with initially low MFA showed the expected linear relationship between stress and strain [22]. In addition, the fracture behavior of wood-based fibers significantly differs with respect to the MFA [168,170]. Unfortunately, little experimental evidence has been achieved to support the idea of changing MFA with the moisture content [5,149,171]. However, the influence of moisture was observed for several plant- and wood-based fibers and was shown to significantly enhance the fiber creep. Thereby a decrease of the fiber strength with the increased moisture content was reported for several plant-based fibers [7,122,125,127]. Whereas it is generally accepted that the fiber strength decreases with moisture content, studies also exist which show an increased fiber strength at lower moisture content [125,172]. The present results support the idea that the time-dependent mechanical behavior of pulp fibers is determined by the moisture content and its effect on the MFA. This is consistent with observed long-time moisture-induced creep behavior of a tracheid [5]. At a moisture content below 5wt%, the present study suggests that the MFA does not significantly change, instead, the adsorbed water stabilizes the cell wall. In contrast to that, at a moisture content above 7wt%, accelerated strain during the long-term exposure to constant RH has been observed, which was attributed to the successive water adsorption at the interface between fibrils and matrix, thereby the MFA might increase. Besides, there is evidence that hemicellulose softens at around 50%RH and 25°C, which additionally induces excessive water adsorption, as the free volume increases. After comparing the obtained stress on the cross-sectional area with the obtained strain-rate at different moisture levels, the results suggest no significant effect of the applied preload on the respective creep strain-rate.

Accordingly, below 5wt%, the water on the one hand allows fibrils to perform stress-relaxation within the surrounding amorphous matrix and on the other hand reinforces the cell wall by cross-linking the load-bearing unit with the matrix by establishing hydrogen bonds. The reinforcing effect was further related to the adsorption of strongly bound water. Such an observed anti-plasticization effect would imply that water preferably adsorbs at the fibril surface at lower moisture content. Notably, this so-called anti-plasticization effect at low moisture content was observed for several cellulose-based materials [173]. The present results are further supported by the information gained from molecular dynamic simulations of a matrix based on hemicellulose reinforced by cellulose-based fibrils during sorption. Besides the amorphous matrix, the interface between the fibrils and the matrix was shown to be a favorable site for water accumulation [174]. The results revealed that water sorption at the interface was particularly enhanced at very low and very high moisture levels and thereby showed that a threshold exists after which the water plasticizes the composite [174,175]. Above 5% moisture content, water adsorbed by the cell wall seems to be sufficiently mobile to significantly increase the shear stresses at the fibrils, allowing them to reduce its angle towards the fiber axis. This would imply that the fiber strength increases above 5% moisture content. On the macroscopic level, although, the strength of wood was shown to decrease upon moisture uptake. This is plausible as the effect of weakening is related to the breaking of hydrogen bonds between wood polymers due to the water uptake. Above the critical moisture content of 5wt% water molecules tend to break more than one hydrogen bond between constitutive polymers, which is related to poly-layer water adsorption [87]. This amount of moisture corresponds to approximately one water molecule per sugar unit, figure 29.
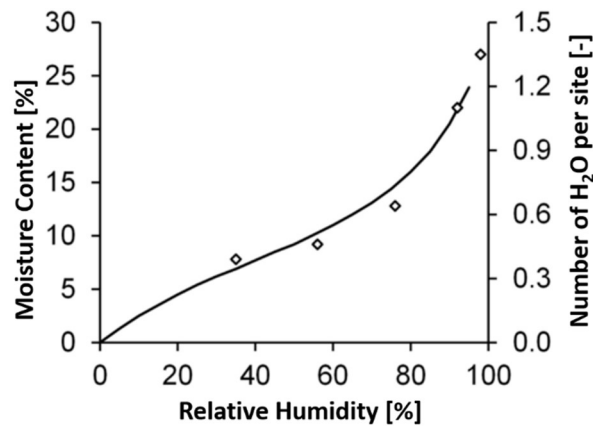
Fig. 29 Sorption isotherm for wood at room temperature (Forest Products Laboratory 2010) and average number of water molecules per sorption site (Berthold et al. 1996).

Below 5wt% moisture content, entering water molecules result in less swelling as seen from the present experiments and perhaps even establishing an ordered hydrogen-bonding pattern which reinforces the fiber cell wall. Above 5wt% moisture content a larger degree of swelling is observed, indicating that a larger number of hydrogen bonds has been broken, and poly-layer water adsorption has begun. Consequently, during moisture uptake, the strength loss is much higher due to the increasing distance between the constitutive polymers than the achieved strength-increase by a changed MFA. On the macroscopic scale of a tracheid it has already been shown that this effect is a marked weakening of the transverse elastic- and shear-moduli accompanied by a reorientation of microfibrils, i.e. a change in MFA [5]. The presently described mechanism of water-induced structural changes of pulp fibers are further supported by dynamic mechanical-analysis of moisturized Sixta spruce. The results have revealed an increased storage modulus up to a moisture content of 5wt%, whereas further moisture uptake led to a decreased storage modulus. In agreement, the observed loss-tangent declined between 1 and 5wt% moisture content and further increased, up to a moisture content of 7wt%. The maximum of the loss-tangent at 7wt% moisture content indicates a glass-transition, most likely that of hemicellulose [172]. The influence of hemicellulose on the creep behavior of wood-based samples was studied by several authors and all agreed that the softening of hemicellulose could enhance the creep behavior [3,41]. Additionally, many determinations of sorption isotherms of cellulosic materials have revealed that they exhibit a reduced sorption hysteresis at progressively higher isotherm temperatures, which is consistent with sorption interactions occurring with a glassy solid below the glass transition temperature [51,75,157]. Accordingly, the assumption that matrix softening adds to the creep

behavior of wood-based materials above 50%RH and 25°C is warranted. The present results support the idea of hemicellulose softening above a moisture content of 7wt% and 25°C. This phase change was shown to significantly increase the swelling strain-rate at 80% RH, and it was further suggested to have a marked influence on the MFA. In order to prove evidence a direct analytical method such as SAXS-measurements enabling the detection of the MFA are necessary. However, the presently obtained swelling strain-rate during sorption and the creep strain-rate during constant ambient humidity at three different moisture levels have shown a significant relationship. Whereas the swelling strain-rate polynomial increased with the moisture content, the creep strain-rate linearly increased with the moisture content. During the sorption process the strain exponentially increased, which is consistent with previously determined sorption kinetics of cellulose-based materials [74]. The results further confirm the observed macroscopic deformation behavior of wood-based materials and provide useful information about the understanding of the mechanical behavior of pulp fibers [29,158].

Chapter 7: Dry fiber creep

Whereas the creep of individual pulp fibers under the influence of moisture has been widely observed, little is known about the fiber creep when moisture is absent from the cell wall. In the dry state, a pulp fiber has an increased contact area between constitutive polymers, a fact which was already suggested to improve the fiber strength. In contrast to this, when a fiber is freely dried, amorphous polymers randomly collapse and fibrils located close to collapsing pores are even forced to change their direction. Thereby the fibrils transversally align towards the fiber axis, a mechanism referred to as tension-buckling. This leads to observable misaligned fibrils throughout the cell wall which can critically affect the mechanical properties of pulp fibers [176]. These regions are also known as kinks, slip planes, nodes, or micro-compressions, and in the following will be referred to as dislocations. It is, however, rather uncertain how dislocations behave during creep and whether they are truly affecting the mechanical properties. For synthetic fibers, it has already been proven, that an applied strain can increase the orientation of the constitutive polymers which leads to an increased fiber strength, a phenomenon known as strain hardening. In the case of individual pulp fibers, strain hardening has not been observed until now. Another objective of this thesis therefore is to observe the mechanism behind the dry pulp-fiber creep and to further evaluate whether the orientation of the constitutive polymers could be improved in order to positively impact their mechanical properties.

For the creep and creep-recovery experiments 9 individual pulp fibers were subjected to the same pre-treatment of drying for 8 hours at 25°C and 0% RH under the tensile load of about 4 MPa. Thereafter, dry fibers were instantaneously stressed by an external load of about 180 MPa, which was kept constant for 20 minutes. 180 MPa correspond to approximate 15% of the ultimate tensile strength of pulp fibers. After 20 minutes of stress exposure the external load was removed, and the fibers were allowed to rest for further 20 minutes before the next load cycle was applied. Prior to the application of the external load, the strain was set to zero. This treatment was repeated six times, while the displacement was recorded, figure 30 (a). In each load cycle, the slope [dε/dt] significantly decreased after 6 to 10 minutes of stress exposure, thereafter the creep rate was evaluated.
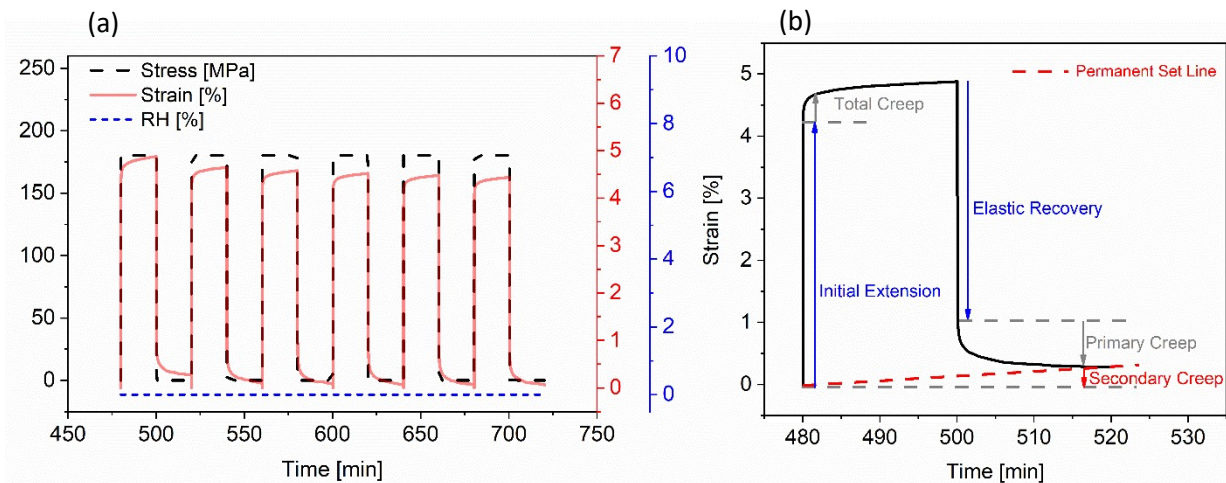
Fig. 30 (a) Measurement schedule, (b) resulting strain function and its interpretation after exposure to a single load cycle.

Each load cycle is described by the initial extension due to the applied external load, by the fiber creep during constant force application, and the recovery after the load has been removed, figure 30 (b). Permanent set or secondary creep was observed during each load cycle, which describes the non-recoverable part of the creep, figure 31 (a+b). During the measurement two fiber specimen broke during the first load cycle, namely SP33 and SP36 (illustrated in light and dark brown). SP31 (green) broke during the fifth load cycle and SP32 (violet) in the final load-cycle. Five of the measured fibers withstood the successive loading and unloading through all six load cycles. The fibers which broke during the initial load cycle, namely SP33 and SP36 were further excluded from the evaluation. The single inter-fiber variation is in accordance with previously published literature and illustrates the variability of the physical structure of natural wood fibers. It is believed that this variation is mainly caused by the load bearing unit, and therefore related to the MFA.
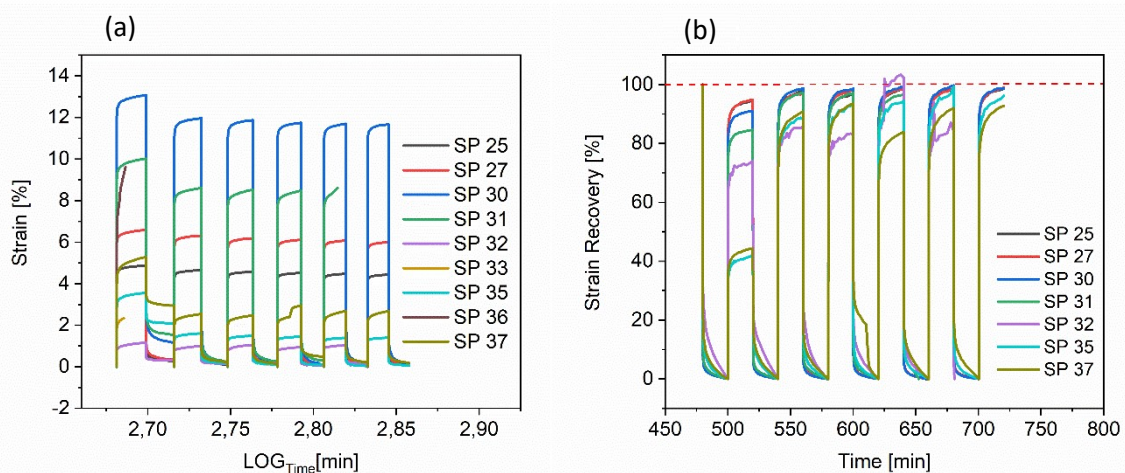

Fig. 31 Resulting (a) strain and (b) strain-recovery functions of 9 individual dry pulp fibers, after their exposure to six load cycles with 180 MPa at 25°C.

The creep and creep-recovery experiments show that, after the externally applied load has been removed, the strain immediately drops down to values close to 0%, which correspond to a recovery of almost 100%. Nevertheless, none of the fibers fully recovered its initial gauche length, which is particularly expressed in the initial load cycle. The obtained permanent set induced during each load cycle is attributed to plastic deformations inside the fiber cell wall. From the results it is further apparent that the initial load cycle has the highest impact on the materials' subsequent deformation pattern, which implies that most of the obtained plastic deformation was already induced during the initial load cycle. When excluding this load cycle, the resulting permanent set was remarkably low and varied between 1% to 5% of the initial gauche length, figure 32 (a).
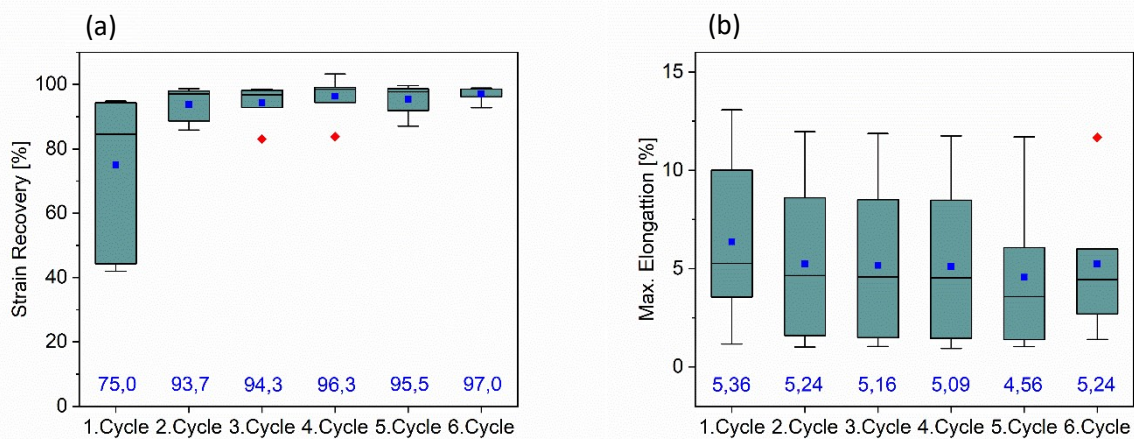
Fig. 32 Data distribution of (a) the strain recovery and (b) the maximum elongation illustrated by a box plot and mean values of the tested fibers during each load cycle illustrated in blue.

At a first glance, the maximum elongation does not significantly vary according to the apparent standard deviations, figure 32 (b). Nonetheless, the mean values of the obtained elongations continuously decrease during the first five load cycles, which leads to continuously increasing values of the strain recovery, seemingly approaching a constant value of 97%. Consequently, after the initial load cycle, the observed recovery indicates a highly elastic material. During the fourth load cycle, the deviation from the mean value for both, the maximum elongation and the recovery strain, is the highest, which might be related to a fully extended fiber state. The underlying natural divergence of the MFA becomes strongly dominant when the fibrils are fully strained and, accordingly, the standard deviation from the apparent mean value is expected to increase. Initially applied load cycles therefore might have increased the

orientation of the fibrils, while during the fifth load cycle premature fiber failure might already have been induced. Captivatingly, the obtained recovery strain significantly varies during the initial load cycle in the range between 42% and 95%. Thereby SP32, SP35 and SP37 recovered only 74%, 42% and 44% of their initial gauche length, whereas the others recovered at least 85% of their initial shape, figure 33 (a+b, SP32, SP35 and SP37 are illustrated in red). Surprisingly, already within the second load cycle, these three samples achieved values of 86%, 89% and 91%, respectively.
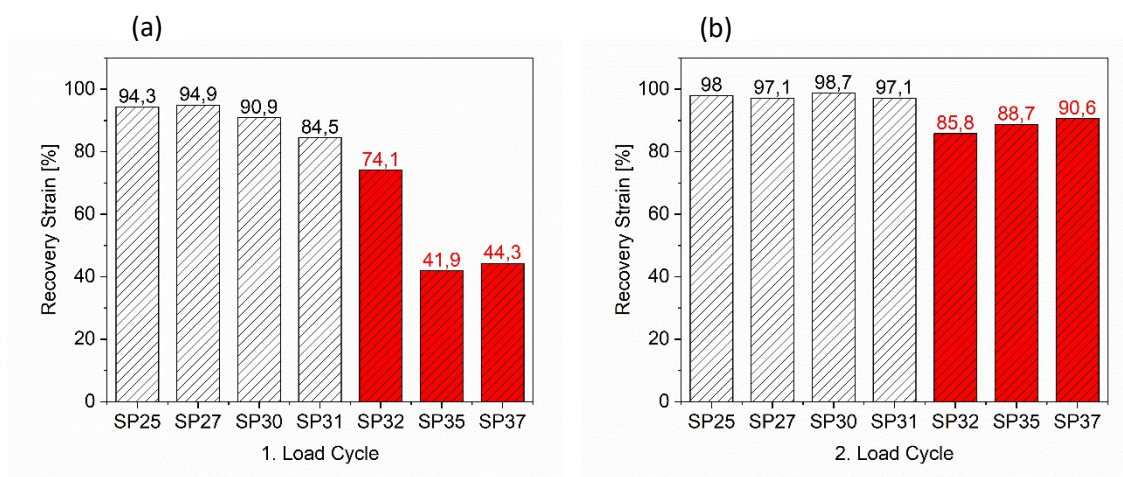
Fig. 33 Mean values of the recovery strain of the (a) initial and (b) the second load cycle.

However, values of the creep-rate vary between 10,02% and 12,11 % per ten minutes, figure 34 (a). The average creep-rate decreases during the first three load cycles and suddenly increases during the fourth load cycle from 9,889 %/LOG(min) to 11,91 %/LOG(min). Consequently, the deviation from the mean value increases. In consistence with the maximum elongation and with the recovery strain the deviation from the mean value obtained its maximum range during the fourth load cycle. Similar to the obtained recoveries, the decreasing ability to creep during the initial three load cycles suggests a strengthening of the fiber network, whereas the increase of the fiber creep rather indicates a strength loss, possibly related to premature fiber failure.
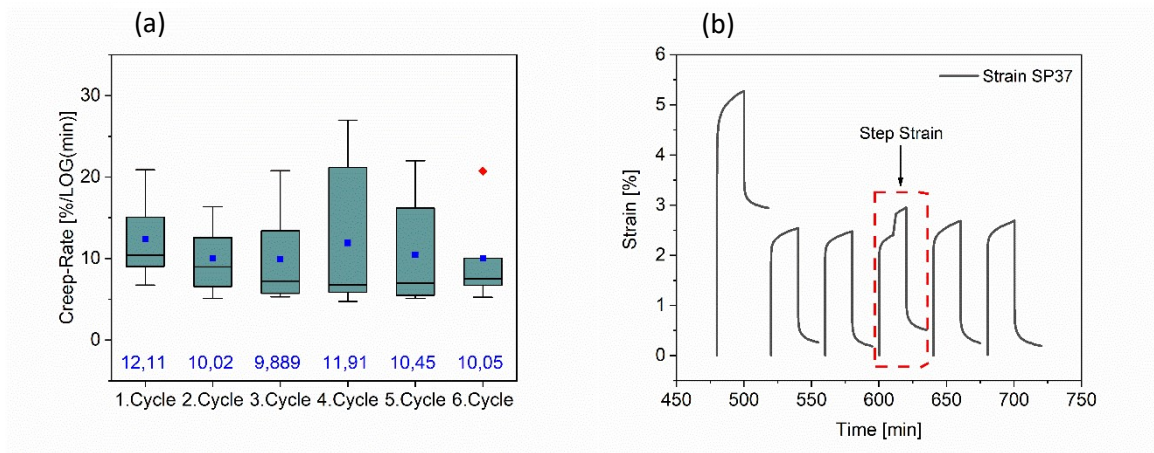
Fig. 34 (a) Data distribution of the maximum elongation and (b) resulting strain-function of the fiber specimen SP37, after their exposure to six load cycles with 180 MPa at 25°C.

Mentionable, the strain pattern of sample SP37 shows an unexpected strain-step during the fourth load cycle. Afterwards, the maximum elongation increases slightly from 2,4% to 2,7%, as does the creep-rate, which increases from 13,4 %/LOG(min) during the third load cycle to 22,0 %/LOG(min) after the step during the fifth load cycle, figure 34 (b). For the same fiber specimen, the recovery after the fourth load cycle significantly decreases from 93,5% to 83,8%. This loss of the ability to recover indicates already induced small damages of the load bearing unit. Captivatingly as well, the fiber sample SP31 spontaneously broke during the fifth load cycle, without any previous sign of failure or crack initiation. This clearly supports the assumption that after the application of four load cycles with 180 MPa some fibers are on the edge of failure.

The results of the relaxation moduli are less conclusive, and obtained values are similarly distributed through each applied load cycle. The relaxation moduli vary between 1600 MPa and 25000 MPa within the initial load cycle and further rather increase, figure 34 (a). At a first glance the stress relaxation of dry pulp fibers similarly behaves during each load cycle, figure 35 (b).
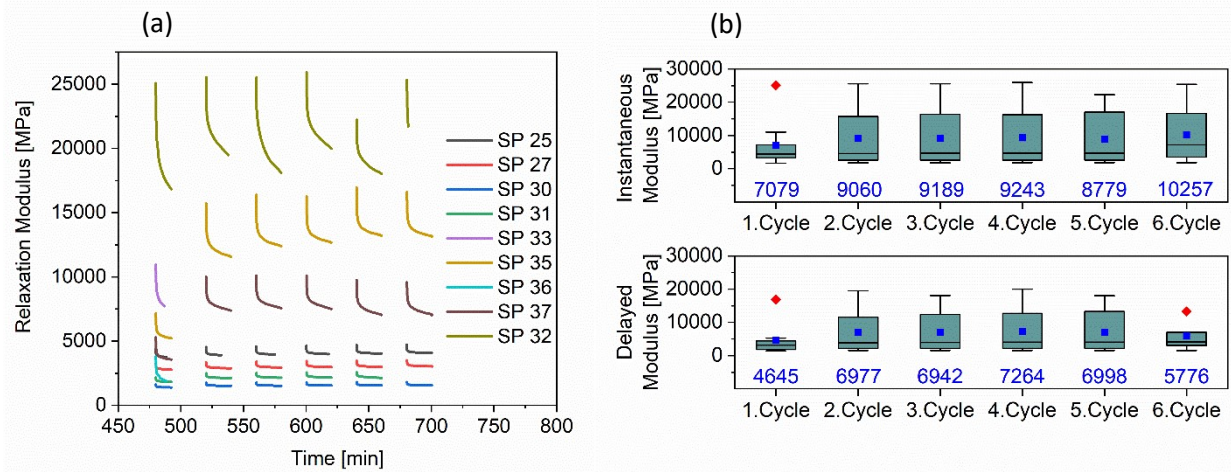
Fig. 35 (a) Resulting relaxation moduli of 9 individual dry pulp fibers, after their exposure to six load cycles with 180 MPa at 25°C, (b) and the obtained instantaneous and delayed moduli visualized by a box plot where the mean value is illustrated in blue.

The data distribution visualized in the boxplots defines either SP32, or SP35 and SP37, which are more than 25% apart from the average value, as outliers. The same fiber specimens have obtained conspicuously high creep-rates and relaxation moduli. In addition to that, there is a marked difference between those samples which have achieved a high relaxation modulus and those obtained a low relaxation modulus. While SP25, SP27, SP30 and SP31 are in an equilibrated state after 6 to 10 minutes of stress exposure, for the fiber samples SP32, SP35 and SP37 the strain and the relaxation moduli still develop, figure 36 (a+b).

Fig. 36 Strain and relaxation modulus after separating the outliers from the sample batch. (a) Fiber specimen which are not more than 25% apart from the mean value, (b) outliers.

It seems therefore possible that the results describe the influence of the dry pulp fibers' load bearing unit during stress exposure. For fibers with initially high MFA, a decrease of the MFA is feasible at much lower shear forces, as the stress concentrates at the interface between fibril surfaces and matrix. Under an applied tensile load, fibers with initially high MFAs could logically be expected to respond to a greater degree than a specimen with a relatively small initial MFA. Thus, fibers with initially high MFA are expected to creep more than fibers with initially low MFA. In addition, an increasing creep implies increased stress relaxation on the molecular level. One possible explanation for the enhanced relaxation moduli of the fiber samples SP32, SP35 and SP37 therefore might be the continuously decreasing MFA under tensile loads [66,171]. Obviously, the behavior of those fibers defined as outliers describes the behavior of fibers with initially high MFA, whereas for those fibers within the defined standard deviation of 25%, the MFA remains rather constant during stress exposure and the creep follows the behavior of fibers with initially low MFA. As stress relaxation is increased for fibers with high MFA, it is also reasonable, that these fibers did not reach an equilibrated state within

the applied set time of 20 minutes. For fibers with initially high MFA, plastic fiber response becomes increasingly imminent as the fibrils move or slip through the matrix. Thus, there is evidence that the fiber response significantly differs with respect to the initial inclination of the fibrils inside the fiber cell wall. After separating the results into two groups, the findings therefore clearly suggest that one observed deformation pattern describes the creep of fibers with initially high MFA (SP32, SP35, SP37), whereas the other deformation pattern describes the creep of fibers with initially low MFA (SP25, SP27, SP30, SP31). The mechanical behavior of these two groups essentially differs in the amount of creep, the amount of recovery and by the amount of stress relaxation, table 3.

Tab. 3 Mechanical behavior upon loading of dry pulp fibers with different initial MFA.

Pulp fibers	MFA	Equilibrium	Creep-Rate	Relaxation	Deformation
MFA$_{low}$	Constant	reached	low	low	elastic
MFA$_{high}$	Decrease	not reached	high	high	plastic

The mechanism behind the plastic deformation becomes obvious by looking at the relaxation moduli and the strain recovery in more detail. The instantaneous moduli of the outlier specimens, further referred to as fibers with initially high MFA, are enhanced fivefold, which suggests increased fibril movement and increased stress levels inside the cell wall, figure 37 (a+b).

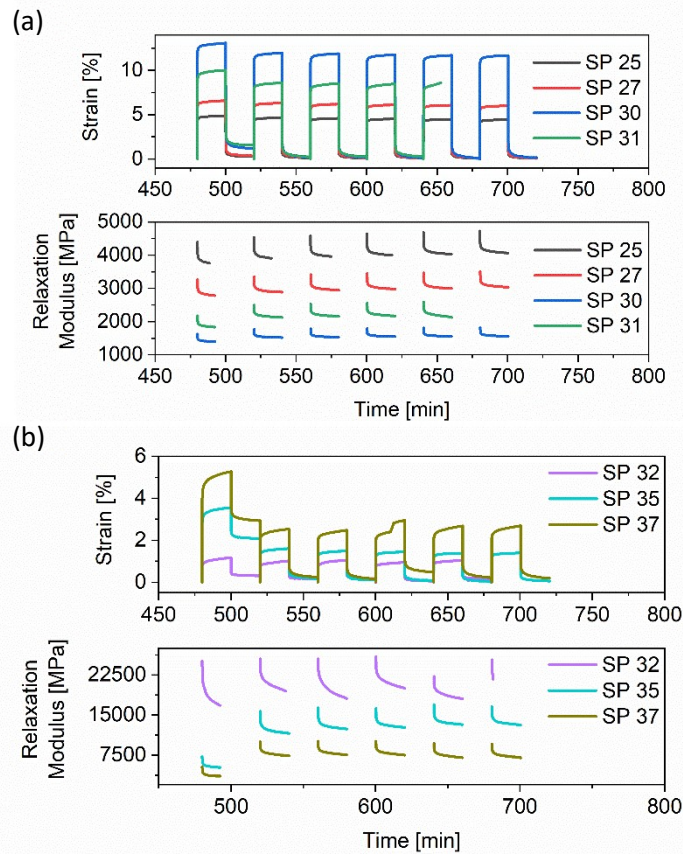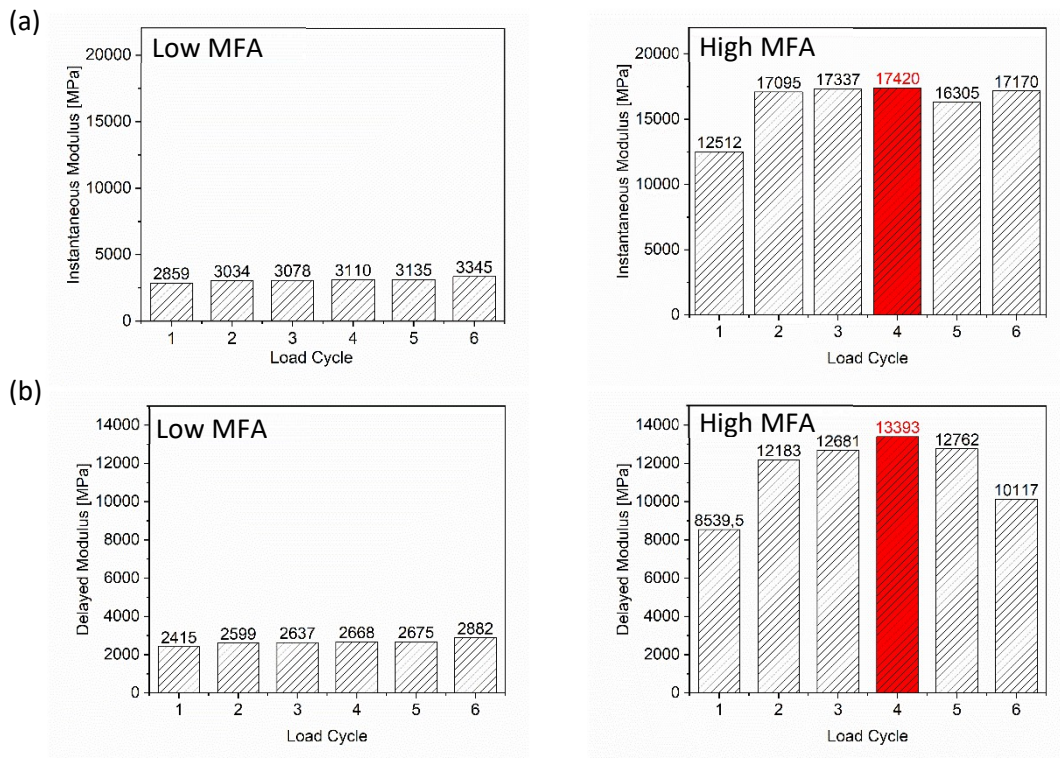**Fig. 37** Instantaneous and delayed moduli after separating the outliers from the sample bath. (a) Fiber specimen which are not more than 25% apart from the mean value, (b) outliers.

Theoretically, the instantaneous modulus of dry pulp fibers describes the polymer-backbone vibration of the load-bearing unit after stress exposure. Accordingly, the instantaneous modulus represents the highest value of the relaxation modulus after the force has been instantaneously applied in tensile direction. The stress further is transported to the polymer sidechains, which represents the hydroxyl-groups of the cellulose chains and the delayed modulus, respectively. Thus, the delayed modulus is obtained from the lowest value of the relaxation modulus during stress exposure. At the fibril surface the hydroxyl-groups of the cellulose chains must be able to relax into the neighboring amorphous matrix to further reduce and distribute stress. In the dry state, this transfer is expected to be reduced or even diminished, due to the rigid and inflexible matrix. Consequently, shear stresses at the interface may additionally increase, causing the decrease of the MFA for fibers with initially high MFAs. Thus, backbone and side-chain relaxation are tremendously enhanced for fibers with initially high MFA, compared to fibers with initially low MFA, where the fibrils are capable of withstanding the applied stress. The results from the relaxation moduli therefore clearly capture the higher overall stress level in fibers with high MFA when an external tensile load is applied. The stress level in fibers with low MFA is reduced, as fibrils are almost parallelly

aligned to the fiber axis, enabling the fibrils to withstand tensile stress to a much higher extent. Consequently, the applied stress can be almost entirely stored elastically and significantly less stress relaxation occurs. The amount of induced stress relaxation of fibers with initially low MFA is therefore related to the realignment of fibrils at the site of dislocations, leading to a strengthening of the fiber. This is supported by the recovery strain of these fibers which continuously increases. The recovery of fibers with initially low MFA is close to 95% already during the initial load application, and further approaches a constant value of 99%. The strain of these fibers therefore describes a highly elastic material that plastically deforms only marginally and rather strengthens through all applied load cycles, figure 38.
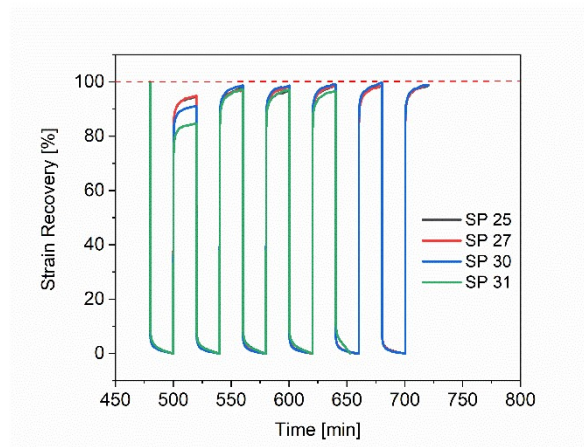
Fig. 38 Strain recovery of fiber specimens with initially low MFA during six load cycles with 180 MPa at 25°C.

In contrast to that, the moduli of fibers with initially high MFA pass through a maximum during the fourth load cycle (figure 37; maximum moduli are illustrated in red). After the initial load cycle, delayed moduli continuously increase from the second to the fourth load cycle, whereas instantaneous moduli stay rather constant. This is related to the hydroxyl-groups seeking for a new partner to re-bond with, enabling the fibrils to fixate in another position. Accordingly, the hydroxyl-groups may not be able to relax towards the matrix and fracture might occur somewhere at the load-bearing unit, yielding maximum stress relaxation within the fourth load cycle. Within the same load cycle the strain function of the sample SP37 shows a strain step, which indicates induced fracture of the load bearing unit. The following load cycle leads to a reduced recovery and decreasing moduli, indicating that the fibrils were further able to interlock in a new position. A similar picture can be gained from the strain recovery of the fiber sample SP32, figure 39 (SP37 illustrated in olive green and SP32 illustrated in violet). The

recovery strain for this fiber even exceeds 100% during the fourth load cycle, in which maximum stress relaxation occurs. This may be explained by an elastic recovery after the load bearing unit has been broken. The same fiber specimen withstood another load cycle before it entirely broke during the last load cycle. In consistence, stress relaxation during the fifth load cycle decreases, which is related to the previous fixation of the broken fibrils in a new position.
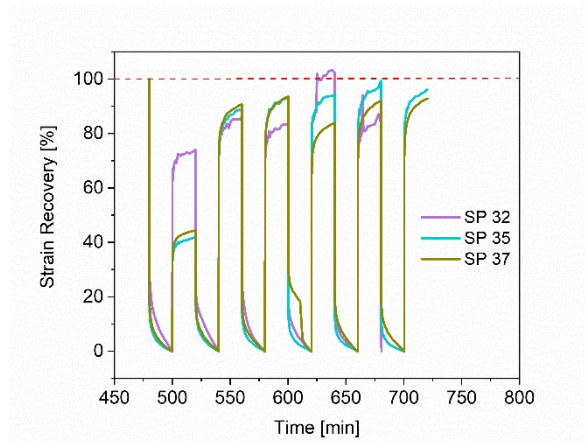
Fig. 39 Strain recovery of fiber specimen with initially high MFA during six load cycle with 180 MPa at 25°C (outlier specimens).

For both categories of pulp fibers, regardless whether they have a high or a low MFA, the realignment of the fibrils at the sites of dislocation is expected [80,170]. Overall, the decrease of the MFA leads to a fourfold increase of the relaxation modulus, compared to the achievable relaxation modulus by dislocation straining.

As mentioned in the literature review, the creep of pulp fibers is influenced by several factors. Besides the effect of moisture, the physical properties of the cell wall, especially the S2-layer is known to control the mechanical properties of pulp fibers. Prior studies have already pointed out the importance of the MFA as load bearing unit in wood-based materials [9,22,66,80,84,176,177]. Mechanical properties, such as the elastic modulus, significantly differ whether the initial MFA is high or low, and the fiber strength accordingly changes [22]. Lotfy et al. suggested that the extent of creep in wood differs according to the initial MFA, which was related to the decrease of the MFA during stress exposure [66]. The present study proves evidence of the existence of two different deformation patterns governing the creep behavior of dry pulp fibers. More precisely, the results show that the extent of creep and induced stress relaxations of dry pulp fibers significantly differ in accordance with the initial inclination of the fibrils to the fiber axis. Plastic deformation of fibers with high MFA can therefore be related to the decrease of the MFA. From the results of the present study it is further apparent that fibers with initially low MFA are able to elastically deform to a high extent, whereas plastic deformation is rather minimized. The small extent of plastic deformation occurring in fibers with initially low MFA is referred to the straining and fixation of the fibrils at the site of dislocations, which leads to a reinforcement of the fiber cell wall. This is in consistence with the observations of Peura et al., who found evidence that the MFA of dry wood specimens with initially low MFA (up to 10 °) does not decrease after straining. Overall, these cases also support the view that has been given by Kim et al., who observed the ultimate tensile strength (UTS) of pulp fibers of different MFA under increasing tension stress during drying. For fibers with initially high MFA, an increased fiber strength during straining was observed, and the obtained UTS achieved a maximum according to the applied stress. In contrast to this, fibers with initially low MFA did not significantly change their initial UTS. Kim et al. concluded that fibers with initially high MFA decrease their MFA in order to respond to the applied stress, while fibers with initially low MFA can be strengthened by the removal of dislocations [80]. The increasing fiber strength reported by Kim et al. mirrors the increasing relaxation moduli for fibers with initially high MFA observed in the present study and further confirms the slightly increased relaxation modulus for fibers with initially low MFA. Whereas the removal of the dislocations contributes to the strengthening of fibers with initially high MFA, for fibers with initially low MFA the removal of such defects is the only mechanism to strengthen the cell wall. This implies that the strengthening of fibers with initially low MFA is

possible to a much lower extent. The observed slightly increased relaxation moduli for those fibers are therefore explained by the presence of dislocations and the possibility to strengthen these areas by the realignment of the fibrils in direction of the applied stress. The strengthening of the sites of dislocation can further explain why dislocations were not found to contribute to the mechanical properties of nature-based fibers. For slightly moisturized wood fibers (tested at 30% RH and 25°C), observations of the elastic properties of the cell wall have shown that dislocations only minorly affect the fiber's tensile strength, but the cell wall fracture has been induced in proximity to these defects [22,141,176]. In contrast to that, Eder et al. showed that, under continuous loading, previously damaged pulp fibers showed nearly the same UTS as compared to an undamaged reference fiber [176]. Although dislocations were reported to minorly influence the mechanical properties of wood-based fibers, evidence exists, that these regions are prone to locally concentrate stress [129,176–178]. During characterization, these regions can be strained, inducing a reinforcement within the cell wall, which has led to the assumption that dislocations do not affect the mechanical properties of wood-based fibers. This, however, is related to a strengthening of the fiber during the process of characterization, as the initial fiber strength can be restored by the realignment of the fibrils at the site of dislocation. Placet et al. studied the mechanical behavior of single hemp fibers at 30% RH and 25°C. For that reason, they applied load cycles to the single fibers similar to the experiments performed in this study. Contrary to our experiments the stress was increased from cycle to cycle, and in sum these stresses exceeded 180 MPa. Additionally, the force was ramped in a way that the applied stress was continuously increased and then kept constant for a time period of 30 minutes as soon as the desired stress was reached. In-situ polarized light microscopy thereby confirmed that fibrils have been re-aligned mainly in the area of dislocations, a process already suggested to occur in wood fibers during straining [178]. The realigned fibrils in the area of dislocations obtained an MFA close to zero, as they oriented themselves nearly parallel to the fiber axis. More importantly, the removal of dislocations was found to be stress- and time-dependent as well as reversible. This additionally adds to the complexity of studying the effect of dislocations on the mechanical properties of wood-based fibers. However, the present study set out with the aim of assessing the role of the MFA of dry pulp fibers during creep experiments, and whether and how dislocations affect the mechanical behavior of pulp fibers. The present study clearly shows that two different mechanisms are

involved during the creep of dry pulp fibers and obtained results largely corroborate the findings of previous work done in this field.

Chapter 8: Conclusion

The present study was designed to independently study the sorption-induced creep and the creep induced by an externally applied load. As the key incentive was the separation of these frequently overlapping effects special focus was put on the experimental design. The results indicate that the applied pre-load does not significantly impact the sorption induced strain-rate, which, indeed, allows studying the long-term deformation behavior of pulp fibers exclusively induced by sorption. In the following, results which could elucidate the relation between molecular mechanisms and macroscopic wood performance are briefly reviewed.

Chapter 8.1: Fiber during drying

The drying strain of pulp fibers can be categorized in three parts, including (1) water desorption from the available outer and inner surface of the cell wall, (2) drying of the porous network, and (3) densification of the molecular structure without significant moisture loss. The strain in part (3) linearly decreases with the logarithmically scaled time, whereas the moisture content remains rather constant. Although the moisture content does not significantly change during the final observation interval in which the ambient humidity is kept at a minimum, the obtained strain rate is enhanced as compared to the strain rate during the first and the second strain segment. Even when the cell wall is almost dry, the pulp fibers still deform significantly. The final strain segment therefore is governed by structural densifications accompanied by an increase of the microfibril angel. This is explained by increasing Van der Waals-forces as the distance between constitutive polymers continuously decreases.

Chapter 8.2: Fiber during rewetting

Corresponding to the abovementioned behavior, the strain during rewetting can be categorized in three parts, including (1) initial surface adsorption, (2) swelling during RH increase, and (3) creep at constant RH. The swelling strain-rate at the applied moisture levels follows a second order polynomial growth, whereas the creep strain-rate linearly increases with elevating moisture levels.

Chapter 8.3: Fiber during adsorption/swelling

When the ambient RH is increased at a rate of 2% per minute the swelling strain develops exponentially, which is in consistence with previously reported sorption kinetics of wood-

based materials. This can be explained by the process of water entering the cell wall: The energy necessary to reopen the porous structure is enhanced as compared to the following facilitated adsorption of water molecules onto already existing layers of water. As a consequence, the strain at the beginning only proceeds slowly and further linearly develops with increasing RH.

Chapter 8.4: Fiber during constant RH

In addition to the aforementioned processes observed during moisture increase, fiber specimens show a different behavior under constant ambient RH. The strain increases linearly with the logarithmically scaled time at constant 25% RH. Thereby, the achieved swelling strain-rate and the creep strain-rate are in the same range. This is in contrast to the strain development during 50% and 80% RH levels, where the swelling strain-rate is significantly enhanced in relation to the creep strain-rate. This implies that the sorption capacity of pulp fibers significantly increases at 50% RH, explained by the water-induced Tg-shift of the matrix polymers. When hemicellulose starts to soften the free volume increases contributing to the observed accelerated creep at 50% and 80% RH. As water preferably adsorbs at the interface between the fibrils and the matrix, intensifying shear stresses might additionally force the fibrils to reduce their inclination towards the cell axis. Accordingly, the decrease of the MFA may add to the sorption-induced accelerated creep at constant 50% and 80% RH, even when no external load is applied.

Chapter 8.5: Fiber during humidity cycling

In general, mechano-sorptive creep is seen as a consequence of a coupling between an externally applied load and the sorption process itself. In the present study, when the fibers were exclusively stressed by the sorption process between 50% and 80% RH, MSC was not observed. Additionally, MSC in pulp fibers only occurred when the ambient humidity was cycled between 30% and 80% RH [7]. The absence of MSC in the present study is related to matrix polymers entering their rubbery state enabling for facilitated stress migration. Also, in other cellulose related materials, MSC is exclusively observed when the matrix was present in its non-softened state. Therefore it seems plausible that interfaces between the fibrils and the matrix play a key role when MSC is observed. Applied stresses are expected to concentrate at this very interface, hence increasing the free volume when the material is alternatingly

exposed to drying and swelling processes. Accordingly, the sorption capacity of the cell wall increases and induces accelerated creep.

Chapter 8.6: Dry fiber creep

While previous sub-chapters mainly referred to the sorption-induced phenomena, the following experiments address the load-induced creep of dry fibers. The results of the creep and creep-recovery experiments show that dry pulp fibers strengthen during exposure to the first three out of six load cycles. This is concluded from the increasing recovery strains and the decreasing creep-rates and attributed to the higher ordering of the supramolecular structures. The findings further suggest that in general the stress response of the fibrils dominate the dry pulp-fiber creep enabling the differentiation of fibers having a high or a low MFA. By separating the sample batch into two groups of fibers with either high or low fibril inclinations, defining of the different mechanisms underlying plastic deformation of the fibers is made possible. Fibers with an initially low MFA barely deform plastically, mainly driven by fibril rearrangement at the fiber dislocations. Fibers with an initially high MFA, however, plastically deform to a high extent as a consequence of the MFA decrease during load application. This different mechanical response of fibers with initially low or high MFA is also clearly visible in the obtained relaxation moduli. From these, it is obvious that stress relaxation in fibers with initially high MFA is significantly enhanced as compared to stress relaxations occurring in fibers with initially low MFA. The increased relaxation moduli of fibers with initially high MFA clearly suggest an increased molecular movement related to the decrease of the MFA during stress exposure in tensile direction.

Chapter 8.7: Summary and outlook

In general, the findings explained above contribute to our knowledge about the viscoelastic nature of pulp fibers and enhance our understanding of plastic deformation in dried pulp fibers during creep. The findings further point towards an interesting new focus of future research. From the obtained results and the literature available, it can be concluded that the creep behavior of pulp fibers may significantly be influenced by the interface between fibrils and matrix. Accordingly, a promising focus of future research could be laid on the observation of said interfaces during drying and/ or wetting. During sorption, these interfaces may grow and further lead to increased and unpredictable creep behavior. In the past, many researchers have claimed that creep of wood mirrors the creep of concrete, which is governed by the

propagation of micro cracks inside the material. As previously discussed, the stress at the interface between fibrils and matrix is expected to continuously increase and, with that, the probability of crack initiation rises. The amount of generated free volume increases as the matrix passes its Tg during each sorption cycle; the matrix in its glassy state is unable to adapt the dimensional changes occurring during the sorption process. With each sorption cycle, interfaces and cracks therefore grow. This may significantly add to the creep of the cell wall and may further explain the observed similarity in the creep behavior between wood and concrete. In the case of individual wood fibers, however, the mechanism behind MSC seems to be more complex. It is expected that the available free volume between fibrils and matrix during the adsorption cycle is continuously occupied by water. Thereby the number of hydroxyl-groups at the interface increases, facilitating stress migration by VdW-interactions further minimizing the stress concentration at these sites. As a consequence, MSC is not observed when the matrix is present in its softened state. As it was shown in previous work, MSC in wood fibers does not occur when the humidity is cycled between 50% and 90% RH, even when an external load is applied [110]. Further work is needed in order to establish the impact of the mechanically applied load elevating the creep of wood fibers during humidity cycling. A logical continuation of this work therefore would be to analyze the creep of pulp fibers in the absence of an applied mechanical load during humidity cycling between 30% and 80% RH. In this moisture interval the matrix passes its Tg, which is supposed to strongly contribute to the phenomenon of MSC. The occurrence of MSC under such conditions would elucidate MSC as a phenomenon originating from the amorphous matrix passing its Tg. The applied mechanical load, however, could additionally amplify the MSC.

Another factor strongly affecting the creep of pulp fibers is related to the initial inclination of the fibrils towards the fiber axis. The mechanical behavior of pulp fibers obviously differs to a high extent according to their initial MFA. From creep experiments of wood-based materials reported in here, it becomes obvious that some specimens never reach steady-state conditions, whereas some specimens quickly achieve a quasi-equilibrium state. The present study further suggests that this difference arises from the initial inclination of the fibrils, which can change during characterization. Plastic deformations in dry pulp-fibers with high MFA is significantly enhanced due to an increased fibril movement. In contrast to that, fibers with low MFA barely plastically deform and show highly elastic response, as the obtained recovery strain approaches 99% of the initial gauche length. For a deeper understanding of creep in

wood and pulp fibers it is therefore necessary to test fibers with initially high and low MFA, separated from each other.

References

1. Xanthos, D. & Walker, T. R. International policies to reduce plastic marine pollution from single-use plastics (plastic bags and microbeads): A review. *Mar. Pollut. Bull.* **118,** 17–26 (2017).

2. Jambeck, J. R. *et al.* Plastic waste inputs from land into the ocean. *Science (80-.).* **347,** 768–771 (2015).

3. Sedlachek, K. M. The Effect Of Hemicelluloses and Cyclic Humidity on the Creep of Singel Fibers. (Ripon College, 1995).

4. Engelund, E. T. Wood – water interactions Linking molecular level mechanisms with macroscopic performance. (Technical University of Denmark, 2011).

5. Engelund, E. T. & Salmén, L. Tensile creep and recovery of Norway spruce influenced by temperature and moisture. *Holzforschung* **66,** 959–965 (2012).

6. Soremark, C. & Fellers, C. N. Mechano-sorptive Creep and Hygroexpansion of Corrugated Board in Bending. *J. pulp Pap. Sci.* **19,** 519–526 (1993).

7. Olsson, A. M. & Salmén, L. Mechano-sorptive creep in pulp fibres and paper. *Wood Sci. Technol.* **48,** 569–580 (2014).

8. Olsson, A. M., Salmén, L., Eder, M. & Burgert, I. Mechano-sorptive creep in wood fibres. *Wood Sci. Technol.* **41,** 59–67 (2007).

9. Salmén, L., Olsson, A. M., Stevanic, J. S., Simonovic, J. & Radotic, K. Structural organisation of the wood polymers in the wood fibre structure. *BioResources* **7,** 521–532 (2012).

10. Hearlejohn, W. S. *Physical structure and fibre properties*. *Regenerated Cellulose Fibres* (2001).

11. Mohan, T., Hribernik, S., Kargl, R. & Stana-Kleinschek, K. *Cellulose- Fundamental Aspects and Current Trends*. *Nanocellulosic Materials in Tissue Engineering Applications* (2015).

12. Goring, D. A. I. & Timell, T. E. Molecular weight of native celluloses. *Tappi J.* **45,** 454–460 (1962).

13. Okita, Y., Saito, T. & Isogai, A. Entire Surface Oxidation of Various Cellulose Microfibrils by TEMPO-Mediated Oxidation. *Biomacromolecules* **11,** 1696–1700 (2010).

14. Park, S., Baker, J. O., Himmel, M. E., Parilla, P. A. & Johnson, D. K. Cellulose crystallinity index : measurement techniques and their impact on interpreting cellulase performance. *Biotechnol. Biofuels* **3,** 1–10 (2010).

15. Lavoine, N., Desloges, I., Dufresne, A. & Bras, J. Microfibrillated cellulose - its barrier properties and applications in cellulosic materials: a review. *Carbohydr. Polym.* **90,** 735–64 (2012).

16. Atalla, R. H. & Vanderhart, D. L. Native Cellulose: A Composite of Two Distinct Crystalline Forms. *Science (80-.).* **223,** 283–285 (1984).

17. Sjöström, E. *Wood chemistry: Fundamentals and applications*. (1993).

18. Koutaniemi, S. Lignin biosynthesis in Norway spruce: from a model system to the tree. (University of Helsinki, 2007).

19. Hinterstoisser, B., Åkerholm, M. & Salmén, L. Load distribution in native cellulose. *Biomacromolecules* **4,** 1232–1237 (2003).

20. Salmén, L. & Akerhom, M. Softening of wood polymers induced by moisture studied by dynamic FTIR spectroscopy. *J. Appl. Polym. Sci.* **94,** 2032–2040 (2004).

21. Berthold, J., Olsson, R. J. O. & Salmén, L. Water Sorption to Hydroxyl and Carboxylic Acid Groups in Carboxymethylcellulose (CMC) Studied with NIR-spectroscopy. *Cellulose* **5,** 281–298 (1998).

22. Salmén, L. & Burgert, I. Cell wall features with regard to mechanical performance. A review. *Holzforschung* **63,** 121–129 (2009).

23. Brändstrom, J. Micro- and ultrastructural aspects of Norway spruce tracheids: A review. *Iawa J.* **22,** 333–353 (2001).

24. Fengel, D. & Stoll, M. Über die Veränderungen des Zellquerschnitts, der Dicke der Zellwand und der Wandschichten von Fichtenholz-Tracheiden innerhalb eines Jahrringes. *Holzforschung* **27,** 1–7 (1973).

25. Berthold, J., Rinaudo, M. & Salmeń, L. Association of water to polar groups; Estimates by an adsorption model for ligno-cellulosic materials. *Colloids Surfaces A Physicochem. Eng. Asp.* **112,** 117–129 (1996).

26. Griffin, D. M. Water Potential and Wood-Decay Fungi. *Ann. Rev. Phytopathol.* **15,** 319–329 (1977).

27. Hernández, R. E. & Bizon, M. Compression Strength of Sugar Maple Below and Above the Fiber. *Wood Fiber Sci.* **26,** 360–369 (1994).

28. Hill, C. A. S. *et al.* An investigation of cell wall micropore blocking as a possible mechanism for the decay resistance of anhydride modified wood. *Int. Biodeterior. Biodegrad.* **55,** 69–76 (2005).

29. Engelund, E. T., Thygesen, L. G., Svensson, S. & Hill, C. A. S. A critical discussion of the physics of wood-water interactions. *Wood Sci. Technol.* **47,** 141–161 (2013).

30. Nakamura, K., Hatakeyama, T. & Hatakeyama, H. Studies on Bound Water of Cellulose by Differential Scanning Calorimetry. *Text. Res. J.* **51,** 607–613 (1981).

31. Thygesen, L. G., Tang Engelund, E. & Hoffmeyer, P. Water sorption in wood and modified wood at high values of relative humidity. Part I: Results for untreated, acetylated, and furfurylated Norway spruce. *Holzforschung* **64,** 315–323 (2010).

32. Zelinka, S. L., Lambrecht, M. J., Glass, S. V., Wiedenhoeft, A. C. & Yelle, D. J. Examination of water phase transitions in Loblolly pine and cell wall components by differential scanning calorimetry. *Thermochim. Acta* **533,** 39–45 (2012).

33. Matthews, J. F. *et al.* Computer simulation studies of microcrystalline cellulose Iβ. *Carbohydr. Res.* **341,** 138–152 (2006).

34. Hartley, I. D., Kamke, F. A. & Peemoeller, H. Cluster theory for water sorption in wood. *Wood Sci. Technol.* **26,** 83–99 (1992).

35. Hartley, I. D., Avramidis, S. & MacKay, A. L. H-NMR studies of water interactions in sitka spruce and western hemlock: moisture content determination and second moments. *Wood Sci. Technol.* **30,** 141–148 (1996).

36. Hatakeyama, T. Effect of bound water on structural change of regenerated cellulose. *Macromol. Chem.* **188,** 1875–1884 (1987).

37. Hatakeyama, H. & Hatakeyama, T. Interaction between water and hydrophilic polymers l. *Thermochim. Acta* **308,** 3–22 (1998).

38. Simpson, W. Sorption Theories Applied To Wood. *Wood Fiber* **12,** 183–195 (1980).

39. O'Sullivan, A. C. Cellulose: the structure slowly unravels. *Cellulose* **4,** 173–207 (1997).

40. Maréchal, Y. & Chanzy, H. The hydrogen bond network in I(β) cellulose as observed by infrared spectrometry. *J. Mol. Struct.* **523,** 183–196 (2000).

41. Hofstetter, K., Hinterstoisser, B. & Salmén, L. Moisture uptake in native cellulose - The roles of different hydrogen bonds: A dynamic FT-IR study using Deuterium exchange. *Cellulose* **13,** 131–145 (2006).

42. Fringant, C. *et al.* Characterisation of sorbed water molecules on neutral and ionic polysaccharides. *Int. J. Biol. Macromol.* **18,** 281–286 (1996).

43. Joly, C., Gauthier, R. & Escoubes, M. Partial masking of cellulosic fiber hydrophilicity for composite applications. Water sorption by chemically modified fibers. *J. Appl. Polym. Sci.* **61,** 57–96 (1996).

44. Brunauer, S., Emmett, P. H. & Teller, E. Adsorption of gases in multimolecular layers. *J. Am. Chem. Soc.* **60,** 309–319 (1938).

45. Park, G. S. Transport Principles—Solution, Diffusion and Permeation in Polymer Membranes. in *Synthetic Membranes: Science, Engineering and Applications* 57–107 (1981).

46. Bessadok, A. *et al.* Study of water sorption on modified Agave fibres. *Carbohydr. Polym.* **76,** 74–85 (2009).

47. Stamm, A. J. The fiber-saturation point of wood as obtained from electrical conductivity measurements. *Ind. Eng. Chem. Anal. Ed.* **1,** 94–97 (1929).

48. Célino, A., Fréour, S., Jacquemin, F. & Casari, P. The hygroscopic behavior of plant fibers: a review. *Front. Chem.* **1,** 43 (2013).

49. Babbitt, J. D. On the adsorption of water vapour by cellulose. *Can. J. Res.* **20a,** 143–172 (1942).

50. Mauze, G. R. & Stern, S. A. The dual-mode solution of vinyl chloride monomer in poly(vinyl chloride). *J. Memb. Sci.* **18,** 99–109 (1984).

51. Vrentas, J. S. A Free-Volume Interpretation of the Influence of the Glass Transition on Diffusion in Amorphous Polymers. *J. Appl. Polym. Sci.* **22,** 2325–2339 (1978).

52. Vrentas, J. S. & Vrentas, C. M. Sorption in Glassy Polymers. *Macromolecules* **24,** 2404–12 (1991).

53. Chow, S.-Z. & Pickles, K. Thermal Softening and Degradation of Wood and Bark. *Wood Fiber Sci.* **3,** 166–178 (1971).

54. Olsson, A.-M. & Salmén, L. The Softening Behavior of Hemicelluloses Related to Moisture. in *Hemicelluloses: Science and Technology* 184–197 (2001).

55. A. Lenth, C. & A. Kamke, F. Moisture dependent softening behavior of wood. *Wood Fiber Sci.* **33,** 492–507 (2001).

56. Wang, J. Z., Dillard, D. a., Wolcott, M. P., Kamke, F. a. & Wilkes, G. L. Transient Moisture Effects in Fibers and Composite Materials. *J. Compos. Mater.* **24,** 994–1009 (1990).

57. Jakes, J. E. *et al.* Mechanism of Transport Through Wood Cell Wall Polymers. *J. For. Prod. Ind.* **2,** 10–13 (2013).

58. Hailwood, A. J. & Horrobin, S. Absorption of water by polymers: analysis in terms of a simple model. *Trans. Faraday Soc.* **42,** 84–102 (1946).

59. Stamm, A. J. Combined bound-water and water vapor diffusion into sitka spruce. *For. Prod. J.* **10,** 644–648 (1960).

60. Gamstedt, E. K., Bader, T. K. & De Borst, K. Mixed numerical-experimental methods in wood micromechanics. *Wood Sci. Technol.* **47,** 183–202 (2013).

61. Krabbenhoft, K. A model for non-Fickian moisture transfer in wood. *Mater. Struct.* **37,** 615–622 (2004).

62. Hozjan, T. & Svensson, S. Theoretical analysis of moisture transport in wood as an open porous hygroscopic material. *Holzforschung* **65,** 97–102 (2011).

63. Péroval, C., Debeaufort, F., Despré, D. & Voilley, A. Edible Arabinoxylan-Based Films. 1. Effects of Lipid Type on Water Vapor Permeability, Film Structure, and Other Physical Characteristics. *J. Agric. Food Chem.* **50,** 3977–3983 (2002).

64. Comstock, G. L. Moisture diffusion coefficients in wood as calculated from adsorption, desorption, and steady state data. *For. Prod. J.* **13,** 97–103 (1963).

65. Christensen, G. N. & Hergt, H. F. A. Effect of Previous History on Kinetics of Sorption by Wood Cell Walls. *J. Polym. Sci.* **7,** 2427–2430 (1969).

66. Lotfy, M., El-Osta, M. & Wellwood, R. W. Short-term creeep as related to microfibril angel. *Wood Fiber Sci.* **4,** 26–32 (1972).

67. Salmén, L. & Olsson, A. M. Physical properties of cellulosic materials related to moisture changes. *Wood Sci. Technol.* **50,** 81–89 (2016).

68. Keckes, J. *et al.* Cell-wall recovery after irreversible deformation of wood. *Nat. Mater.* **2,** 810–4 (2003).

69. Crank, J. A theoretical investigation of the influence of molecular relaxation and internal stress on diffusion in polymers. *J. Polym. Sci.* **11,** 151–168 (1953).

70. Engelund, E. T. & Svensson, S. Predicting the reorientation of microfibrils in plant fibres under tensile strain. (2011).

71. Hill, S. J. *et al.* Effect of drying and rewetting of wood on cellulose molecular packing. *Holzforschung* **64,** 421–427 (2010).

72. Gouanvé, F., Bessadok, A., Langevin, D. & Métayer, M. Kinetics of water sorption in flax and PET fibers. *Journal, Eur. Polym.* **43,** 586–598 (2007).

73. Xie, Y., Hill, C. A. S., Xiao, Z., Mai, C. & Militz, H. Dynamic water vapour sorption properties of wood treated with glutaraldehyde. *Wood Sci. Technol.* **45,** 49–61 (2011).

74. Xie, Y., Hill, C. A. S., Jalaludin, Z. & Sun, D. The water vapour sorption behaviour of three celluloses: Analysis using parallel exponential kinetics and interpretation using the Kelvin-Voigt viscoelastic model. *Cellulose* **18,** 517–530 (2011).

75. Hill, C. A. S., Norton, A. & Newman, G. The water vapor sorption behavior of natural fibers. *J. Appl. Polym. Sci.* **112,** 1524–1537 (2009).

76. Eichhorn, S. J. *et al.* Current international research into cellulosic fibres and composites. *J. Mater. Sci.* **36,** 2107–2131 (2001).

77. Chen, W., Lickfield, G. C. & Yang, C. Q. Molecular modeling of cellulose in amorphous state part II: effects of rigid and flexible crosslinks on cellulose. *Polymer (Guildf).* **45,** 7357–7365 (2004).

78. Hossain, D. *et al.* Molecular dynamics simulations of deformation mechanisms of amorphous polyethylene. *Polymer (Guildf).* **51,** 6071–6083 (2010).

79. Fan, C. F. Yielding of a Model Glassy Polycarbonate under Tension: A Molecular Mechanics Simulation. *Macromolecules* **28,** 5215–5224 (1995).

80. Kim, C. Y., Page, D., El-Hosseiny, F. & Lancaster, A. P. S. The mechanical properties of single wood pulp fibers. III. The Effect of Drying Stress on Strength. *J. Appl. Polym. Sci.* **19,** 1549–1561 (1975).

81. Burgert, I., Frühmann, K., Keckes, J., Fratzl, P. & Stanzl-Tschegg, S. E. Microtensile Testing of Wood Fibers Combined with Video Extensometry for Efficient Strain Detection. *Holzforschung* **57,** 661–664 (2003).

82. Mott, L., Groom, L. & Shaler, S. Mechanical properties of individal southern pine fibers. Part II. Comparison of earlywood and latewood fibers with respect to tree height and juvenility. *Wood Fiber Sci.* **34,** 221–237 (2002).

83. Lichtenegger, H. *et al.* Variation of Cellulose Microfibril Angles in Softwoods and Hardwoods: A Possible Strategy of Mechanical Optimization. *J. Struct. Biol.* **128,** 257–269 (1999).

84. Peura, M. *et al.* The effect of axial strain on crystalline cellulose in Norway spruce. *Wood Sci. Technol.* **41,** 565–583 (2007).

85. Kamiyama, T., Suzuki, H. & Sugiyama, J. Studies of the structural change during deformation in Cryptomeria japonica by time-resolved synchrotron small-angle X-ray scattering. *J. Struct. Biol.* **151,** 1–11 (2005).

86.   Groom, L., Shaler, S. & Mott, L. Mechanical properties of individual southern pine fibers. Part III: Global relationships between fiber properties and fiber location within. *Wood Fiber Sci.* **34,** 238–250 (2002).

87.   Nissan, A. H. H-Bond Dissociation in Hydrogen Bond Dominated Solids. *Macromolecules* **9,** 840–850 (1976).

88.   Chen, W., Lickfield, G. C. & Yang, C. Q. Molecular modeling of cellulose in amorphous state. Part I: model building and plastic deformation study. *Polymer (Guildf).* **45,** 1063–1071 (2004).

89.   Holland, H. D., Halsey, G. & Eyring, H. Mechanical Properties of Textiles: VI. A Study of Creep of Fibers. *Text. Res. J.* **16,** 201–210 (1946).

90.   Eyring, H. The Activated Complex and the Absolute Rate of Chemical Reactions. *Chem. Rev.* **17,** 65–77 (1935).

91.   Eyring, H. Viscosity, Plasticity, and Diffusion as Examples of Absolute Reaction Rates. *J. Chem. Phys.* **4,** 283–291 (1936).

92.   Kauzmann, W. & Eyring, H. The Viscous Flow of Large Molecules. *J. Am. Chem. Soc.* **62,** 3113–3125 (1940).

93.   Jeffrey, G. A. & Saenger, W. *Hydrogen bonding in biological structures.* (Springer-Verlag, New York, 2012).

94.   Halsey, G., White, H. J. & Eyring, H. Mechanical Properties of Textiles, I. *Text. Res. J.* **15,** 295–311 (1945).

95.   Tobolsky, A. & Eyring, H. Mechanical Properties of Polymeric Materials. *J. Chem. Phys.* **11,** 125–134 (1943).

96.   Hidaka, H., Kim, U. J. & Wada, M. Synchrotron X-ray fiber diffraction study on the thermal expansion behavior of cellulose crystals in tension wood of Japanese poplar in the low-temperature region. *Holzforschung* **64,** 167–171 (2010).

97.   Kelley, S. S., Rials, T. G. & Glasser, W. G. Relaxation behaviour of the amorphous components of wood. *J. Mater. Sci.* **22,** 617–624 (1987).

98.   Byrd, V. L. Effect of relative humidity changes during creep on handsheet paper properties. *Tappi J.* **55,** 247–252 (1972).

99.   Armstrong, L. D. & Kingston, R. S. T. Effect of Moisture Changes on Creep in Wood. *Nature* **185,** 862–863 (1960).

100.   Gunderson, D. E. A Method for Compressive Creep Testing of Paperboard. *Tappi J.* **64,** 67–71 (1981).

101.   Haslach, H. W. The Mechanics of Moisture Accelerated Creep in Paper. *Tappi J.* **77,** 179–186 (1994).

102.   Salmén, L. & Fellers, C. N. Moisture Induced Transients and Creep of Paper and Nylon 6,6: a Comparison. *Nord. Pulp Pap. Res. J.* **11,** 186–191 (1996).

103.   Urbanik, T. J. & Lee, K. S. Swept Sine Wave Humidity Cycle Period Effect on Creep. *Wood Fiber Sci.* **27,** 68–78 (1995).

104. Gibson, E. J. Creep of Wood: Role of Water and Effect of a Changing Moisture Content. *Nature* **206,** 213–215 (1965).

105. Armstrong, L. D. Deformation of Wood in Compression During Moisture Movement. *Wood Sci. Technol.* **5,** 81–86 (1972).

106. Ranta-Maunus, A. The viscoelasticity of wood at varying moisture content. *Wood Sci. Technol.* **9,** 189–205 (1975).

107. Hunt, D. G. The Mechano-Sorptive Creep Susceptibility of Two Softwoods and Its Relation to Some Other Material Properties. *J. Mater. Sci.* **21,** 2088–2096 (1986).

108. Hanhijarvi, A. Deformation Kinetics Based Rheological Model for Time-Dependent and Moisture Induced Deformation of Wood. *Wood Sci. Technol.* **29,** 191–199 (1995).

109. Salmén N. L. & Back, E. L. Moisture-dependent thermal softening of paper evaluated by its elastic modulus. *Tappi J.* **63,** 117 (1980).

110. Habeger, C. C., Coffin, D. W. & Hojjatie, B. Influence of humidity cycling parameters on the moisture-accelerated creep of polymeric fibers. *J. Polym. Sci. Part B Polym. Phys.* **39,** 2048–2062 (2001).

111. Pickett, G. J. The Effect of Change in Moisture-Content on the Creep of Concrete Under a Sustained Load. *J. Amer. Concr. Inst.* **13,** 333–355 (1942).

112. Dounis, D. V., Moreland, J. C., Wilkes, G. L. & Turner, R. B. The Mechano-Sorptive Behavior of Flexible Water-Blown Polyurethane Foams. *J. Appl. Polym. Sci.* **50,** 293–301 (1993).

113. Lindström, S. B., Karabulut, E., Kulachenko, A., Sehaqui, H. & Wagberg, L. Mechanosorptive creep in nanocellulose materials. *Cellulose* **19,** 809–819 (2012).

114. Lindström, S. & Karabulut, E. Discriminating between different mechanosorptive creep hypotheses. *Prog. Pap. …* 121–123 (2011).

115. Coffin, D. W., Gruyter, D. & K., N. Creep and relaxation. in *Mechanics of paper products* Chapter 7 (2012).

116. Vlahinic, I., Thomas, J. J., Jennings, H. M. & Andrade, J. E. Transient creep effects and the lubricating power of water in materials ranging from paper to concrete and Kevlar. *J. Mech. Phys. Solids* **60,** 1350–1362 (2012).

117. Alfthan, J. Micro-mechanical modelling of mechano-sorptive creep in paper. (2002).

118. Alfthan, J. The effect of humidity cycle amplitude on accelerated tensile creep of paper. *Mech. Time-Dependent Mater.* **8,** 289–302 (2004).

119. Alfthan, J. & Gudmundson, P. An anisotropic fibre-network model for mechano-sorptive creep in paper. *Int. J. Solids Struct.* **45,** 5765–5787 (2008).

120. Haslach, H. W. Time-dependent mechanisms in fracture of paper. *Mech. Time-Dependent Mater.* **13,** 11–35 (2009).

121. Haslach Jr., H. W. The Moisture and Rate-Dependent Mechanical Properties of Paper: A Review. *Mech. Time-Dependent Mater.* **4,** 169–210 (2000).

122. Guicheret-Retel, V. *et al.* Creep behaviour of single hemp fibres. Part II: Influence of loading level, moisture content and moisture variation. *J. Mater. Sci.* **50,** 2061–2072 (2015).

123. Marrot, L., Lefeuvre, A., Pontoire, B., Bourmaud, A. & Baley, C. Analysis of the hemp fiber mechanical properties and their scattering (Fedora 17). *Ind. Crops Prod.* **51,** 317–327 (2013).

124. Cisse, O., Placet, V., Guicheret-Retel, V., Trivaudey, F. & Boubakar, M. L. Creep behaviour of single hemp fibres. Part I: viscoelastic properties and their scattering under constant climate. *J. Mater. Sci.* **50,** 1996–2006 (2015).

125. Placet, V., Cisse, O. & Boubakar, M. L. Influence of environmental relative humidity on the tensile and rotational behaviour of hemp fibres. *J. Mater. Sci.* **47,** 3435–3446 (2012).

126. Ciss, O., Placet, V. & Boubakar, L. Mechanosorptive creep in single hemp fibres. in *Composites week @Leuven and Texcomp-11 Conference* 1–7 (2013).

127. Keryvin, V. *et al.* Analysis of flax fibres viscoelastic behaviour at micro and nano scales. *Compos. Part A Appl. Sci. Manuf.* **68,** 219–225 (2015).

128. Stamboulis, A., Baillie, C. A. & Peijs, T. Effects of environmental conditions on mechanical and physical properties of flax fibers. *Compos. Part A Appl. Sci. Manuf.* **32,** 1105–1115 (2001).

129. Baley, C. Influence of kink bands on the tensile strength of flax fibers. *J. Mater. Sci.* **39,** 331–334 (2004).

130. Dong, F., Olsson, A. M. & Salmén, L. Fibre morphological effects on mechano-sorptive creep. *Wood Sci. Technol.* **44,** 475–483 (2010).

131. Sun, N. & Frazier, C. E. Time/temperature equivalence in the dry wood creep response. *Holzforschung* **61,** 702–706 (2007).

132. Kaboorani, A., Blanchet, P. & Laghdir, A. A Rapid Method to Assess Viscoelastic and Mechanosorptive Creep in Wood. *Wood Fiber Sci.* **45,** 370–382 (2013).

133. Navi, P., Pittet, V. & Plummer, C. J. G. Transient moisture effects on wood creep. *Wood Sci. Technol.* **36,** 447–462 (2002).

134. Zhan, T., Jiang, J., Peng, H. & Lu, J. Evidence of mechano-sorptive effect during moisture adsorption process under hygrothermal conditions: Characterized by static and dynamic loadings. *Thermochim. Acta* **633,** 91–97 (2016).

135. Zhan, T., Jiang, J., Peng, H. & Lu, J. Dynamic viscoelastic properties of Chinese fir (Cunninghamia lanceolata) during moisture desorption processes. *Holzforschung* **70,** 547–555 (2016).

136. Placet, V., Passard, J. & Perré, P. Viscoelastic properties of green wood across the grain measured by harmonic tests in the range 0-95°C: Hardwood vs. softwood and normal wood vs. reaction wood. *Holzforschung* **61,** 548–557 (2007).

137. Hanhijarvi, H. D. Experimental indication of interaction between viscoelastic and mechano-sorptive creep. *Wood Sci. Technol.* **32,** 57–70 (1998).

138. Hunt, D. G. Creep trajectories for beech during moisture changes under load. *J. Mater. Sci.* **19,** 1456–1467 (1984).

139. Menard, K. P. *Dynamic mechanical analysis: a practical introduction.* (1999).

140. Ebrahimzadeh, P. R. & Kubat, J. Mechanosorptive effects in cellophane, polyamide 6 and some other polymers studied by dynamic mechanical analysis. *Doktorsavhandlingar vid Chalmers Tek. Hogsk.* **2,** 4227–4235 (1997).

141. Navi, P. & Stanzl-Tschegg, S. E. Micromechanics of creep and relaxation of wood. A review. *Holzforschung* **63,** 186–195 (2009).

142. Navi, P. & Pizzi, A. Property changes in thermo-hydro-mechanical processing. *Holzforschung* **69,** 863–873 (2015).

143. Habeger, C. C. & Coffin, D. W. The role of stress concentrations in accelerated creep and sorption-induced physical aging. *J. pulp Pap. Sci.* **26,** 145–157 (2000).

144. Jajcinovic, M., Fischer, W. J., Hirn, U. & Bauer, W. Strength of individual hardwood fibres and fibre to fibre joints. *Cellulose* **23,** 2049–2060 (2016).

145. Ehrnrooth, E. & Kolseth, P. The Tensile Testing of Single Wood Pulp Fibers in Air and in Water. *Wood Fiber Sci.* **16,** 549–566 (1984).

146. Lorbach. Automated 3D measurement of fiber cross section morphology in handsheets. *Nord. Pulp Pap. Res. J.* **27,** 264–269 (2012).

147. Abe, K. & Yamamoto, H. Change in mechanical interaction between cellulose microfibril and matrix substance in wood cell wall induced by hygrothermal treatment. *J. Wood Sci.* **52,** 107–110 (2006).

148. Abe, K. & Yamamoto, H. Behavior of the cellulose microfibril in shrinking woods. *J. Wood Sci.* **52,** 15–19 (2006).

149. Zabler, S., Paris, O., Burgert, I. & Fratzl, P. Moisture changes in the plant cell wall force cellulose crystallites to deform. *J. Struct. Biol.* **171,** 133–141 (2010).

150. Toba, K., Yamamoto, H. & Yoshida, M. Mechanical interaction between cellulose microfibrils and matrix substances in wood cell walls induced by repeated wet-and-dry treatment. *Cellulose* **19,** 1405–1412 (2012).

151. Peura, M. *et al.* Negative poisson ratio of crystalline cellulose in kraft cooked Norway spruce. *Biomacromolecules* **7,** 1521–1528 (2006).

152. Peura, M. *et al.* X-ray microdiffraction reveals the orientation of cellulose microfibrils and the size of cellulose crystallites in single Norway spruce tracheids. *Trees - Struct. Funct.* **22,** 49–61 (2008).

153. Rayirath, P., Avramidis, S. & Mansfield, S. D. The Effect of Wood Drying on Crystallinity and Microfibril Angle in Black Spruce (Picea mariana). *J. Wood Chem. Technol.* **28,** 167–179 (2008).

154. Leppänen, K. *et al.* X-ray scattering and microtomography study on the structural changes of never-dried silver birch, European aspen and hybrid aspen during drying. *Holzforschung* **65,** 865–873 (2011).

155. Lube, V., Lazarescu, C., Mansfield, S. D. & Avramidis, S. Wood microfibril angle variation after drying. *Holzforschung* **70,** 485–488 (2016).

156. Grignon, J. & Scallan, A. M. Effect of pH and neutral salts upon the swelling of cellulose gels. *J. Appl. Polym. Sci.* **25,** 2829–2843 (1980).

157. Vrentas, J. S. & Vrentas, C. M. Hysteresis effects for sorption in glassy polymers. *Macromolecules* **29,** 4391–4396 (1996).

158. Murata, K. & Masuda, M. Microscopic observation of transverse swelling of latewood tracheid: Effect of macroscopic/mesoscopic structure. *J. Wood Sci.* **52,** 283–289 (2006).

159. Watt, I. C. & Kabir, M. Sorption of Water Vapor in Jute Fibers. *Text. Res. J.* **45,** 42–48 (1975).

160. Okubayashi, S., Griesser, U. J. & Bechtold, T. Water accessibilities of man-made cellulosic fibers – effects of fiber characteristics. 403–410 (2005). doi:10.1007/s10570-005-2179-y

161. Okubayashi, S., Griesser, U. & Bechtold, T. A kinetic study of moisture sorption and desorption on lyocell fibers. *Carbohydr. Polym.* **58,** 293–299 (2004).

162. Chirkova, J., Andersons, B. & Andersone, I. Study of the structure of wood-related biopolymers by sorption methods. *BioResources* **4,** 1044–1057 (2009).

163. Lee, J. M., Pawlak, J. J. & Heitmann, J. A. Longitudinal and concurrent dimensional changes of cellulose aggregate fibrils during sorption stages. *Mater. Charact.* **61,** 507–517 (2010).

164. Frandsen, H. L., Damkilde, L. & Svensson, S. A revised multi-Fickian moisture transport model to describe non-Fickian effects in wood. *Holzforschung* **61,** 563–572 (2007).

165. Burgert, I., Gierlinger, N. & Zimmermann, T. Properties of chemically and mechanically isolated fibres of spruce (Picea abies [L.] Karst.). Part 1: Structural and chemical characterisation. *Holzforschung* **59,** 240–246 (2005).

166. Habeger, C. C. & Coffin, D. W. The Role of Stress Concentrations in Accelerated Creep and Sorption-Induced Physical Aging. (1999).

167. Vishtal, A. & Retulainen, E. Boosting the extensibility potential of fibre networks: A review. *BioResources* **9,** 7951–8001 (2014).

168. Eder, M., Arnould, O., Dunlop, J. W. C., Hornatowska, J. & Salmén, L. Experimental micromechanical characterisation of wood cell walls. *Wood Sci. Technol.* **47,** 163–182 (2013).

169. Burgert, I., Frühmann, K., Keckes, J., Fratzl, P. & Stanzl-Tschegg, S. Structure-function relationships of four compression wood types: micromechanical properties at the tissue and fibre level. *Trees* **18,** 480–485 (2004).

170. Eder, M., Stanzl-Tschegg, S. & Burgert, I. The fracture behaviour of single wood fibres is governed by geometrical constraints: In situ ESEM studies on three fibre types. *Wood Sci. Technol.* **42,** 679–689 (2008).

171. Jentzen, C. The effect of stress applied during drying on some of the properties of individual pulp fibers. *Tappi J.* **47,** 412 (1964).

172. Obataya, E., Norimoto, M. & Gril, J. The effects of adsorbed water on dynamic mechanical properties of wood. *Polymer (Guildf).* **39,** 3059–3064 (1998).

173. Seow, C. C., Cheah, P. B. & Chang, Y. P. Antiplasticization by Water in Reduced-Moisture Food Systems. **64,** 576–581 (1999).

174. Kulasinski, K., Guyer, R., Derome, D. & Carmeliet, J. Water Adsorption in Wood Microfibril-Hemicellulose System: Role of the Crystalline-Amorphous Interface. *Biomacromolecules* **16,** 2972–2978 (2015).

175. Kulasinski, K. Effects of water adsorption in hydrophilic polymers. *Polym. Sci. Res. Adv. Pract. Appl. Educ. Asp.* 217–223 (2016).

176. Eder, M., Terziev, N., Daniel, G. & Burgert, I. The effect of (induced) dislocations on the tensile properties of individual Norway spruce fibres. *Holzforschung* **62,** 77–81 (2008).

177. Thygesen, L. G., Eder, M. & Burgert, I. Dislocations in single hemp fibres-investigations into the relationship of structural distortions and tensile properties at the cell wall level. *J. Mater. Sci.* **42,** 558–564 (2007).

178. Placet, V., Trivaudey, F., Cisse, O., Gucheret-Retel, V. & Boubakar, M. L. Diameter dependence of the apparent tensile modulus of hemp fibres: A morphological, structural or ultrastructural effect? *Compos. Part A Appl. Sci. Manuf.* **43,** 275–287 (2012).

179. Page, D. H., Elhosseiny, F., Winkler, K. & Lancaster, A. P. S. Elastic modulus of single wood pulp fibers. *Tappi J.* **60,** 114–117 (1977).

180. Page, D. H. & El-Hosseiny, F. Mechanical properties of single wood pulp fibres. Part VI. Fibril angle and the shape of the stress-strain curve. *Pulp Pap. Canada* **84,** TR99-100 (1983).